OPTICALLY-INDUCED POPULATION DISCHARGE THRESHOLD TESTING: A NOVEL INVESTIGATION OF A MURINE MODEL OF ALCOHOL WITHDRAWAL INDUCED CNS HYPEREXCITABILITY

BY:

GREGORY ERICK ALBERTO

A Dissertation Submitted to the Graduate Faculty of

WAKE FOREST UNIVERSITY GRADUATE SCHOOL OF ARTS AND SCIENCES

In Partial Fulfillment of the Requirements

for the Degree of

DOCTOR OF PHILOSOPHY

Neuroscience

August 2017

Winston-Salem, North Carolina

Approved by:

Dwayne W. Godwin, Ph.D., Advisor
Jeff Weiner, PhD., Chair
Jennifer Stapleton-Kotloski, Ph.D.
Evgeny Budygin, Ph.D.
James Daunais, Ph.D.

ACKNOWLEDGMENTS

My journey through graduate school is a story of collaboration and unparalleled support without which I would not be in the position I am today. I'd like to take this opportunity to thank some people who have been instrumental in my life and education.

First, I have to acknowledge the institution that has allowed me to follow my passion and develop along a path that is not exactly traditional. I began my training at Wake Forest School of Medicine in 2011 and quickly realized that my interest in Neuroscience research that had been fostered in undergraduate under the mentorship of Dr. Erik Johnson was not fleeting. In the summer of 2012, I reached out to the medical school Council of Deans to investigate the possibility of taking leave from my medical training to pursue a PhD. As is common at Wake Forest, they were extremely supportive of this idea. So I applied to Wake Forest Graduate School of Arts and Sciences. I must extend a deep sentiment of gratitude to the School for being willing to assist me in pursuing a non-traditional path toward a combined MD/PhD.

In addition to the School of Medicine and the institution of Wake Forest, I would like to acknowledge the Departments of Neuroscience and Neurology. The Neurology department did not hesitate to bring me on as a training fellow, and funded my first year of graduate school. I am deeply grateful to Dr. Popli and the whole department of Neurology for taking a risk on an untested young mind. My funding then transitioned to the Neuroscience Program where I was placed on the T32NS073553 Multisensory Training Grant. This funding supported me while

I conducted magnetoencephalographic investigations of language laterality, and explored potential PhD projects. The support from the Neuroscience Program and the Neurology Department were essential to my success in graduate school.

I would like to also take the opportunity to thank my mentor, Dr. Dwayne Godwin. Dr. Godwin was immediately willing to take me into his lab and allowed me the freedom to develop my own path. With little more than a vague interest in neurophysiology he was willing to give me access to all of his knowledge, skills, and available tools for investigation. The Godwin Lab is a place where curiosity is rewarded and no question is unfit for some level of investigation. Under his guidance I was successful in receiving an NRSA training fellowship. Dr. Godwin encouraged me to take risks and put myself out there. As a result of Dwayne's encouragement, I was fortunate to be selected by NIDA and the NIAAA to participate in the Early Career Investigator Showcase. Dwayne also thought it would be appropriate to nominate me for the Norman Sulkin Award in Neuroscience, which I was honored to receive. Dr. Godwin's kindness, support, and true passion for the sciences will follow me through my career. Thank you.

I would like also to thank my committee members: Drs. Jennifer Stapleton-Kotloski, Jeff Weiner, Evgeny Budygin, and James Daunais. I need to extend special thanks to Dr. Stapleton-Kotloski who was instrumental in my training in MEG experimentation and analysis. Her patience and level of positive support is unparalleled. Additionally, Dr. Daunais showed me that a passion for investigation and lifelong learning are key ingredients to a successful career as a researcher.

I need to thank all of the members of the Godwin lab, specifically Dr. David Klorig. I can ascribe a great deal of my success to Dr. Klorig, nearly all of it. His passion for and uncompromising dedication to the scientific method are inspiring. He does not take shortcuts in science, and the entire scientific community is better to have him. He trained me in electrophysiology, data analysis, surgical techniques, experimental design, and on and on. We spoke late into the evenings about the mysteries of the brain, and he became a friend to me. He supported me when work became frustrating and difficult. He is caring, empathetic, patient, and compassionate. Dr. Klorig is truly deserving of more praise and recognition than I could possibly give him here.

Finally, I need to thank my friends and family. To my parents, Gino and Karen Alberto; thanks for being patient mom and dad. I know this is a long, circuitous route to finally getting a job, but I appreciate your unwavering support and encouragement. The way you brag about me to the family, even if unwarranted, is really sweet. Thank you to Anne Koch who has been a constant source of encouragement and motivation. You keep me grounded and your kind and caring heart reminds me why we do research at all. I hope that I can serve humanity in a way that would make you proud. To Anne's parents, Ken and Elizabeth Koch, thank you for being a family to me when mine was so far away. For four years, you welcomed me into your home for Holidays and treated me with such love and support, thank you. To my friends who have no idea what I do, thanks. You folks are as important to me as anyone. You gave me the gift of distraction. Thank you.

TABLE OF CONTENTS

LIST OF FIGURES AND TABLES

CHAPTER 1: ALCOHOL USE DISORDER, WITHDRAWAL, AND CENTRAL NERVOUS SYSTEM HYPEREXCITABILITY

CHAPTER 2: OPTOGENETICALLY INDUCED POPULATION DISCHARCE THRESHOLD (OPDT) AS A SENSITIVE MEASURE OF EXCITABILITY

LIST OF ABBREVIATIONS

$5\text{-}HT_3$	5-hydroxytryptamine type 3
AD	After Discharge
ANOVA	Analysis of Variance
AUD	Alcohol Use Disorder
AWS	Alcohol Withdrawal Syndrome
BEC	Blood Ethanol Concentration
BSE	Brief Spindle Episode
BZD	Benzodiazepine
CA1	Cornu ammonis 1
Ca^{2+}	Calcium Ion
CA3	Cornu ammonis 3
CAMKIIα	Calcium/Calmodulin dependent protein kinase II-alpha
ChR2	channel-rhodopsin 2
CIE	Chronic Intermittent Ethanol
Cl^-	Chloride ion
CNS	Central Nervous System
EEG	Electroencephalogram
EtOH	Ethanol
ETX	Ethosuximide
$GABA_AR$	gamma-aminobutryic acid type A Receptor
GIRK	G protein-activated inwardly rectifying K^+
HIC	Handling Induced Convulsion
I_{50}	Light intensity at which there is half maximum PS occurrence

K^+	Potassium Ion
$K_{Ca}2$	calcium-activated potassium
LED	Light Emitting Diode
LEV	Levetiracetam
LFP	Local Field Potential
LGICs	Ligand Gated Ion Channel
LTP	Long Term Potentiation
L-type	Long-type Ca^{2+} channel
MEG	Magnetoencephalography
Mg^{2+}	Magnesium Ion
mTORC1	Mammalian Target of Rapamycin Complex 1
NIAAA	National Institute on Alcohol Abuse and Alcoholism
NMDAR	N-methyl-D-aspartate Receptor
oPDT	optically-induced Population Discharge Threshold
PS	Population Spike
PTZ	Pentylenetetrazole
PYR	Pyrazole
SSW	Spike and Sharp Wave
T-type	transient-type Ca^{2+} channel
WD	Withdrawal

ABSTRACT

Alcohol Use Disorder is a major, costly problem in society. Alcohol use is the third highest risk factor for health problems with much of that burden attributable to problems associated with alcohol withdrawal (WD). During WD the central nervous system (CNS) is described as being hyperexcitable. Hyperexcitability is a consequence of homeostatic pressure to compensate for alcohol's potentiation of inhibitory systems. When the drug is removed from the system the compensatory changes in excitability are revealed leading to excess activity. The increase in activity is associated with the symptoms of WD including seizure. Seizure represents the most severe symptom of WD, and is responsible for a significant portion of WD associated mortality. Treatment of alcohol WD relies on potentiating the inhibitory system with benzodiazepines (BZD). This is largely effective, but some individuals still experience WD symptoms even with BZD treatment and there is a risk of respiratory depression from BZD treatment and BZDs can be abused.

Here we demonstrate a platform in which CNS excitability during WD is probed called the optically-induced Population Discharge Threshold (oPDT). We demonstrate that the metric is sensitive to WD hyperexcitability and represents a novel model for experimentation. We propose that oPDT can be used for pharmacological screening for new, more effective treatment options. Furthermore, we demonstrate that oPDT is not altered with treatment with the drug ethosuximide (ETX) during WD. ETX is a Ca^{2+} channel blocker which has been shown to reduce WD anxiety-like behavior, certain seizure types associated

with thalamic dysfunction, and mortality in an animal model of WD. Our results indicate that the hyperexcitability measured by oPDT represents a change in circuit function that is insensitive to ETX. This suggests that the symptoms of WD may be differentiable, and that while hyperexcitability is ubiquitous during WD it may be the circuit and population context in which the hyperexcitability exists rather than the hyperexcitability itself that is relevant to symptomology. In summary, we have demonstrated a novel method for investigating WD hyperexcitability and shown that circuit level investigations of excitability can differentiate pharmacologic efficacy. We suggest that while hyperexcitability is an underlying feature of WD symptoms its role and the modulation of hyperexcitability are dependent on the neurobiological context in which it exists.

CHAPTER 1

ALCOHOL USE DISORDER, WITHDRAWAL, AND CENTRAL NERVOUS SYSTEM HYPEREXCITABILITY

G.E. Alberto

Abstract

Alcohol use has nearly ubiquitous effects on the molecular underpinnings of central nervous system (CNS) function, ranging from the major neurotransmitters to the intrinsic modulators of neuron excitability. The overwhelming effect of acute alcohol consumption is to increase inhibitory tone and reduce excitatory drive. Chronic alcohol abuse puts enormous homeostatic pressure on the system to rectify the shift in balance away from inhibition to restore normal excitatory tone. When alcohol is removed from the system following these homeostatic changes, there is a profound rebound hyperexcitability of the central nervous system. Here I review the major advancements in our understanding of the molecular mechanisms of central nervous system hyperexcitability during alcohol withdrawal with particular emphasis on the inhibitory and excitatory neurotransmitter systems as well as intrinsic modulators of neuronal excitability. I then describe how these changes interact to cause population wide hyperexcitability, priming the system for seizure. I provide an overview of existing models of CNS hyperexcitability during alcohol withdrawal and suggest a new method for probing excitability, optically-induced Population Discharge Threshold (oPDT) testing. I provide evidence for the mechanisms of pharmacotherapeutics during alcohol withdrawal and outline how oPDT testing may provide a more sensitive model for understanding these mechanisms. Utilizing circuit wide electrophysiological recordings combined with behavioral observation and experimenter controlled optical probes of the state of excitability I am able to detect subtle changes in the balance of excitation and

inhibition. In the future oPDT testing can be applied to a wide variety of experimental questions regarding CNS excitatory tone.

Alcohol Use Disorder and Alcohol Withdrawal

Although alcohol use is common and largely socially accepted, unhealthy patterns of use develop in a significant subset of individuals. According to the National Institute on Alcohol Abuse and Alcoholism (NIAAA), nearly 18 million individuals qualify as having an alcohol use disorder (AUD) resulting in more than $220 billion dollars lost annually. AUD is defined primarily by psychosocial features such as compulsive drinking, sacrificing regular activity for drinking, and drinking more than one wants (*Diagnostic and Statistical Manual of Mental Disorders* 2013). This unhealthy relationship with alcohol predisposes people to be at risk for alcohol withdrawal syndrome (AWS) upon cessation of alcohol consumption. AWS is composed of an array of psychological and physiological symptoms, which may seem unrelated, but that ultimately can be ascribed to the complex interactions of underlying neurobiological systems and the homeostatic pressure on those systems from the constant presence of alcohol. These symptoms include anxiety, hyperactivity, tremor, nausea, and in the most severe cases seizure

Figure 1.1. Cycle of alcohol abuse and relapse. The relationship between AUD and AWS is a consequence of a complex suite of neuroadaptive changes that occur in response to chronic exposure to alcohol. It is therefore necessary to develop useful tools for understanding AWS in order to better address AUD. From Becker 2008.

(Begleiter and Platz, 1972). It is believed that the symptoms of AWS as well as the fear related to the appearance of such symptoms are primary causes for relapse into, or maintenance of, alcohol abuse (Koob and Moal 2008; Howard C. Becker 2008; B. A. Johnson et al. 2006), and therefore understanding the neurobiology of AWS is paramount in alleviating the personal and societal burden of AWS (Fig. 1 (Howard C. Becker 2008)). Here I will describe the effects of chronic ethanol exposure on discrete neurobiological systems each of which represent potential targets for the treatment of AWS; demonstrate the response of those systems to the presence of alcohol and how that response leads to AWS, and finally I will argue for a new approach to understanding alcohol withdrawal (WD) that respects the complex, multisystem effect of alcohol in the context of the intact brain. Specifically, I will focus on the relationship between the presence of chronic alcohol in neural systems and the resultant circuit hyperexcitability as it relates to WD seizure.

Ligand-Gated Ion Channels

Ligand-gated ion channels (LGICs) represent a widespread family of receptor types present throughout the CNS. LGICs have a role in regulating the excitability state of individual neurons and subsequently how populations of neurons transmit and receive synaptic signals. Alcohol has a direct modulatory effect on a wide range of LGICs including the gamma-aminobutryic acid type A ($GABA_A$), N-methyl-D-aspartate (NMDA), glycine, nicotinic, and 5-hydroxytryptamine type 3 ($5\text{-}HT_3$) receptors (M. Davies 2003; Morisot and Ron 2017; Cardoso et al. 1999; Valenzuela et al. 1998). The effect of ethanol on each

of these different LGICs is specific causing some to gain function while others are functionally inhibited. It is believed that the specificity of action and the resultant homeostatic pressure on each of these systems is responsible for the increased excitability of the CNS during WD. As the scope of this document is not to comprehensively review the addiction process, but instead the consequences of chronic ethanol exposure and withdrawal, the major focus of my discussion of LGICs will be on the two major receptor systems responsible for excitation (NMDA-R) and inhibition ($GABA_AR$). Importantly, the $GABA_AR$ system is the main target for treatment of AWS (Schaefer and Hafner 2013; B. A. Johnson et al. 2006).

Gamma-Aminobutyric Acid type A Receptor

Electron microscopy revealed that the structure of the $GABA_AR$ consists of five subunits surrounding an enclosed central ion channel (Nayeem et al. 1994). The second of four transmembrane domains (TM2) of each of the five subunits form the central ion channel of the $GABA_AR$ and selectively allow for the passage of the chloride ion (Cl^-) (Smith and Olsen 1995). GABA binding occurs at the interface between the α and β subunits to cause a conformational change in the receptor allowing chloride ions to flow through (Stephens et al. 2017). Under normal conditions signaling through $GABA_AR$ leads to Cl^- influx causing hyperpolarization of the neuron. However, during development and when there is a high concentration of intracellular Cl^- (e.g. during seizure) GABA signaling can cause Cl^- efflux resulting in depolarization of the neuron (Sipilä et al. 2005; Spitzer 2010; de Curtis and Avoli 2016). Under normal conditions the influx of Cl^-

reduces the probability of an action potential; it is therefore considered to be involved in inhibitory signaling.

Over the past few decades a body of evidence supporting the role for the receptor subunits in the addictive process has begun to build (for a comprehensive review see (Stephens et al. 2017)). There have been 19 different subunit families identified with each family potentially having multiple members (Olsen and Sieghart 2009); additionally there is the potential for alternative splicing within some subunit isoforms providing even more variability in the system (Petrie et al. 2001). In total, there are over 1 million possible $GABA_AR$ permutations, but a very small subset are thought to actually participate in normal function (Olsen and Sieghart 2009; Fritschy and Panzanelli 2014). In the mammalian brain the most common $GABA_AR$ subtypes contain α1, β2, and γ2 subunits (M. Davies 2003). It is also important to discuss the α4 and δ subunits in the context of alcohol exposure as there are relevant changes in their expression levels in response to alcohol exposure (Liang et al. 2007; Cagetti et al. 2003). While the precise location (i.e., hippocampus, limbic system, brainstem, etc.) of any particular subunit being expressed is the major determinant for associated behavioral output, sophisticated genetic manipulations are being used to illuminate the particular role specific subunits play in behavior and therefore the rewarding, potentially addictive, aspects of alcohol use. For example, the reinforcing anxiolytic effect of alcohol may in part be attributable to α2, α3, and α5 subunits whereas the sedative and amnestic affects may be attributable to the α1 subunit, but not the others (Rudolph et al. 1999; McKernan et al. 2000). This

complex distribution of effects and the subsequent shift in subunit expression following alcohol abuse contributes to some of the symptoms of AWS. When exposed to ethanol the $GABA_AR$ is potentiated allowing increased influx of Cl^- for a longer time thereby increasing overall inhibitory tone (Allan and Harris 1987; D. L. Davies and Alkana 2001a, 2001b; M. Davies 2003). It is this chronic potentiation of the $GABA_AR$ that provides the homeostatic pressure to reduce the inhibitory drive of the $GABA_AR$. In a series of chronic ethanol administration experiments Kang et. al. demonstrated that changes in the GABAR system in hippocampus are responsible for reductions in inhibitory drive (Kang et al. 1996; Kang et al. 1998). Subsequently, the same group used Western blot and PCR to demonstrate

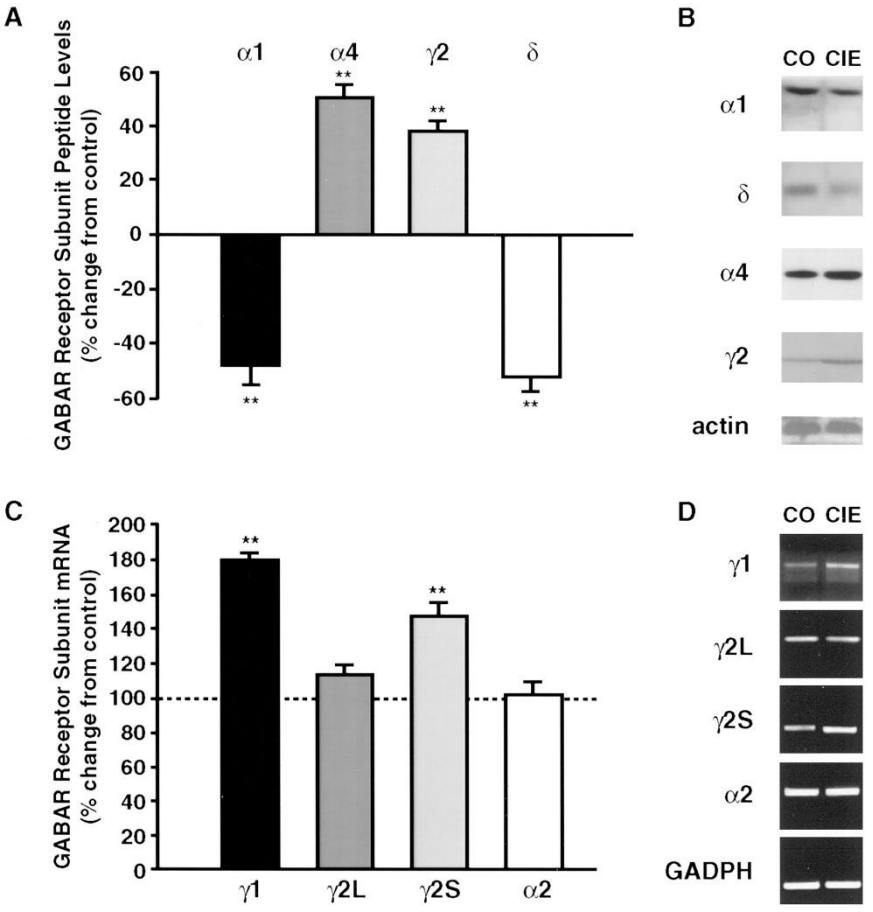

Figure 1.2 Changes in the expression of $GABA_AR$ subunit mRNA and peptide levels. Investigations into the molecular adaptions which occur in response to chronic ethanol exposure indicate a shift in the expression profile of the $GABA_A$ receptor system. These changes result in lower overall expression of $GABA_AR$ as well as changes in the expression of specific subunits which lead to less overall inhibitory tone through GABA signaling. From Cagetti et al. 2003.

specifically that the dysregulation of inhibition in hippocampus can be attributed, at least in part, to changes in the distribution of the $GABA_AR$ subunit expression (Fig. 1.2) (Cagetti et al. 2003; Mahmoudi et al. 1997). Furthermore, altered receptor trafficking and increased endocytosis of $GABA_AR$ has been shown (Petrie et al. 2001; Liang et al. 2007; Fritschy and Panzanelli 2014). Finally, using repeated pentobarbital administration as a control for chronic $GABA_AR$ activation it was demonstrated that the receptor subunit changes that occur are specific to ethanol exposure rather than simply over activation of the receptor (Morrow et al. 1990). Functionally, these changes to the $GABA_AR$ system result in increased channel opening time and a shorter time open, resulting in a reduction in Cl^- ion passage across the membrane and therefore reduced inhibitory drive in the neuron (Allan and Harris 1987; Kang et al. 1996; Mahmoudi et al. 1997; Tatebayashi et al. 1998; Cagetti et al. 2003). An overview of the discussed changes and their functional impacts as they relate to the hippocampus can be found in Table I (Grobin et al. 1998). The sum total effect of these GAB_AR subunit changes as well as the downregulation of total receptor numbers and endocytosis of membrane bound receptors amounts to increased excitability of affected neurons. However, the GABA system represents only one aspect of the balance of excitation and inhibition in the brain.

Receptor property	Alteration	Source
GABA-mediated Cl^- channel function	No change	(Tremwel et al. 1994)
GABA-mediated Cl^- channel function	Decreased	(Kang et al. 1996)
Paired-pulse inhibition	Decreased	(Kang et al. 1996)
Electrical stimulation of [^{3}H] GABA release	Increase	(Tremwel et al. 1994)
[^{3}H]Flunitrazepam binding	No change	(Rastogi et al. 1986; Negro et al. 1992a,b)
[^{35}S]TBPS binding	No change	(Rastogi et al. 1986)
[^{3}H]Zolpidem binding	No change	(Devaud and Morrow 1994)
[^{3}H]Ro-15–4513 binding	No change	(Mhatre et al. 1988)
α_1 Subunit mRNA[a]	Decreased	(Charlton et al. 1997)
α_1 Subunit peptides[a]	Decreased	(Charlton et al. 1997)
α_1 Subunit peptides[b,c]	No change	(Matthews et al. 1998)
α_2 Subunit peptides[b,c]	No change	(Matthews et al. 1998)
α_3 Subunit peptides[b,c]	No change	(Matthews et al. 1998)
α_4 Subunit peptides[b]	No change	(Matthews et al. 1998)
α_4 Subunit mRNA and peptides[c,d]	Increased	(Mahmoudi et al. 1997; Matthews et al. 1998)
α_5 Subunit mRNAs[a]	Increased	(Charlton et al. 1997)
α_6 Subunit mRNAs[d]	No change	(Mahmoudi et al. 1997)
$\beta_{2/3}$ Subunit peptides[b,c]	No change	(Matthews et al. 1998)
γ_2 Subunit peptides[b,c]	No change	(Matthews et al. 1998)

[a]12 weeks chronic ethanol consumption
[b]14 days chronic ethanol consumption
[c]40 days chronic ethanol consumption
[d]60 days chronic intermittent ethanol consumption

Table I Review of changes to GABA receptor system in response to chronic ethanol exposure. The above table from Grobin et al. 1998 illustrates the wide-ranging influence that chronic ethanol exposure has on the GABA system contributing to withdrawal mediated CNS hyperexcitability.

N-methyl-D-aspartate Receptor (NMDAR)

The NMDAR channel is one of the three major receptor subtypes for which glutamate acts as a ligand. Amongst the three glutamate receptors, the NMDA receptor is unique due to its dual gating properties, being both voltage- and ligand-gated (Mori and Mishina 1995). The voltage-gated property of the NMDAR is governed by a Mg^{2+} ion that resides within the ion channel preventing passage of cations at resting membrane potentials. The NMDAR is made of four subunits, each of which may have multiple splice variants and expression profiles across different regions of the brain (Mori and Mishina 1995; R. R. Johnson et al. 1996). There is one obligatory subunit GluN2A-D and GluN3A-B (Traynelis et al. 2010). The regulatory subunits can be modified to affect receptor localization in the membrane as well as binding efficacy and channel properties (Traynelis et al. 2010). Importantly, under normal conditions signaling through the NMDAR removes the Mg^{2+} block and leads to neuron depolarization, increasing the

likelihood of an action potential. As described, early studies suggested that ethanol (EtOH) increased GABA-activated Cl^- flux thereby hyperpolarizing neurons, however additional studies suggest that EtOH also inhibits the NMDA receptor current (Lovinger et al. 1989; White et al. 1990). This discovery further complicated the understanding of how chronic alcohol abuse caused hyperexcitability in the brain during withdrawal. Further investigation revealed specific changes in the NMDAR system as a result of chronic EtOH exposure that were in many ways similar to those changes observed in the $GABA_AR$ system (Snell et al. 1996; Kalluri et al. 1998).

More recent work indicates that the development of AUD and excessive alcohol intake is in part mediated by molecular modification of the NMDAR system (Ron and Barak 2016; Morisot and Ron 2017). These changes occur as a result of downstream activation of the mammalian target of rapamycin complex 1 (mTORC1) and occur in a regionally specific way (Morisot and Ron 2017). mTORC1 has been implicated as a major second messenger in the learning process, and its activation during alcohol consumption has led to the development of a hypothesis that regards AUD as being a consequence of a pathological learning process whereby the rewarding experiences of alcohol consumption are embedded as strong memories (Torregrossa et al. 2011). This hypothesis is consistent with observations of upregulated NMDA receptors after long term potentiation (LTP) as well as during learning tasks (Riedel et al. 2003; Mayford et al. 2012). In a series of studies it was demonstrated that alcohol exposure mimics the activation of Fyn kinase, the major substrate of which is

GluN2B (Gibb et al. 2011; Darcq et al. 2014; Morisot and Ron 2017). As described, GluN2B is a modulatory subunit of the NMDAR, and when phosphorylated it leads to NMDAR stabilization in the membrane as well as facilitates NMDAR activity (Wang et al. 2010, 2011). These observations are consistent with a learning-like hypothesis of alcohol use disorder, but also demonstrate important, long-lasting changes to the balance of excitation. These changes in excitation will be unmasked when alcohol access is removed, thereby contributing to rebound hyperexcitability during WD (Grant et al. 1990). Electrophysiological studies support this hypothesis demonstrating that not only is there an increase of NMDAR in the membrane, but also that the excitatory post-synaptic potential is increased during WD (Nelson et al. 2005).

Intrinsic excitability

Intrinsic excitability of a neuron can be defined as those features of a neuron, other than synaptic transmission, that enhance or reduce the likelihood that a neuron will fire an action potential (e.g. voltage-gated ion channels). Intrinsic excitability, while it may occur through separate mechanisms, may interact with more conventional synaptic sources of excitability (Graef and Godwin 2010). In recent years more attention has been paid to the role of intrinsic excitability in the addiction process and how it may relate to WD (Kourrich et al. 2015). The number of modulators of intrinsic excitability is vast; essentially including every channel that exists outside of the synapse (Kourrich et al. 2015). Many of these channels are simple voltage-gated channels, while others are coupled to G-protein-mediated pathways (Lomazzi et al. 2008).

Significant work has been done to characterize the role of modulators of intrinsic excitability during the addiction and withdrawal process, however the high diversity of heterogeneous channel types has made it difficult to identify a unified understanding of the effect of drugs on these systems. The most well characterized target of ethanol and ethanol withdrawal is the voltage-gated Ca^{2+} channel system (Twombly et al. 1990; Baliño et al. 2010; Broadbent 2013; Shan et al. 2013; Graef et al. 2011). There are two major types of Ca^{2+} channel: long-type (L-type) and transient-type (T-type) (Simms and Zamponi 2014). Activation of voltage-gated Ca^{2+} channels leads to an influx of Ca^{2+} and an increased likelihood of neuronal firing. Both types of channel appear to be inhibited by the presence of EtOH (Twombly et al. 1990; Shan et al. 2013; Walter and Messing 1999; Mu et al. 2003). In response to chronic ethanol exposure the Godwin lab has demonstrated an upregulation of T-type calcium channels, specifically the CaV3.2 isoform (Graef et al. 2011; Nordskog et al., Hammarback, and Godwin 2006). Furthermore, work in our lab demonstrates that blocking T-type calcium channels with the drug ethosuximide (ETX) reduces pentylenetetrazole (PTZ) induced seizure during WD (Riegle et al. 2015) as well as behavioral correlates of WD (Riegle et al. 2014).

An additional regulator of excitatory drive is the G protein-activated inwardly rectifying K^+ (GIRK) channel. These channels are located near the synapse and provide a slow inhibitory current that reduces the likelihood of action potential firing (Lüscher and Slesinger 2010). GIRK channel opening is modulated through a second messenger cascade in response to a number of neurotransmitters,

including acetylcholine, dopamine, GABA, and others (Pfaffinger et al. 1985). Once activated by the G protein the GIRK channel is opened allowing the passage of K^+ from the cell thereby decreasing excitability. Studies of the crystalline structure of the GIRK channel have identified a binding pocket for ethanol in the channel (Aryal et al. 2009). When bound ethanol opens the channel leading to inhibition of the neuron (Kobayashi et al. 1999). Using genetic knockout mice it was shown that symptoms of alcohol withdrawal, including anxiety and convulsions, are in part mediated by the GIRK channel (Blednov et al. 2001).

Finally, there are calcium-activated potassium ($K_{Ca}2$) channels, which open in response to transient increases in Ca^{2+} (Allen et al. 2007). These channels act as Ca^{2+} sensors and aid in NMDA dependent plasticity (Faber et al. 2008; Faber 2010; Lin et al. 2008). Ethanol exposure results in a reduction in the $K_{Ca}2$-mediated after-hyperpolarization (AHP) (Mulholland et al. 2011). When ethanol is chronically administered there is a subsequent reduction in the number of $K_{Ca}2$ channels and a correlated increase in NMDAR (Mulholland et al. 2011; Mulholland 2012). These observations regarding the role of $K_{Ca}2$ channels in alcohol withdrawal lead to the hypothesis that restoring $K_{Ca}2$ activity may reduce the severity of alcohol withdrawal. When a positive modulator of the channel was applied Mulholland et al. saw a reduction in the epileptiform discharges and cell death in cornu ammonis 1 (CA1) of hippocampus (Mulholland et al. 2011).

The results of these studies provide evidence for much broader alterations in the balance of excitation and inhibition than simply changes to the NMDA and

$GABA_AR$ system. In the search for novel pharmaceutical options for treating AWS our lab, and others, have broadened the search to include targets outside of traditional LGIC systems. In order to test efficacy of novel pharmaceuticals the field would benefit from a standardized way to probe the balance of excitation and inhibition.

Models of Alcohol Withdrawal

A prerequisite to studying alcohol withdrawal *in vivo* is developing alcohol dependence in the animal being studied by exposing the animals to sufficient levels of the drug. There are three major strategies for exposure to accomplish this goal, each with a variety of available modifications (for a comprehensive review see; Becker 2000). The first strategy involves forced exposure to alcohol either through gastric lavage or exposure to ethanol vapor for some period of time. This strategy allows for a high level of experimenter control of blood alcohol levels, but does not allow for investigations of animal preference or drug seeking. A second strategy utilizes animals with a genetic predisposition for alcohol consumption. In these models animals are given ethanol to consume and certain animals will choose to self-administer the drug. Allowing for animal self-administration provides the experimenter with insights into drug preference and drinking behaviors in different conditions, but suffers from low control over the total amount of drug consumed as determined by blood alcohol levels. Finally, the third strategy is a variation of the first two whereby the experimenter adds alcohol to the animal's food, or other source of nutrition. This strategy allows the experimenter to control when and for how long an animal has access to the drug,

but fails to control the overall dose given the animal may or may not choose to eat. Importantly, each of these strategies is capable of inducing symptoms of ethanol withdrawal (Becker 2000).

In humans, there is a long list of symptoms associated with alcohol withdrawal, and many of those symptoms have analogous signs in animal models (Table II; (Becker 2000)). Due to the fact that animals cannot convey their subjective

Withdrawal Signs and Symptoms in Humans	Corresponding Withdrawal Signs in Animals
Signs and symptoms as defined in the Clinical Institute Withdrawal Assessment for Alcohol, Revised (CIWA-Ar) questionnaire	
Gastrointestinal disturbances (e.g., nausea and vomiting)	Reduced food and water intake; diarrhea
Tremor	Tremor
Autonomic hyperreactivity (e.g., excessive sweating)	Rapid heart beat (i.e., tachycardia); elevated blood pressure; central and behavioral thermal dysregulation; piloerection
Anxiety	Behavioral measures of anxiety (e.g., avoidance of bright, open spaces)
Agitation	Behavioral signs of irritability and aggressiveness
Sensory disturbances (i.e., tactile, auditory, and visual disturbances)	Sensory hyperreactivity (e.g., enhanced startle response)
Headache	N/A*
Disorientation and clouding of sensorium	N/A*
Other clinical withdrawal symptoms used as diagnostic criteria as defined in the Diagnostic and Statistical Manual of Mental Disorders, Fourth Edition	
Psychomotor agitation	Abnormalities in body posture, gait, and locomotor activity; stereotypic movements
Grand mal seizures	Electrographic and behavioral signs of central nervous system hyperexcitability
Insomnia	*Abnormalities in the electroencephalogram*

Table II Overview of human alcohol withdrawal symptoms and corresponding animal models. This table modified from Becker 2000 illustrates the long list of symptoms associated with CNS hyperexcitability during alcohol withdrawal.

experience researchers must rely solely on objective physiologic or behavioral measures.

Interestingly, withdrawal severity is not solely predicated on the total amount of ethanol an animal has been exposed to, but is instead highly correlated with the number of exposures and withdrawals (Becker and Hale 1993; Becker 1994).

This profound observation led to the development of the chronic intermittent ethanol (CIE) exposure paradigm whereby animals are exposed to ethanol vapor for a prescribed period of time after which they are withdrawn from alcohol. This process is repeated typically for four exposure and four withdrawal periods; this block of intermittent exposure can be repeated. Becker and Hale first described the effect of multiple withdrawals compared to an equivalent exposure period using the handling induced convulsion (HIC; further discussion to follow) model of CNS hyperexcitability (Becker and Hale 1993). These observations strengthened the proposal of the “kindling” hypothesis of alcohol withdrawal that dates back to 1978 (Ballenger and Post 1978; Becker and Hale 1993; Becker 1996, 1998). Kindling is a term previously ascribed to seizure studies in which a stimulus that did not initially provoke a behavioral seizure would eventually do so upon repeated exposures. In the context of alcohol withdrawal it refers to the phenomenon in which exposure to repeated doses of ethanol and subsequent withdrawal slowly ramps up the severity of withdrawal symptoms over time.

Measures of CNS Hyperexcitability

As described, alcohol causes a general increase in inhibitory tone in the CNS. As a consequence of extended inhibition there is a homeostatic response by the neurons in the brain to downregulate inhibitory drive and increase excitatory tone. This occurs through increased numbers of NMDAR, decreases in $GABA_AR$, reduced efficacy of $GABA_AR$ subunits, and changes to the intrinsic excitability of the cell. Koob and others have also suggested that there is an additional learning component to addiction whereby positive associations are made with ethanol

intake as well as negative reinforcement from relieving the symptoms of withdrawal (Koob and Moal 2008; Hyman 2005; Hyman et al. 2006; Torregrossa et al. 2011). These learning associated changes also lead to increases in expression of NMDAR, which may contribute to the shift in the balance of excitation and inhibition in the CNS. Many of the symptoms of alcohol withdrawal syndrome can be attributed to hyperexcitability of the CNS, including seizure. For this discussion, I will avoid discussion of anxiety-like phenotypes and focus instead on physiologic and behavioral measures of CNS excitability *in vivo* related to seizure and electrophysiology.

Electroencephalography (EEG)

Measuring the electrical potentials of wide swaths of neural tissue provides insight into the population wide activity patterns of the CNS. Using implanted electrodes researchers are able to measure population based activity of the brain to identify normal and pathological activity in order to gain an understanding of changes that may occur in the brain as a result of chronic exposure to ethanol. Work from the Godwin lab indicates that EEG can be used to distinguish baseline activity from activity during WD using the sleep EEG. The shift in baseline is indicated by changes in the architecture of the EEG when analyzed with the Fourier transform (Wiggins et al. 2013). Baseline activity of the brain is in part contingent on the genotype of the animals being studied. For example, the DBA/2J mouse, which is resistant to alcohol intake, has characteristic brief spindle episodes (BSE) during baseline whereas the C57/Bl6 mouse, which is alcohol preferring, does not (Ryan 1984). The frequency of occurrence of such

BSE can be used as an EEG indicator of CNS excitability following withdrawal. In C3/He mice (Veatch and Becker 2002) as well as DBA/2J mice (Riegle et al. 2014) the frequency of such BSE increases during withdrawal indicating that the CNS has become hyperexcitable. Furthermore, the appearance of spike and sharp wave (SSW) discharges in Sprague-Dawley rats was identified as being an indicator of CNS hyperexcitability following alcohol WD (Figure 1.3; Veatch and Gonzalez 1996). The increased frequency of such SSWs, here referred to as population spikes (PS), is a consistent EEG measure of CNS hyperexcitability.

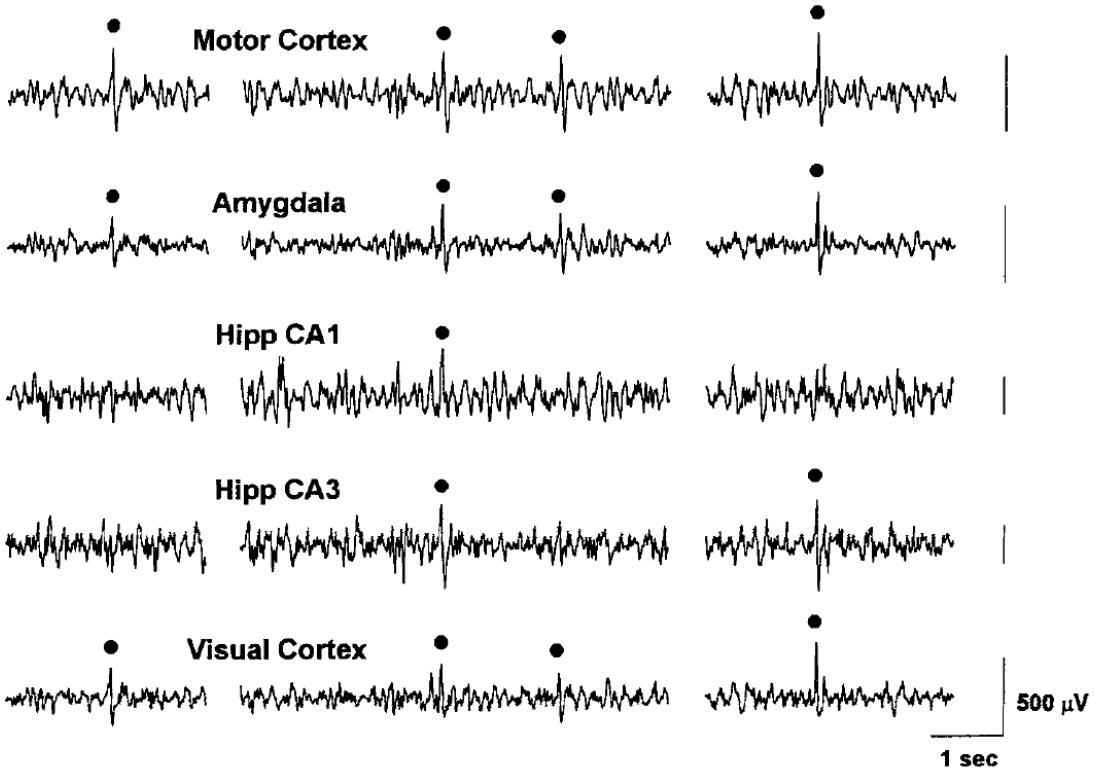

Figure 1.3 EEG measures of CNS hyperexcitability during alcohol withdrawal. Veatch and Gonzalez 1996 measured EEG from male Sprague-Dawley rats and found an increase in SSWs as a result of repeated withdrawal episodes from alcohol. The appearance of this PS as an indicator of CNS hyperexcitability forms the basis for investigation using a newly developed optogenetic model of CNS tone.

Recently, the Godwin lab has developed an optogenetic measure of PS sensitivity that correlates highly with seizure threshold and functions to probe CNS excitability (Chapter 2). From work conducted in our lab we have determined that induction of optogenetically induced seizure following a modified kindling protocol tracks closely with the sensitivity for optogenetically induced PS in a test termed optically-induced Population Discharge Threshold (oPDT; Figure 1.4; Chapter 2). The PS, whether measured with EEG or local field potential (LFP), indicates that a population of neurons has overwhelmed surround inhibition resulting in a high amplitude, highly synchronous discharge of a group of neurons. Veatch and Gonzalez demonstrated that the frequency PS is directly related to the amount of ethanol exposure and the number of withdrawal periods (Veatch and Gonzalez 1996). The morphology and time course of the optically induced PS is analogous to that observed by Veatch and Gonzalez, suggesting that it may prove a good metric for CNS hyperexcitability during withdrawal.

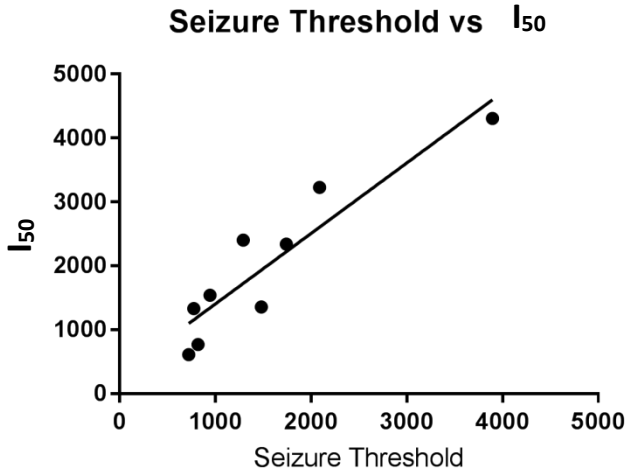

Figure 1.4 Optical seizure threshold plotted against the level at which optical stimulation elicits a PS 50% of the time. The oPDT indicates the sensitivity a population of neurons has to synchronous discharge. The PS that results during oPDT testing is morphologically similar to that observed by Veatch and Gonzalez 1996, and serves as a surrogate metric for seizure susceptibility and CNS tone. These results from 9 animals are significantly correlated $R = 0.9202$; $p<0.0004$.

Audiogenic Seizure

The audiogenic seizure model of alcohol withdrawal relies on the susceptibility of some rodents to have seizures in response to a loud, sudden tone, notably the DBA/2J mouse (Rogawski 2005; Neumann and Collins 1991). The susceptibility of an animal to audiogenic seizure during withdrawal is increased and the method has been used extensively as a model for CNS hyperexcitability during withdrawal representing one of the first models developed (Hunter et al. 1973; Rogawski 2005). Interestingly, there appears to be no electrographic correlate of audiogenic seizure when measured by cortical EEG, which has led researchers to suggest that it is subcortical in origin, likely stemming from inferior colliculus in the brainstem (Maxson and Sze 1976). There have been indications however that audiogenic seizure does engage the hippocampus (Hunter et al. 1973), which is more consistent with typical seizure seen during withdrawal (Jesse et al. 2017).

Handling Induced Convulsion (HIC)

The HIC measure of CNS hyperexcitability was developed by Dora Goldstein in 1972 (Goldstein 1972). The scoring system represents the severity of convulsion associated with experimenter handling of the subject animal (Kosobud and Crabbe 1990; Becker and Hale 1993). This measure of CNS sensitization relies on the response of the experimental subject to being picked up by the tail (Table III).

0	No activity on tail lift, or after gentle 360° spin
1	No activity on tail lift, but facial grimace after 360° spin
1.5	Facial grimace on tail lift
2	Tonic convulsion after 360° spin
3	Tonic/clonic convulsion after 360° spin
4	Tonic convulsion on tail lift
5	Tonic/clonic on tail lift, often delayed by 1 to 2 sec
6	Severe tonic/clonic on tail lift, no delay
7	Severe tonic/clonic prior to tail lift

Table III. Handling induced convulsion scoring table. The HIC score has been a widely used metric for CNS hyperexcitability during ethanol withdrawal. While the mechanism of its effect is unclear it is well described and vetted as an indicator of the severity of withdrawal. There are questions regarding whether there is coincident electrographic seizure during HIC. Modified from Crabbe and Kosobud 1990 in Becker and Hale 1993.

This measure of CNS excitability has been used by a number of labs, and has been well vetted as a metric for WD hyperexcitability (Crabbe et al. 1980, 1991; Veatch and Becker 2002; Riegle et al. 2014). While the metric is a strong indication of CNS hyperexcitability during withdrawal; there have been no studies to date that have measured CNS electrophysiology, either through EEG or LFP, during the HIC (Veatch and Becker 2005). Preliminary studies conducted in the Godwin lab indicate that there is no electrophysiological correlate to the HIC maneuver (Supplemental Video 1). While this does not negate the relevance of HIC to understanding withdrawal hyperexcitability, it does call into question the mechanism of HIC, which has never been fully described (Goldstein 1972; Crabbe et al. 1991; Kosobud and Crabbe 1990; Becker and Hale 1993). Importantly however, HIC scores are sensitive to withdrawal interventions, including traditional pharmacologic intervention with benzodiazepines making the HIC metric a reliable indication of WD severity and efficacy of intervention (Becker and Veatch 2002).

Chemoconvulsants

Administration of drugs known to elicit seizure while an animal is in withdrawal allows researchers to test the susceptiblity of a model animal to seizure (Squires et al. 1984; Szabó et al. 1984; Grant et al. 1990; Kokka et al. 1993). Notably, pentylenetetrazol (PTZ) has been used to measure not only CNS hyperexcitability but also mortality during WD (Kokka et al. 1993; Riegle et al. 2015). When PTZ is applied to alcohol naïve animals it increases the likelihood of optogenetically induced PS occurring at any given level of stimulation indicating that it acts to sensitize the CNS to stimuli related to seizure (Figure 1.5; Chapter 2). In the context of alcohol withdrawal administration of PTZ interacts with the underlying hyperexcitability to cause seizure at doses that would not typically do so. Well controlled dosing of PTZ can then be used to measure the extent of sensitization in the CNS as a result of alcohol withdrawal (Riegle et al. 2014, 2015). Importantly, as shown in Figure 1.5b (Chapter 2) as well as in (Riegle et al. 2014) anticonvulsants reduce the susceptibility for PTZ seizure during withdrawal and the likelihood of a PS at any given optogenetic stimulus intensity after PTZ treatment.

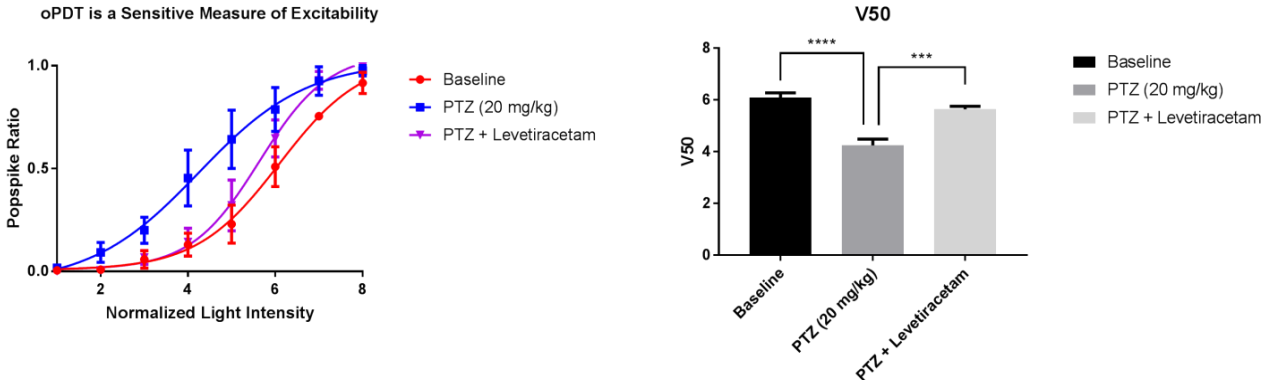

Figure 1.5 optically-induced Population Discharge Threshold (oPDT) testing is a sensitive measure of CNS excitability. A. The oPDT metric was developed in the Godwin lab as a way to probe the balance of excitation and inhibition in a given neural circuit. Here it is shown that treatment with the chemoconvulsant PTZ (blue) shifts the oPDT curve in the direction of hyperexcitability and this can be reversed with the anti-convulsant levetiracetam (PTZ+Levetiracetam; purple). **B.** Plotting the V50, level at which 50% of stimulus presentations elicit PS, demonstrates that the shift in the oPDT curve resulting from PTZ is significant and that Levetiracetam returns this to a baseline level. These results from 6 mice are significant *** = p<0.0001

Alcohol Withdrawal Seizure in the Clinic

A number of molecular changes occur at the level of the neuron in response to chronic exposure to ethanol, which lead to an increase in the excitatory tone of the CNS. These alterations to the GABAR and NMDAR systems as well as modulators of intrinsic excitability occur in response to alcohol induced CNS depression thereby allowing the organism to attain some level of normal neuronal signaling while alcohol is present (Manasco et al. 2012; Jesse et al. 2017). Sudden cessation of alcohol intake reveals these compensatory changes to the CNS in the form of hyperexcitability, as previously described. In human patients, this hyperexcitability often manifests as alcohol withdrawal seizure and occurs in up to 15% of patients with an alcohol use disorder (Mennecier et al. 2008; Chan et al. 2009). These alcohol withdrawal seizures confer significant complications in the treatment of patients with AUDs and warrant immediate and aggressive

treatment as the occurrence of seizure during withdrawal increases risk of mortality related to cardiac arrhythmias (Kattimani and Bharadwaj 2013; Jesse et al. 2017; Holbrook et al. 1999; Mainerova et al. 2015). Seizures in patients with AUD typically occur within 48-72 hours of cessation of alcohol intake (Bråthen et al. 1999; Victor and Brausch 1967). The time course, severity, and ubiquity of seizure during withdrawal necessitates that high-quality treatments be available.

Currently, the gold-standard treatment for alcohol withdrawal seizure is with the benzodiazepine (BZD) class of drugs with dosing dependent on the severity of withdrawal (Jesse et al. 2017; Mainerova et al. 2015). BZDs bind to the $GABA_AR$ to increase Cl^- flux across the membrane, thereby mimicking the effect of ethanol acting to reduce the likelihood of seizure. Interestingly, while using BZDs is effective for preventing withdrawal seizure it has been difficult to determine if BZDs are effective for improving outcomes during alcohol withdrawal in general (Amato et al. 2010; Schaefer and Hafner 2013). In many cases, the use of other anti-convulsant drugs that do not act on the GABAR system have been shown to be effective in reducing alcohol withdrawal seizure (Müller et al. 2010; Barrons and Roberts 2010). However, because those studies have been underpowered and lacked appropriate placebo control there has been no recommendation to use alternatives to BZDs (Minozzi et al. 2010).

High quality pre-clinical investigations of the mechanisms and efficacy of non-BZD based therapy for alcohol withdrawal seizure is essential for improving outcomes in the patient population. While there are a number of available models for CNS hyperexcitability during withdrawal described above, the majority are

limited to measuring behavioral phenotype without corresponding electrophysiology (Crabbe et al. 1991; Veatch and Becker 2005; Maxson and Sze 1976) or recording spontaneous electrographic events without the benefit of experimenter control (Veatch and Gonzalez 1996; Veatch and Becker 2005). A system in which CNS excitability could be probed in a highly controlled manner under a variety of conditions would allow for identifying relevant molecular targets for pharmacologic intervention.

A new model for probing CNS excitability

There appears to be a trade-off between direct measures of CNS hyperexcitability using EEG or LFP (e.g. BSE; PS) and measures of CNS excitability using behavioral methods (e.g. HIC; PTZ). Using methods developed in the Godwin Lab (Klorig and Godwin 2014; D. Klorig, n.d.) we have been able to directly measure electrophysiological correlates of CNS excitability *in vivo* (Chapter 2). By applying subthreshold optogenetic stimuli to discrete target areas of the brain while simultaneously monitoring the electrographic activity of a distributed neural circuit, we are able to probe the balance of excitation and inhibition in a given neural circuit (Figures 1.4 and 1.5). Optogenetics is a technique in which a given cell type is transfected with a light sensitive ion channel (Boyden et al. 2005; Yizhar et al. 2011). This technique allows experimenters to influence with fine temporal and spatial resolution the activity of a discrete population of neurons. Using the transgenic protein Channel-rhodopsin 2 (ChR2) driven by the genetic promoter Calcium/Calmodulin dependent protein kinase II-alpha (CAMKIIα) it is possible to selectively depolarize glutamatergic

neurons (Lein et al. 2007). Work from the Godwin Lab indicates that a specific line of transgenic mouse, Thy1-ChR2(line 18), expresses CAMKIIα promoted ChR2 uniquely in the excitatory neurons of hippocampus (Figure 1.6). Using an optogenetically based modified kindling protocol we are able to reliably induce seizures in these animals while recording from discrete locations of the brain (Chapter 2). Furthermore, by stimulating populations of neurons with very low intensity light we are able to probe the level of excitatory tone in the system (Figure 1.5). This measure, oPDT, allows the experimenter to measure subtle changes in populations of reciprocally connected neurons to determine the level of inhibitory or excitatory drive. By inducing a PS, much like that observed by Veatch and Gonzalez, we detect the threshold at which excitation overwhelms surround inhibition to allow for a population based discharge (Veatch and Gonzalez 1996). oPDT testing relies on the complex interplay of populations of neurons rather than the behavior of a single neuron or the activity patterns of a single area of the brain. As such oPDT testing gives an indication of system wide changes that may occur in response to an experimental intervention. This level of control and distributed observation gives unprecedented insight into the role of

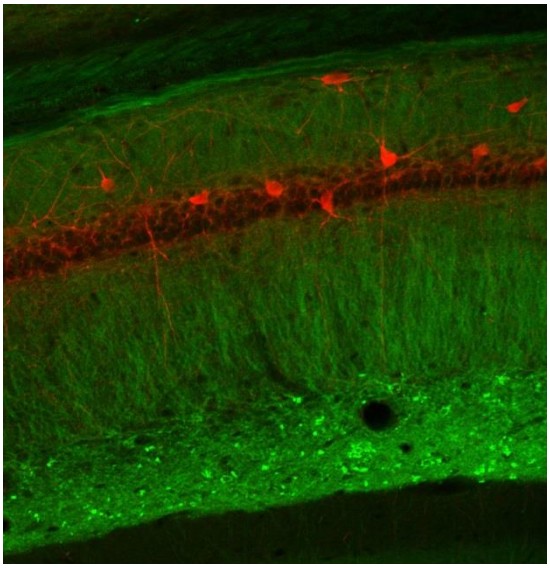

Figure 1.6 Confocal imaging of eYFP (green) in Thy1-ChR2 line 18 mouse co-labeled with parvalbumin antibody (red) indicates specific expression of ChR2 in excitatory neurons of hippocampus. Limited expression of ChR2 to excitatory neurons allows for a high level of control during oPDT testing and optical kindling.

circuit level interactions in CNS excitability. One such area of application for oPDT testing is to the homeostatic changes that occur in response to chronic ethanol exposure. The upregulation of NMDAR and downregulation of $GABA_AR$ as well as changes to modulators of intrinsic excitability may be detectable using oPDT. Additionally, it may be possible to apply targeted pharmacologic intervention *in vivo* to determine which molecular changes are most relevant to treating hyperexcitability during withdrawal and to determine or develop potential novel pharmacotherapies.

Conclusion

Alcohol Use Disorder and Alcohol Withdrawal Syndrome represent complex pathophysiologies with near ubiquitous consequences throughout the CNS. The result of chronic exposure to alcohol is a change in the fundamental balance of neuronal function leading to profound hyperexcitability of the brain. This hyperexcitability is the underlying mechanism through which many of the symptoms of alcohol withdrawal manifest, and is a major contributor to the cycle of alcohol abuse, withdrawal, and relapse. While the molecular changes that occur in response to chronic ethanol exposure are fairly well characterized and some models for withdrawal hyperexcitability are available the field lacks a paradigm in which experimenters have the ability to manipulate and observe the CNS in such a way as to investigate with fine granularity the effect of CNS hyperexcitability on neural circuits. To follow will be a characterization of how optical Population Discharge Threshold testing can be applied to chronic ethanol exposure to determine the extent of hyperexcitability during withdrawal. I will then

apply the newly developed methodology to investigate efficacy of currently used as well as other promising pharmacologic interventions.

References

Allan, Andrea M., and R. Adron Harris. 1987. “Acute and Chronic Ethanol Treatments Alter GABA Receptor-Operated Chloride Channels.” *Pharmacology Biochemistry and Behavior* 27 (4): 665–70. doi:10.1016/0091-3057(87)90192-4.

Allen, Duane, Bernd Fakler, James Maylie, and John P. Adelman. 2007. “Organization and Regulation of Small Conductance Ca2+-Activated K+ Channel Multiprotein Complexes.” *The Journal of Neuroscience: The Official Journal of the Society for Neuroscience* 27 (9): 2369–76. doi:10.1523/JNEUROSCI.3565-06.2007.

Amato, Laura, Silvia Minozzi, Simona Vecchi, and Marina Davoli. 2010. “Benzodiazepines for Alcohol Withdrawal.” *The Cochrane Database of Systematic Reviews*, no. 3 (March): CD005063. doi:10.1002/14651858.CD005063.pub3.

Aryal, Prafulla, Hay Dvir, Senyon Choe, and Paul A. Slesinger. 2009. “A Discrete Alcohol Pocket Involved in GIRK Channel Activation.” *Nature Neuroscience* 12 (8): 988–95. doi:10.1038/nn.2358.

Baliño, Pablo, Raúl Pastor, and Carlos M. G. Aragon. 2010. “Participation of L-Type Calcium Channels in Ethanol-Induced Behavioral Stimulation and Motor Incoordination: Effects of Diltiazem and Verapamil.” *Behavioural Brain Research* 209 (2): 196–204. doi:10.1016/j.bbr.2010.01.036.

Ballenger, J. C., and R. M. Post. 1978. “Kindling as a Model for Alcohol Withdrawal Syndromes.” *The British Journal of Psychiatry: The Journal of Mental Science* 133 (July): 1–14.

Barrons, R., and N. Roberts. 2010. “The Role of Carbamazepine and Oxcarbazepine in Alcohol Withdrawal Syndrome.” *Journal of Clinical Pharmacy and Therapeutics* 35 (2): 153–67. doi:10.1111/j.1365-2710.2009.01098.x.

Becker, H. C. 1996. “The Alcohol Withdrawal ‘kindling’ phenomenon: Clinical and Experimental Findings.” *Alcoholism, Clinical and Experimental Research* 20 (8 Suppl): 121A–124A.

Becker, H C. 1998. “Kindling in Alcohol Withdrawal.” *Alcohol Health and Research World* 22 (1): 25–33.

———. 2000. “Animal Models of Alcohol Withdrawal.” *Alcohol Research & Health: The Journal of the National Institute on Alcohol Abuse and Alcoholism* 24 (2): 105–13.

Becker, H. C., and R. L. Hale. 1993. “Repeated Episodes of Ethanol Withdrawal Potentiate the Severity of Subsequent Withdrawal Seizures: An Animal Model of Alcohol Withdrawal ‘kindling.’” *Alcoholism, Clinical and Experimental Research* 17 (1): 94–98.

Becker, Howard C. 1994. “Positive Relationship between the Number of Prior Ethanol Withdrawal Episodes and the Severity of Subsequent Withdrawal Seizures.” *Psychopharmacology* 116 (1): 26–32.

———. 2008. “Alcohol Dependence, Withdrawal, and Relapse.” *Alcohol Research & Health* 31 (4): 348–61.

Becker, Howard C., and Lynn M. Veatch. 2002. “Effects of Lorazepam Treatment for Multiple Ethanol Withdrawals in Mice.” *Alcoholism, Clinical and Experimental Research* 26 (3): 371–80.

Blednov, Y. A., M. Stoffel, S. R. Chang, and R. A. Harris. 2001. “Potassium Channels as Targets for Ethanol: Studies of G-Protein-Coupled Inwardly Rectifying Potassium Channel 2 (GIRK2) Null Mutant Mice.” *The Journal of Pharmacology and Experimental Therapeutics* 298 (2): 521–30.

Boyden, Edward S., Feng Zhang, Ernst Bamberg, Georg Nagel, and Karl Deisseroth. 2005. “Millisecond-Timescale, Genetically Targeted Optical Control of Neural Activity.” *Nature Neuroscience* 8 (9): 1263–68. doi:10.1038/nn1525.

Bråthen, G., E. Brodtkorb, G. Helde, T. Sand, and G. Bovim. 1999. “The Diversity of Seizures Related to Alcohol Use. A Study of Consecutive Patients.” *European Journal of Neurology* 6 (6): 697–703.

Broadbent, Julie. 2013. “The Role of L-Type Calcium Channels in the Development and Expression of Behavioral Sensitization to Ethanol.” *Neuroscience Letters* 553 (October): 196–200. doi:10.1016/j.neulet.2013.08.008.

Cagetti, Elisabetta, Jing Liang, Igor Spigelman, and Richard W. Olsen. 2003. “Withdrawal from Chronic Intermittent Ethanol Treatment Changes Subunit Composition, Reduces Synaptic Function, and Decreases Behavioral Responses to Positive Allosteric Modulators of $GABA_A$ Receptors.” *Molecular Pharmacology* 63 (1): 53–64. doi:10.1124/mol.63.1.53.

Cardoso, R. A., S. J. Brozowski, L. E. Chavez-Noriega, M. Harpold, C. F. Valenzuela, and R. A. Harris. 1999. “Effects of Ethanol on Recombinant Human Neuronal Nicotinic Acetylcholine Receptors Expressed in Xenopus Oocytes.” *The Journal of Pharmacology and Experimental Therapeutics* 289 (2): 774–80.

Chan, Gar Ming, Robert S. Hoffman, Jeffrey A. Gold, Paula J. Whiteman, Lewis R. Goldfrank, and Lewis S. Nelson. 2009. “Racial Variations in the Incidence of Severe Alcohol Withdrawal.” *Journal of Medical Toxicology: Official Journal of the American College of Medical Toxicology* 5 (1): 8–14.

Crabbe, J. C., J. S. Janowsky, E. R. Young, and H. Rigter. 1980. “Handling Induced Convulsions in Twenty Inbred Strains of Mice.” *Substance and Alcohol Actions/Misuse* 1 (2): 159–63.

Crabbe, J. C., C. D. Merrill, and J. K. Belknap. 1991. “Effects of Convulsants on Handling-Induced Convulsions in Mice Selected for Ethanol Withdrawal Severity.” *Brain Research* 550 (1): 1–6.

Curtis, Marco de, and Massimo Avoli. 2016. “GABAergic Networks Jump-Start Focal Seizures.” *Epilepsia* 57 (5): 679–87. doi:10.1111/epi.13370.

Darcq, Emmanuel, Sami Ben Hamida, Su Wu, Khanky Phamluong, Viktor Kharazia, Jian Xu, Paul Lombroso, and Dorit Ron. 2014. “Inhibition of Striatal-Enriched Tyrosine Phosphatase 61 in the Dorsomedial Striatum Is Sufficient to Increased Ethanol Consumption.” *Journal of Neurochemistry* 129 (6): 1024–34. doi:10.1111/jnc.12701.

Davies, D. L., and R. L. Alkana. 2001a. “Ethanol Enhances GABAA Receptor Function in Short Sleep and Long Sleep Mouse Brain Membranes.” *Alcoholism, Clinical and Experimental Research* 25 (3): 478–83.

———. 2001b. “Direct Evidence for a Cause-Effect Link between Ethanol Potentiation of GABA(A) Receptor Function and Intoxication from Hyperbaric Studies in C57, LS, and SS Mice.” *Alcoholism, Clinical and Experimental Research* 25 (8): 1098–1106.

Davies, Martin. 2003. “The Role of GABAA Receptors in Mediating the Effects of Alcohol in the Central Nervous System.” *Journal of Psychiatry and Neuroscience* 28 (4): 263.

Diagnostic and Statistical Manual of Mental Disorders. 2013. 5th ed. American Psychiatric Association.

Faber, E. S. L. 2010. “Functional Interplay between NMDA Receptors, SK Channels and Voltage-Gated Ca2+ Channels Regulates Synaptic Excitability in the Medial Prefrontal Cortex.” *The Journal of Physiology* 588 (Pt 8): 1281–92. doi:10.1113/jphysiol.2009.185645.

Faber, E. S. Louise, Andrew J. Delaney, John M. Power, Petra L. Sedlak, James W. Crane, and Pankaj Sah. 2008. “Modulation of SK Channel Trafficking by Beta Adrenoceptors Enhances Excitatory Synaptic Transmission and Plasticity in the Amygdala.” *The Journal of Neuroscience: The Official Journal of the Society for Neuroscience* 28 (43): 10803–13. doi:10.1523/JNEUROSCI.1796-08.2008.

Fritschy, Jean-Marc, and Patrizia Panzanelli. 2014. “GABAA Receptors and Plasticity of Inhibitory Neurotransmission in the Central Nervous System.” *The European Journal of Neuroscience* 39 (11): 1845–65. doi:10.1111/ejn.12534.

Gibb, Stuart L., Sami Ben Hamida, Maria Fe Lanfranco, and Dorit Ron. 2011. “Ethanol-Induced Increase in Fyn Kinase Activity in the Dorsomedial Striatum Is Associated with Subcellular Redistribution of Protein Tyrosine Phosphatase α.” *Journal of Neurochemistry* 119 (4): 879–89. doi:10.1111/j.1471-4159.2011.07485.x.

Goldstein, Dora B. 1972. “Relationship of Alcohol Dose to Intensity of Withdrawal Signs in Mice.” *Journal of Pharmacology and Experimental Therapeutics* 180 (2): 203–215.

Graef, J. D., T. W. Huitt, B. K. Nordskog, J. H. Hammarback, and D. W. Godwin. 2011. “Disrupted Thalamic T-Type Ca2+ Channel Expression and Function During Ethanol Exposure and Withdrawal.” *Journal of Neurophysiology* 105 (2): 528–40. doi:10.1152/jn.00424.2010.

Graef, John D, and Dwayne W Godwin. 2010. “Intrinsic Plasticity in Acquired Epilepsy: Too Much of a Good Thing?” *The Neuroscientist: A Review Journal Bringing Neurobiology, Neurology and Psychiatry*, April. doi:10.1177/1073858409358776.

Grant, K. A., P. Valverius, M. Hudspith, and B. Tabakoff. 1990. “Ethanol Withdrawal Seizures and the NMDA Receptor Complex.” *European Journal of Pharmacology* 176 (3): 289–96.

Grobin, A. C., D. B. Matthews, L. L. Devaud, and A. L. Morrow. 1998. “The Role of GABA(A) Receptors in the Acute and Chronic Effects of Ethanol.” *Psychopharmacology* 139 (1–2): 2–19.

Holbrook, A. M., R. Crowther, A. Lotter, C. Cheng, and D. King. 1999. “Diagnosis and Management of Acute Alcohol Withdrawal.” *CMAJ: Canadian Medical Association Journal = Journal de l’Association Medicale Canadienne* 160 (5): 675–80.

Hunter, B. E., C. A. Boast, D. W. Walker, and S. F. Zornetzer. 1973. “Alcohol Withdrawal Syndrome in Rats: Neural and Behavioral Correlates.” *Pharmacology, Biochemistry, and Behavior* 1 (6): 719–25.

Hyman, Steven E. 2005. “Addiction: A Disease of Learning and Memory.” *The American Journal of Psychiatry* 162 (8): 1414–22. doi:10.1176/appi.ajp.162.8.1414.

Hyman, Steven E., Robert C. Malenka, and Eric J. Nestler. 2006. “Neural Mechanisms of Addiction: The Role of Reward-Related Learning and Memory.” *Annual Review of Neuroscience* 29: 565–98. doi:10.1146/annurev.neuro.29.051605.113009.

Jesse, S., G. Bråthen, M. Ferrara, M. Keindl, E. Ben-Menachem, R. Tanasescu, E. Brodtkorb, M. Hillbom, M.a. Leone, and A.c. Ludolph. 2017. “Alcohol Withdrawal Syndrome: Mechanisms, Manifestations, and Management.” *Acta Neurologica Scandinavica* 135 (1): 4–16. doi:10.1111/ane.12671.

Johnson, Bankole A., George F. Koob, Marc A. Schuckit, Barbara J. Mason, and Nassima Ait-Daoud. 2006. “Understanding and Treating Alcohol Dependence.” *Alcoholism: Clinical and Experimental Research* 30 (3): 567–84. doi:10.1111/j.1530-0277.2005.00066.x.

Johnson, R.R., X. Jiang, and A. Burkhalter. 1996. “Regional and Laminar Differences in Synaptic Localization of NMDA Receptor Subunit NR1 Splice Variants in Rat Visual Cortex and Hippocampus.” *J Comp Neurol.* 368 (3): 335–55.

Kalluri, Haviryaji S. G, Ashok K Mehta, and Maharaj K Ticku. 1998. “Up-Regulation of NMDA Receptor Subunits in Rat Brain Following Chronic Ethanol Treatment.” *Molecular Brain Research* 58 (1–2): 221–24. doi:10.1016/S0169-328X(98)00112-0.

Kang, M. H., I. Spigelman, and R. W. Olsen. 1998. “Alteration in the Sensitivity of GABA(A) Receptors to Allosteric Modulatory Drugs in Rat Hippocampus after Chronic Intermittent Ethanol Treatment.” *Alcoholism, Clinical and Experimental Research* 22 (9): 2165–73.

Kang, M., I. Spigelman, D. W. Sapp, and R. W. Olsen. 1996. “Persistent Reduction of GABA(A) Receptor-Mediated Inhibition in Rat Hippocampus after Chronic Intermittent Ethanol Treatment.” *Brain Research* 709 (2): 221–28.

Kattimani, Shivanand, and Balaji Bharadwaj. 2013. “Clinical Management of Alcohol Withdrawal: A Systematic Review.” *Industrial Psychiatry Journal* 22 (2): 100–108. doi:10.4103/0972-6748.132914.

Klorig, David. n.d. United States Patent Application: 9151.146PR - IMPLANTABLE CANNULA CONNECTOR SYSTEMS HAVING MAGNETIC PORTIONS THEREON AND RELATED METHODS, filed 2010 2010.

Klorig, David C., and Dwayne W. Godwin. 2014. “A Magnetic Rotary Optical Fiber Connector for Optogenetic Experiments in Freely Moving Animals.” *Journal of Neuroscience Methods* 227 (April): 132–39. doi:10.1016/j.jneumeth.2014.02.013.

Kobayashi, Toru, Kazutaka Ikeda, Hiroshi Kojima, Hiroaki Niki, Ryoji Yano, Tohru Yoshioka, and Toshiro Kumanishi. 1999. “Ethanol Opens G-Protein-Activated Inwardly Rectifying K+ Channels.” *Nature Neuroscience* 2 (12): 1091–97. doi:10.1038/16019.

Kokka, N., D. W. Sapp, A. M. Taylor, and R. W. Olsen. 1993. “The Kindling Model of Alcohol Dependence: Similar Persistent Reduction in Seizure Threshold to Pentylenetetrazol in Animals Receiving Chronic Ethanol or Chronic Pentylenetetrazol.” *Alcoholism, Clinical and Experimental Research* 17 (3): 525–31.

Koob, George F., and Michel Le Moal. 2008. “Addiction and the Brain Antireward System.” *Annual Review of Psychology* 59 (1): 29–53. doi:10.1146/annurev.psych.59.103006.093548.

Kosobud, A. E., and J. C. Crabbe. 1990. “Genetic Correlations among Inbred Strain Sensitivities to Convulsions Induced by 9 Convulsant Drugs.” *Brain Research* 526 (1): 8–16.

Kourrich, Saïd, Donna J. Calu, and Antonello Bonci. 2015. “Intrinsic Plasticity: An Emerging Player in Addiction.” *Nature Reviews. Neuroscience* 16 (3): 173–84. doi:10.1038/nrn3877.

Lein, Ed S., Michael J. Hawrylycz, Nancy Ao, Mikael Ayres, Amy Bensinger, Amy Bernard, Andrew F. Boe, et al. 2007. “Genome-Wide Atlas of Gene Expression in the Adult Mouse Brain.” *Nature* 445 (7124): 168–76. doi:10.1038/nature05453.

Liang, Jing, Asha Suryanarayanan, Alana Abriam, Bradley Snyder, Richard W. Olsen, and Igor Spigelman. 2007. “Mechanisms of Reversible $GABA_A$ Receptor Plasticity after Ethanol Intoxication.” *Journal of Neuroscience* 27 (45): 12367–77. doi:10.1523/JNEUROSCI.2786-07.2007.

Lin, Mike T., Rafael Luján, Masahiko Watanabe, John P. Adelman, and James Maylie. 2008. “SK2 Channel Plasticity Contributes to LTP at Schaffer Collateral-CA1 Synapses.” *Nature Neuroscience* 11 (2): 170–77. doi:10.1038/nn2041.

Lomazzi, Marta, Paul A. Slesinger, and Christian Lüscher. 2008. “Addictive Drugs Modulate GIRK-Channel Signaling by Regulating RGS Proteins.” *Trends in Pharmacological Sciences* 29 (11): 544–49. doi:10.1016/j.tips.2008.07.011.

Lovinger, D. M., G. White, and F. F. Weight. 1989. “Ethanol Inhibits NMDA-Activated Ion Current in Hippocampal Neurons.” *Science (New York, N.Y.)* 243 (4899): 1721–24.

Lüscher, Christian, and Paul A. Slesinger. 2010. “Emerging Roles for G Protein-Gated Inwardly Rectifying Potassium (GIRK) Channels in Health and Disease.” *Nature Reviews Neuroscience* 11 (5): 301–15. doi:10.1038/nrn2834.

Mahmoudi, M., M. H. Kang, N. Tillakaratne, A. J. Tobin, and R. W. Olsen. 1997. “Chronic Intermittent Ethanol Treatment in Rats Increases GABA(A) Receptor alpha4-Subunit Expression: Possible Relevance to Alcohol Dependence.” *Journal of Neurochemistry* 68 (6): 2485–92.

Mainerova, Barbora, Jan Prasko, Klara Latalova, Karel Axmann, Monika Cerna, Rostislav Horacek, and Romana Bradacova. 2015. “Alcohol Withdrawal Delirium - Diagnosis, Course and Treatment.” *Biomedical Papers of the Medical Faculty of the University Palacky, Olomouc, Czechoslovakia* 159 (1): 44–52. doi:10.5507/bp.2013.089.

Manasco, Anton, Shannon Chang, Joseph Larriviere, L. Lee Hamm, and Marcia Glass. 2012. “Alcohol Withdrawal.” *Southern Medical Journal* 105 (11): 607–12. doi:10.1097/SMJ.0b013e31826efb2d.

Maxson, S. C., and P. Y. Sze. 1976. “Electroencephalographic Correlates of Audiogenic Seizures during Ethanol Withdrawal in Mice.” *Psychopharmacology* 47 (1): 17–20.

Mayford, Mark, Steven A. Siegelbaum, and Eric R. Kandel. 2012. “Synapses and Memory Storage.” *Cold Spring Harbor Perspectives in Biology* 4 (6). doi:10.1101/cshperspect.a005751.

McKernan, R. M., T. W. Rosahl, D. S. Reynolds, C. Sur, K. A. Wafford, J. R. Atack, S. Farrar, et al. 2000. “Sedative but Not Anxiolytic Properties of Benzodiazepines Are Mediated by the GABA(A) Receptor alpha1 Subtype.” *Nature Neuroscience* 3 (6): 587–92. doi:10.1038/75761.

Mennecier, D., M. Thomas, P. Arvers, D. Corberand, L. Sinayoko, S. Bonnefoy, F. Harnois, and C. Thiolet. 2008. “Factors Predictive of Complicated or Severe Alcohol Withdrawal in Alcohol Dependent Inpatients.” *Gastroenterologie Clinique Et Biologique* 32 (8–9): 792–97. doi:10.1016/j.gcb.2008.06.004.

Minozzi, Silvia, Laura Amato, Simona Vecchi, and Marina Davoli. 2010. “Anticonvulsants for Alcohol Withdrawal.” *The Cochrane Database of Systematic Reviews*, no. 3 (March): CD005064. doi:10.1002/14651858.CD005064.pub3.

Mori, H., and M. Mishina. 1995. “Structure and Function of the NMDA Receptor Channel.” *Neuropharmacology* 34 (10): 1219–37. doi:10.1016/0028-3908(95)00109-J.

Morisot, N., and D. Ron. 2017. “Alcohol-Dependent Molecular Adaptations of the NMDA Receptor System.” *Genes, Brain and Behavior* 16 (1): 139–48. doi:10.1111/gbb.12363.

Morrow, A. Leslie, Pascale Montpied, Anne Lingford-Hughes, and Steven M. Paul. 1990. “Chronic Ethanol and Pentobarbital Administration in the Rat: Effects on GABAA Receptor Function and Expression in Brain.” *Alcohol*, National Institute on Alcohol Abuse and Alcoholism NBRB Workshop on the Neurochemical Bases of Alcohol-Related Behavior, 7 (3): 237–44. doi:10.1016/0741-8329(90)90012-2.

Mu, Jian, W. Breckinridge Carden, Nuwan C. Kurukulasuriya, Georgia M. Alexander, and Dwayne W. Godwin. 2003. “Ethanol Influences on Native T-Type Calcium Current in Thalamic Sleep Circuitry.” *The Journal of Pharmacology and Experimental Therapeutics* 307 (1): 197–204. doi:10.1124/jpet.103.053272.

Mulholland, Patrick J. 2012. “K(Ca)2 Channels: Novel Therapeutic Targets for Treating Alcohol Withdrawal and Escalation of Alcohol Consumption.” *Alcohol (Fayetteville, N.Y.)* 46 (4): 309–15. doi:10.1016/j.alcohol.2011.11.002.

Mulholland, Patrick J., Howard C. Becker, John J. Woodward, and L. Judson Chandler. 2011. “Small Conductance Calcium-Activated Potassium Type 2 Channels Regulate Alcohol-Associated Plasticity of Glutamatergic Synapses.” *Biological Psychiatry* 69 (7): 625–32. doi:10.1016/j.biopsych.2010.09.025.

Müller, C. A., M. Schäfer, S. Schneider, H. M. Heimann, A. Hinzpeter, K. Volkmar, A. Förg, A. Heinz, and J. Hein. 2010. “Efficacy and Safety of Levetiracetam for Outpatient Alcohol Detoxification.” *Pharmacopsychiatry* 43 (5): 184–89. doi:10.1055/s-0030-1249098.

Nayeem, N., T. P. Green, I. L. Martin, and E. A. Barnard. 1994. “Quaternary Structure of the Native GABAA Receptor Determined by Electron Microscopic Image Analysis.” *Journal of Neurochemistry* 62 (2): 815–18.

Nelson, T. E., C. L. Ur, and D. L. Gruol. 2005. “Chronic Intermittent Ethanol Exposure Enhances NMDA-Receptor-Mediated Synaptic Responses and NMDA Receptor Expression in Hippocampal CA1 Region.” *Brain Research* 1048 (1–2): 69–79. doi:10.1016/j.brainres.2005.04.041.

Neumann, P E, and R L Collins. 1991. “Genetic Dissection of Susceptibility to Audiogenic Seizures in Inbred Mice.” *Proceedings of the National Academy of Sciences of the United States of America* 88 (12): 5408–12.

Nordskog, B. K., J. A. Hammarback, and D. W. Godwin. 2006. “Diurnal Gene Expression Patterns of T-Type Calcium Channels and Their Modulation by Ethanol.” *Neuroscience* 141 (3): 1365–73. doi:10.1016/j.neuroscience.2006.04.031.

Olsen, Richard W., and Werner Sieghart. 2009. “GABA A Receptors: Subtypes Provide Diversity of Function and Pharmacology.” *Neuropharmacology* 56 (1): 141–48. doi:10.1016/j.neuropharm.2008.07.045.

Petrie, J., D. W. Sapp, R. F. Tyndale, M. K. Park, M. Fanselow, and R. W. Olsen. 2001. “Altered Gabaa Receptor Subunit and Splice Variant Expression in Rats Treated with Chronic Intermittent Ethanol.” *Alcoholism, Clinical and Experimental Research* 25 (6): 819–28.

Pfaffinger, P. J., J. M. Martin, D. D. Hunter, N. M. Nathanson, and B. Hille. 1985. “GTP-Binding Proteins Couple Cardiac Muscarinic Receptors to a K Channel.” *Nature* 317 (6037): 536–38.

Riedel, Gernot, Bettina Platt, and Jacques Micheau. 2003. “Glutamate Receptor Function in Learning and Memory.” *Behavioural Brain Research* 140 (1): 1–47. doi:10.1016/S0166-4328(02)00272-3.

Riegle, Melissa A., Melissa L. Masicampo, Erin H. Caulder, and Dwayne W. Godwin. 2014. “Ethosuximide Reduces Electrographical and Behavioral Correlates of Alcohol Withdrawal Seizure in DBA/2J Mice.” *Alcohol (Fayetteville, N.Y.)* 48 (5): 445–53. doi:10.1016/j.alcohol.2014.01.010.

Riegle, Melissa A., Melissa L. Masicampo, Hong Qu Shan, Victoria Xu, and Dwayne W. Godwin. 2015. “Ethosuximide Reduces Mortality and Seizure Severity in Response to Pentylenetetrazole Treatment During Ethanol Withdrawal.” *Alcohol and Alcoholism (Oxford, Oxfordshire)* 50 (5): 501–8. doi:10.1093/alcalc/agv033.

Rogawski, Michael A. 2005. “Update on the Neurobiology of Alcohol Withdrawal Seizures.” *Epilepsy Currents* 5 (6): 225. doi:10.1111/j.1535-7511.2005.00071.x.

Ron, Dorit, and Segev Barak. 2016. “Molecular Mechanisms Underlying Alcohol-Drinking Behaviours.” *Nature Reviews. Neuroscience* 17 (9): 576–91. doi:10.1038/nrn.2016.85.

Rudolph, Uwe, Florence Crestani, Dietmar Benke, Ina Brunig, and et al. 1999. “Benzodiazepine Actions Mediated by Specific Gamma-Aminobutyric acidA Receptor Subtypes.” *Nature; London* 401 (6755): 796–800. doi:http://dx.doi.org.go.libproxy.wakehealth.edu/10.1038/44579.

Ryan, Lawrence J. 1984. “Characterization of Cortical Spindles in DBA/2 and C57BL/6 Inbred Mice.” *Brain Research Bulletin* 13 (4): 549–58. doi:10.1016/0361-9230(84)90037-6.

Schaefer, Timothy J., and John W. Hafner. 2013. “Are Benzodiazepines Effective for Alcohol Withdrawal?” *Annals of Emergency Medicine* 62 (1): 34–35. doi:10.1016/j.annemergmed.2012.03.017.

Shan, Hong Qu, James A. Hammarback, and Dwayne W. Godwin. 2013. “Ethanol Inhibition of a T-Type Ca^{2}+ Channel through Activity of Protein Kinase C.” *Alcoholism, Clinical and Experimental Research* 37 (8): 1333–42. doi:10.1111/acer.12098.

Simms, Brett A., and Gerald W. Zamponi. 2014. “Neuronal Voltage-Gated Calcium Channels: Structure, Function, and Dysfunction.” *Neuron* 82 (1): 24–45. doi:10.1016/j.neuron.2014.03.016.

Sipilä, Sampsa T., Kristiina Huttu, Ivan Soltesz, Juha Voipio, and Kai Kaila. 2005. “Depolarizing GABA Acts on Intrinsically Bursting Pyramidal Neurons to Drive Giant Depolarizing Potentials in the Immature Hippocampus.” *The Journal of Neuroscience: The Official Journal of the Society for Neuroscience* 25 (22): 5280–89. doi:10.1523/JNEUROSCI.0378-05.2005.

Smith, G. B., and R. W. Olsen. 1995. “Functional Domains of GABAA Receptors.” *Trends in Pharmacological Sciences* 16 (5): 162–68.

Snell, L. D., K. R. Nunley, R. L. Lickteig, M. D. Browning, B. Tabakoff, and P. L. Hoffman. 1996. “Regional and Subunit Specific Changes in NMDA Receptor mRNA and Immunoreactivity in Mouse Brain Following Chronic Ethanol Ingestion.” *Brain Research. Molecular Brain Research* 40 (1): 71–78.

Spitzer, Nicholas C. 2010. “How GABA Generates Depolarization.” *The Journal of Physiology* 588 (Pt 5): 757–58. doi:10.1113/jphysiol.2009.183574.

Squires, R. F., E. Saederup, J. N. Crawley, P. Skolnick, and S. M. Paul. 1984. “Convulsant Potencies of Tetrazoles Are Highly Correlated with Actions on GABA/Benzodiazepine/Picrotoxin Receptor Complexes in Brain.” *Life Sciences* 35 (14): 1439–44.

Stephens, D. N., S. L. King, J. J. Lambert, D. Belelli, and T. Duka. 2017. “GABAA Receptor Subtype Involvement in Addictive Behaviour.” *Genes, Brain and Behavior* 16 (1): 149–84. doi:10.1111/gbb.12321.

Szabó, G., G. L. Kovács, and G. Telegdy. 1984. “Increased Sensitivity to Picrotoxin as an Index of Physical Dependence on Alcohol in the Mouse.” *Drug and Alcohol Dependence* 14 (2): 187–95.

Tatebayashi, H., H. Motomura, and T. Narahashi. 1998. “Alcohol Modulation of Single GABA(A) Receptor-Channel Kinetics.” *Neuroreport* 9 (8): 1769–75.

Torregrossa, Mary M., Philip R. Corlett, and Jane R. Taylor. 2011. “Aberrant Learning and Memory in Addiction.” *Neurobiology of Learning and Memory* 96 (4): 609–23. doi:10.1016/j.nlm.2011.02.014.

Traynelis, Stephen F., Lonnie P. Wollmuth, Chris J. McBain, Frank S. Menniti, Katie M. Vance, Kevin K. Ogden, Kasper B. Hansen, Hongjie Yuan, Scott J. Myers, and Ray Dingledine. 2010. “Glutamate Receptor Ion Channels: Structure, Regulation, and Function.” *Pharmacological Reviews* 62 (3): 405–96. doi:10.1124/pr.109.002451.

Twombly, D. A., M. D. Herman, C. H. Kye, and T. Narahashi. 1990. “Ethanol Effects on Two Types of Voltage-Activated Calcium Channels.” *The Journal of Pharmacology and Experimental Therapeutics* 254 (3): 1029–37.

Valenzuela, C. F., R. A. Cardoso, M. J. Wick, J. L. Weiner, T. V. Dunwiddie, and R. A. Harris. 1998. “Effects of Ethanol on Recombinant Glycine Receptors Expressed in Mammalian Cell Lines.” *Alcoholism, Clinical and Experimental Research* 22 (5): 1132–36.

Veatch, L. M., and L. P. Gonzalez. 1996. “Repeated Ethanol Withdrawal Produces Site-Dependent Increases in EEG Spiking.” *Alcoholism, Clinical and Experimental Research* 20 (2): 262–67.

Veatch, Lynn M., and Howard C. Becker. 2002. “Electrographic and Behavioral Indices of Ethanol Withdrawal Sensitization.” *Brain Research* 946 (2): 272–82. doi:10.1016/S0006-8993(02)02895-0.

———. 2005. “Lorazepam and MK-801 Effects on Behavioral and Electrographic Indices of Alcohol Withdrawal Sensitization.” *Brain Research* 1065 (1–2): 92–106. doi:10.1016/j.brainres.2005.10.047.

Victor, M., and C. Brausch. 1967. “The Role of Abstinence in the Genesis of Alcoholic Epilepsy.” *Epilepsia* 8 (1): 1–20.

Walter, H. J., and R. O. Messing. 1999. “Regulation of Neuronal Voltage-Gated Calcium Channels by Ethanol.” *Neurochemistry International* 35 (2): 95–101.

Wang, Jun, Maria Fe Lanfranco, Stuart L. Gibb, and Dorit Ron. 2011. “Ethanol-Mediated Long-Lasting Adaptations of the NR2B-Containing NMDA Receptors in the Dorsomedial Striatum.” *Channels (Austin, Tex.)* 5 (3): 205–9.

Wang, Jun, Maria Fe Lanfranco, Stuart L. Gibb, Quinn V. Yowell, Sebastien Carnicella, and Dorit Ron. 2010. “Long-Lasting Adaptations of the NR2B-Containing NMDA Receptors in the Dorsomedial Striatum Play a Crucial Role in Alcohol Consumption and Relapse.” *The Journal of Neuroscience: The Official Journal of the Society for Neuroscience* 30 (30): 10187–98. doi:10.1523/JNEUROSCI.2268-10.2010.

White, Geoffrey, David M. Lovinger, and Forrest F. Weight. 1990. “Ethanol Inhibits NMDA-Activated Current but Does Not Alter GABA-Activated Current in an Isolated Adult Mammalian Neuron.” *Brain Research* 507 (2): 332–36. doi:10.1016/0006-8993(90)90292-J.

Wiggins, Walter F., John D. Graef, Tiffany W. Huitt, and Dwayne W. Godwin. 2013. "Ethosuximide Reduces Ethanol Withdrawal-Mediated Disruptions in Sleep-Related EEG Patterns." *Alcoholism, Clinical and Experimental Research* 37 (3): 372–82. doi:10.1111/j.1530-0277.2012.01938.x.

Yizhar, Ofer, Lief E. Fenno, Thomas J. Davidson, Murtaza Mogri, and Karl Deisseroth. 2011. "Optogenetics in Neural Systems." *Neuron* 71 (1): 9–34. doi:10.1016/j.neuron.2011.06.004.

Chapter 2

Optogenetically Induced Population Discharge Threshold (oPDT) as a Sensitive Measure of Excitability

Klorig, D.C., Alberto, G., Godwin, D.W.

Abstract

Current pre-clinical methods for characterizing the efficacy of anti-epileptic drugs and/or surgical interventions rely on the ability to prevent, delay, or lessen the severity of artificially induced seizures, either as a result of electric shock or the administration of pro-convulsant drugs. These measures exhibit a large degree of baseline variability, requiring large numbers of replicates to achieve the statistical power required to demonstrate efficacy. We have developed a new method to detect small shifts in network excitability (e.g. seizure susceptibility) using optogenetically induced population discharge thresholds (oPDT), in mice, as a surrogate for seizure. By combining optogenetic stimulation of the hippocampus with chronic multi-site recording in peri-hippocampal structures of awake behaving animals, we can induce and detect abnormal network wide population discharges that mirror spontaneous interictal spikes in terms of waveform shape and latency. By varying the intensity of light we can compare the magnitude of the optogenetically mediated current to the probability of population discharge. This probability curve is well fit by a Boltzmann curve, allowing calculation of a V50. Here we demonstrate that the V50 is a sensitive and reliable metric of network excitability. Manipulations known to increase excitability such as chronic EtOH withdrawal, or sub-convulsive doses (20 mg/kg) of pentylenetetrazol (PTZ) produce a leftward shift in the curve compared to baseline. Anti-epileptic drugs, in combination with pro-convulsive manipulations, produce a rightward shift to baseline. oPDT baselines are remarkably stable over time, allowing for within-subject experimental design with multiple

pharmacological manipulations, reducing the total number of animals needed. Furthermore we have fully characterized the close relationship between the oPDT and optogenetically induced seizure thresholds, thus demonstrating that the oPDT is a useful surrogate. The oPDT is the first example of a sensitive measure of subconvulsive network excitability, with broad applicability to a number of areas of investigation.

Introduction

The basic pathophysiological event in epilepsy is the synchronous population discharge (de Curtis and Avanzini, 2001). The electrographic signature of this event is a high amplitude interictal spike detectable in EEG recordings (Chatrian et al., 1974; Gotman, 1980), and rhythmic population discharges underlie seizure itself (Adrian and Matthews, 1934; Avoli et al., 2002; Miles et al., 1984).

Synchronous firing is also a feature of normally functioning brain circuitry. However, it has been estimated that the most synchronous non-pathological events involves between 10 and 15% of a local population firing (Buzsaki, 2006). When the size, strength, or timing of a synchronous event exceeds that of the normal range, and compensatory mechanisms fail, a pathological population discharge can result (Connors, 1984). Optogenetic methods, because they involve simultaneous modulation of a population of cells, are well suited to exploring the effects of synchronous firing on networks of cells (Khoshkhoo et al., 2017; Osawa et al., 2013).

We have developed a method using optogenetic light dose-response curves that allows for sensitive measurement of the population discharge threshold in awake behaving animals. Furthermore, we show that the optogenetic population discharge threshold (oPDT) is a useful surrogate for the seizure threshold (without the need to induce seizure) and thus allows for a sensitive measurement of network excitability.

Results

In order to explore network propagation of seizure and spike activity, we developed a multi-site satellite array system consisting of individually placed microwires in perihippocampal structures. Targets include prefrontal cortex (PFC), antero-medial thalamus (AMT), entorhinal cortex (Ent), dentate gyrus (DG), subiculum (Sub), hippocampal area CA3 (CA3), and area CA1 bilaterally (CA1-L and CA1-R) (Figure 1a and S3). A fiber optic was placed 0.2 mm above CA1 for optogenetic stimulation and coupled to a high quality LED light source with a magnetic rotary fiber coupler (Klorig and Godwin, 2014b). We used Thy1 line 18 mice which primarily express ChR2 in area CA1, subiculum, and layer 5 of cortex (Arenkiel et al., 2007). In area CA1, expression is specific to excitatory pyramidal neurons and is concentrated in calbindin-negative cells in the deep pyramidal cell sublayer (Fig. 1a,c and S2). These mice can be bred as homozygotes, which ensures consistent expression levels and patterns from animal to animal, a significant advantage.

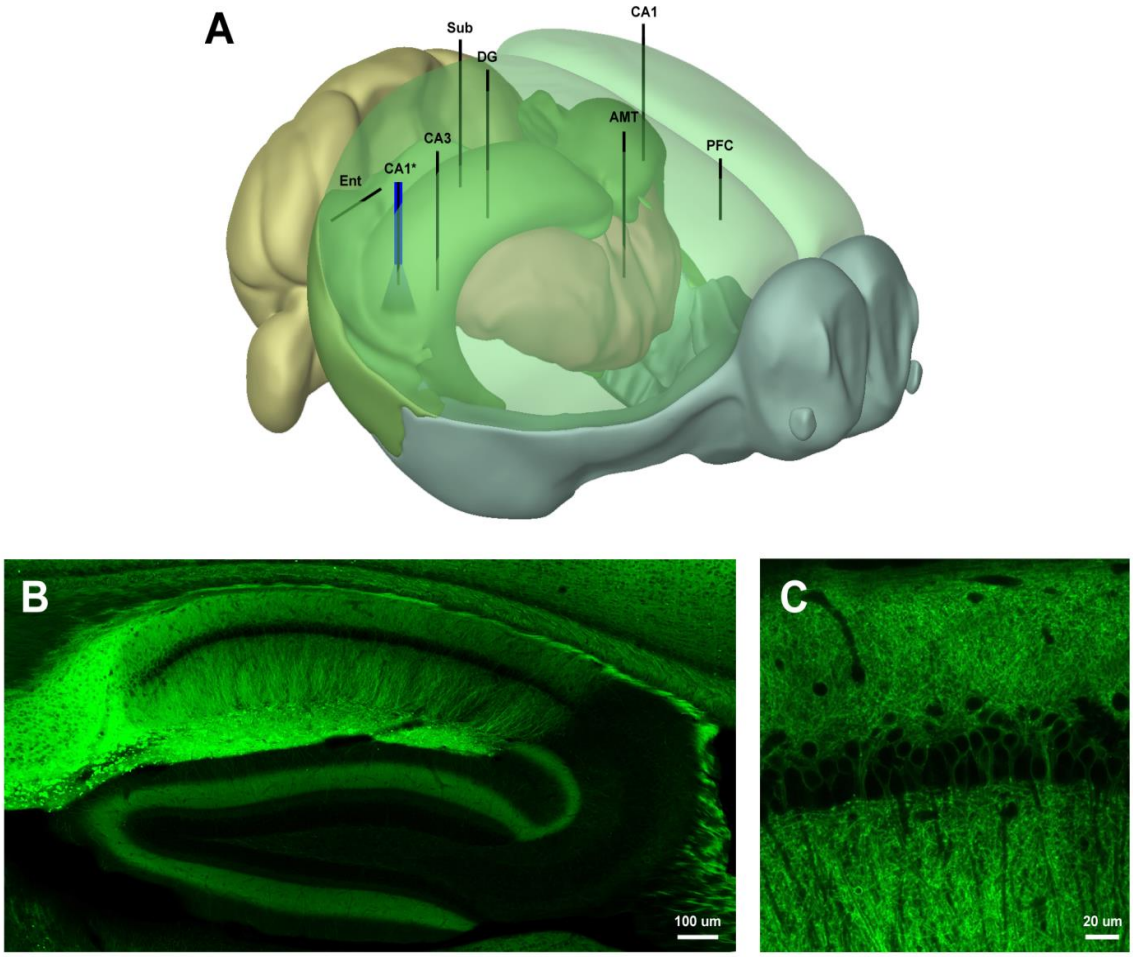

Figure 1: Electrode placement and expression patterns in the Thy1-ChR2 (line 18) mouse. A. Schematic showing the placement of the electrode array and fiber optics. 3D model was generated using Brain Explorer Software courtesy of the Allen Brain Institute (http://mouse.brain-map.org/static/brainexplorer). B. Distribution of ChR2-EYFP in the hippocampus of the thy1 (line 18) mouse. Note high expression levels in CA1 and subiculum and the placement of the fiber over intermediate CA1. 10x tiled confocal image C. ChR2-EYFP is expressed in pyramidal neurons in CA1. 63x oil immersion confocal image.

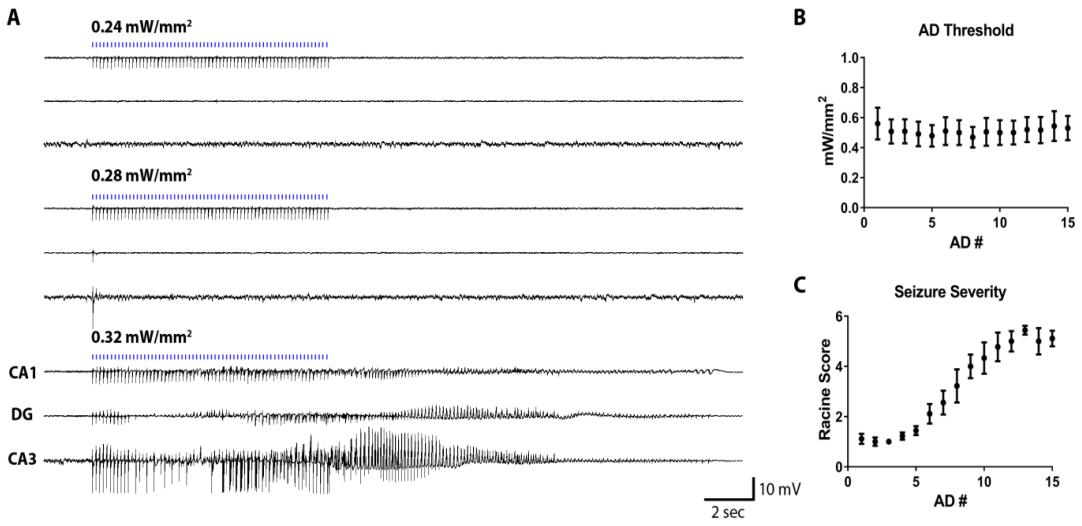

Figure 2: Repetitive optogenetic activation (6.67 Hz, 10 s) produces an AD and daily AD produces behavioral seizure (kindling). A. Superthreshold but not subthreshold stimulation levels (for AD) produce network wide activation ($p < 0.0001$ Fishers exact test, n = 135 seizures). At lower intensity levels, activation was observed only at the stimulation site. B. After discharge thresholds remained stable throughout the kindling period (no significant correlation between threshold and AD#). C. Behavioral seizure severity increased with each after discharge and was strongly correlated with stimulation number ($r = 0.9681$, $p < 0.0001$, n= 9).

We found that rhythmic pulsatile stimuli (6.67 Hz, 10 sec) of sufficient intensity in CA1 produced an unambiguous epileptic after-discharge (AD) (Fig2a). Furthermore, this activity quickly spread throughout the entire network of recording sites with latencies (5-20 ms) far shorter than the interpulse interval (150ms) and occurred even on the first pulse of the train. AD thresholds were measured by presenting stimulus trains at increasing light intensity until an AD occurred. Using this thresholding procedure, we took a subset of animals (n=9) through a modified kindling procedure (Fig2b and c). Threshold ADs were presented daily for 15 days. AD threshold remained stable (uncorrelated with presentation #) over the course of kindling (Pearson's r = 0.146, p = 0.6, ns, n=9) (Fig. 2B). The mean AD threshold was 1.703 mW +/- 0.01987, n=9). However, repeated AD induction was strongly correlated with increasingly severe

behavioral seizures as quantified using a modified Racine scale ($r = 0.9681$, $p < 0.0001$, $n = 9$) (Fig. 2C and S1).

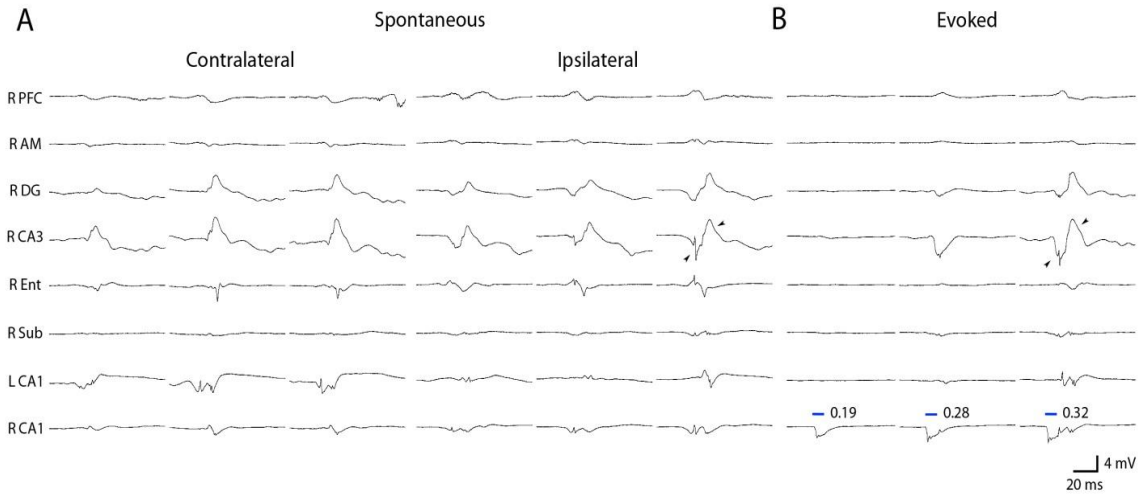

Figure 3: Optogenetic Stimulation Evokes Network Wide Population Discharges that Resemble Spontaneous Interictal Spikes

A. Comparison of spontaneous interictal discharges to optogenetically evoked PDs. Spontaneous contralateral spikes are characterized by leading activity in contralateral (left) CA1. Note the positive going (presumably inhibitory) wave in DG and CA3. Ipsilateral spikes are characterized by near synchronous activation in DG, CA3, and R CA1, and delayed activation in L CA1. B. Evoked population spikes are led by short latency activation in CA1 (stim site) followed by near synchronous activation of DG, CA3, and CA1 with a latency of ~10 ms. Note similar timing and wave shape between post-stimulus evoked population spikes and spontaneous ipsilateral spikes (arrow heads). Blue bars indicate onset and duration of light stimulus in CA1.

Fully kindled animals routinely had stage 6 (running and jumping) evoked seizures. Because these events present a significant hazard to the animals and the experimental preparation, we sought to develop an alternative measure of excitability. We noticed that kindled animals had spontaneous interictal discharges that were nearly identical to those evoked by super-threshold optogenetic stimulation (Fig. 3a and b). They occur in two characteristic patterns, those initiated on the contralateral side and those on the ipsilateral side (Fig. 3a).

The initiation site appears to be CA3 although we can't rule out sites outside of our recording array (Fig3a).

The optogenetically evoked population discharges were similar in terms of waveform shape and latencies, with the exception of preceding activation in CA1 (Fig. 3a). Furthermore we found that they occurred only at a sufficient light intensity similar to that of the AD thresholds (Fig. 3c and 4, also quantified in Fig.6a). However, they did not occur on each presentation of super-threshold light, but rather occur with higher probability as the light intensity is increased (Fig. 4b and c).

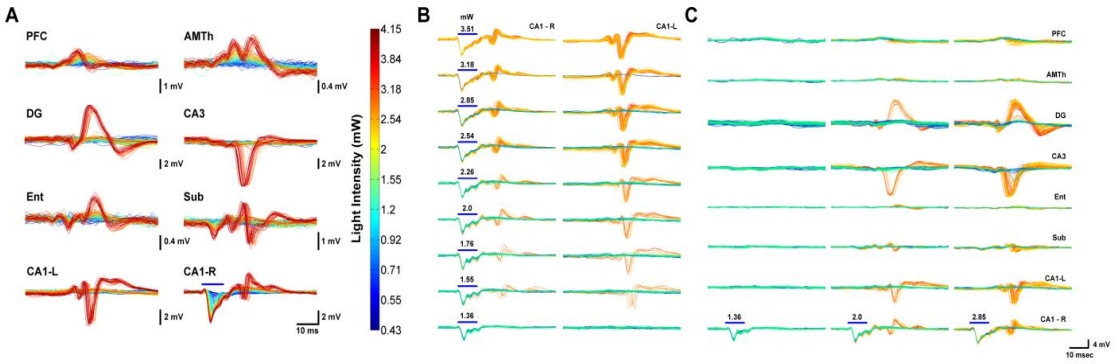

Figure 4: Evoked Population Discharges Depend on Light Intensity A. B. Optogenetic stimulation produces a fast light intensity dependent depolarizing shift in the LFP recorded from stimulation site in area CA1. Blue bars indicate the onset and duration of the optogenetic pulse (10 ms) and labels refer to the light intensity. In area CA3, a longer latency response is accompanied by a high amplitude population spike at intensities above 0.24 mW/mm^2. The gold colored traces are those in which a population spike was detected, the blue are traces where it was absent. Each plot is an overlay of 60 trials and the color gradient indicates chronological order (dark blue/red for early trials, light blue/yellow for late trials). The white dotted line serves as a visual aid for judging latencies. Scale bars in C apply to B as well. **C.** The population spike in CA3 is accompanied by a nearly synchronous response across the network. Three intensity levels from B are shown across channels.

In order to quantify the probability of population discharge (oPD), we developed a randomized dose response procedure. Twenty intensity levels were presented in randomized blocks with a 3 sec ISI, with 60 repetitions over the course of an hour

for a total of 1200 stimuli. The intensity levels were selected to produce a linearized optogenetic dose response curve as measured by the amplitude of the shortest latency peak (Fig. 5a-d). Network population discharges were detected by thresholding a sliding window RMS of the 2nd derivative of the peri-stimulus activity (Fig. 5e-g). The proportion of population discharges to total stimuli presentations at each level can then plotted to generate an optogenetic population discharge threshold curve (oPDT). Perhaps as a reflection of the underlying biophysical basis of the oPD probability, these curves were very well fit by the Hodgin and Huxley formulation of the Boltzmann distribution:

$$f(x) = \frac{1}{1 + e^{\left(\frac{a-x}{b}\right)}}$$

where a is the V50 or oPD50, and b is the slope (Fig. 5h).

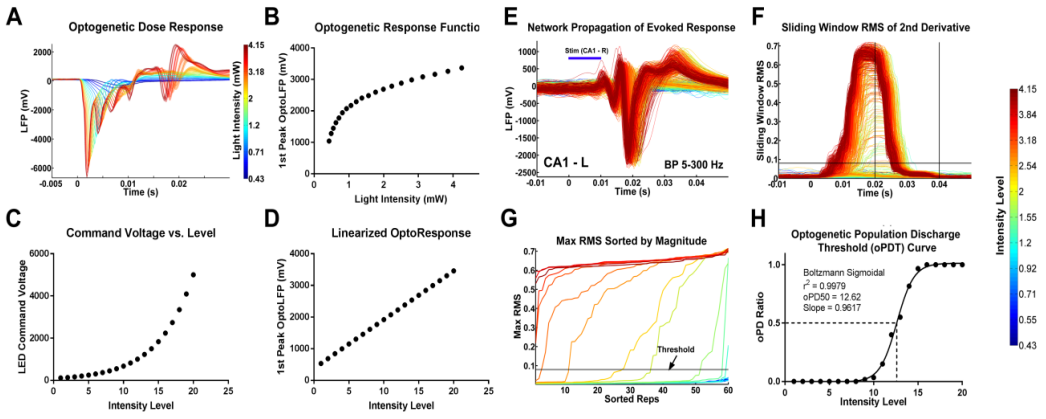

Figure 5: Summary of the optogenetic population discharge threshold procedure. A. Average LFP response to optogenetic activation at varying light intensities. Shaded bars = 95% confidence intervals. **B.** The short latency LFP response was used as an approximation of ChR2 mediated current to generate a light dose response curve. **C.** A series of light intensities were chosen to produce a linearized optogenetic response **D**. **E.** The network propagation of evoked activity from the stimulation site (CA1-R, blue bar) to CA1-L. Individual replicates plotted as bandpass filtered (5-300Hz) traces. Colors correspond to the intensity level of the light stimulus (shown in mW on colorbar). 20 levels, 60 replicates, 1200 total stimuli. Note high amplitude population discharges. **F.** Sliding window RMS of the 2nd derivative calculated from E. Vertical lines indicate threshold time window and horizontal line indicates the magnitude threshold. **G.** Max RMS (within time window) for each light intensity level sorted by magnitude. Note relatively steep

transition between sub-PD and PD RMS values. Threshold is set just above the inflection point. **H.** oPD ratio plot fit by a Boltzmann sigmoidal curve of the form f(x) = 1/(1+exp((a-x)/b)) allows for calculation of an oPD50, or the LED intensity at which 50% of the light pulses produce a population discharge.

Because the oPD appears to represent a surrogate for seizure threshold (Fig. 6a) it should reflect any underlying changes in the brain which govern network excitability. In order to test this hypothesis, we used a well-known pro-epileptic drug (PTZ) at sub-convulsive doses. Although the animals did not exhibit outward behavioral signs after low dose PTZ, their oPD curve was significantly shifted to the left relative to baseline (Baseline = 6.976 +/- 0.099, PTZ = 5.281 +/- 0.246, $p<0.0001$, n = 4) (Fig. 6b and c). Co-treatment of PTZ with the anti-epileptic levetiracetam (Lev) (40 mg/kg) reverses the leftward shift (Baseline 2 = 6.609 +/- 0.196, PTZ+Lev = 6.500 +/- 0.174, ns) (Fig.6c). The low variance of the oPDT is worth noting. Power calculations demonstrate that with only 4 animals, the oPDT procedure can detect shifts in the oPD50 as low as 0.4.

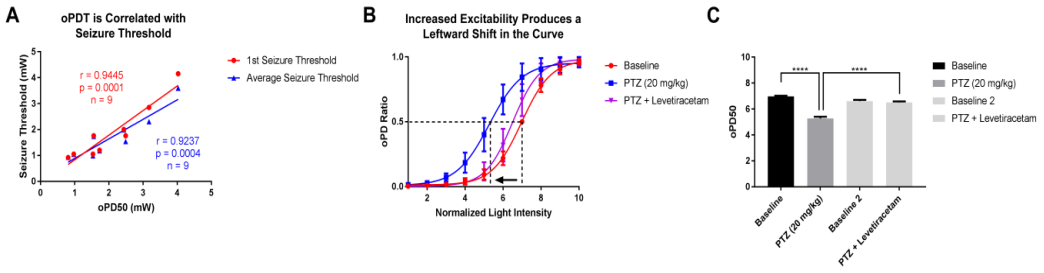

Figure 6: oPD50 is a useful surrogate for seizure threshold and is a sensitive measure of network excitability. A. The relationship between pre-seizure oPD50 and the 1st seizure threshold (red) or the average seizure threshold throughout 15 kindling sessions (blue). The two metrics are strongly correlated (1st Seizure: Pearson's r = 0.9445, p = 0.0001, n = 9, Avg Seizure: Pearson's r = 0.9237, p = 0.0004, n = 9). **B and C.** The GABAa antagonist PTZ (20 mg/kg) shifts the oPD curve leftward (Baseline = 6.976 +/- 0.099, PTZ = 5.281 +/- 0.246) and treatment with levetiracetam (40 mg/kg) reverses the shift (Baseline 2 = 6.609 +/- 0.196, PTZ+Lev = 6.500 +/- 0.174).

Discussion

The purpose of this study was to characterize optogenetically induced population discharges in the hippocampal formation, and their relation to AD activity and behavioral seizure. Population discharges are compound excitatory potentials produced by synchronous network activity (Johnston and Brown, 1981, 1984). Optogenetic stimulation, by virtue of its ability to produce widespread synchronous activation, is ideal for generating population spikes, both in the area directly stimulated, and in downstream synaptic targets. The Thy1 mouse expresses high levels of ChR2-EYFP in pyramidal neurons across the extent of CA1 with a higher degree of consistency and structural specificity than could be achieved with virus injection alone. In this way, optogenetic activation mimics the downstream effects of spontaneously occurring population spikes. Importantly, optogenetic activation allows for sub-to-super threshold depolarization in a large population whereas electrical stimulation would require higher currents to achieve widespread activation, thus affecting fibers of passage. In addition, by selectively targeting excitatory neurons only, the inhibitory population is free to respond, which is important given the emerging role of inhibition in synchronizing activity during seizure (Khoshkhoo et al., 2017).

Organization of Hippocampal Circuitry

The functional organization of the hippocampus has traditionally been described in terms of the tri-synaptic circuit (Ent → DG → CA3 →CA1). However,

recent appreciation of the interactions between hippocampus and entorhinal cortex suggests that the hippocampus is best conceptualized as a series of nested loops. CA1 projects to subiculum and directly to the deep layers of entorhinal cortex (Cenquizca and Swanson, 2006, 2007). The superficial layers of entorhinal cortex then project directly to DG, and CA3 through the perforant path and to CA1 via the temporoammonic pathway, resulting in near simultaneous post-synaptic potentials in these areas (Yeckel and Berger, 1990). Therefore, the shortest loop proceeds from Ent → CA1 → Ent and the longest proceeds via the trisynaptic pathway from Ent → DG → CA3 → CA1. Numerous studies in brain slices have demonstrated that functional connections between the hippocampus and entorhinal cortex are required for experimentally induced epileptiform activity, see (Avoli et al., 2002) for review. In addition, entorhinal cortex can drive epileptiform activity in CA1, even in the absence of input from CA3 after cutting the Shaffer collaterals (Barbarosie and Avoli, 1997; Barbarosie et al., 2000). We selected CA1 as the site for stimulation since it is a readily accessible area directly upstream from entorhinal cortex. Optogenetic stimulation of CA1 produces synchronous activation of entorhinal cortex, which in turn synchronously activates multiple hippocampal areas. Under normal physiological conditions, non-synchronous activation of this pathway produces sharp-wave ripples associated with memory reconsolidation (Klorig and Godwin, 2017a). As we show here, under conditions of super-physiological synchrony, this pathway generates spiking activity that is consistent with interictal spikes.

Optogenetically Induced Population Discharges Resemble Spontaneous Interictal Spikes

We found that optogenetic activation of CA1 produced near synchronous population bursts in DG, CA3, and CA1 with a delay of ~9 ms between recording sites. The spike waveforms in CA1 and CA3 were similar to those evoked by Shaffer collateral stimulation in kindled rats or in the subcortically denervated hippocampus (Buzsáki et al., 1991; Wadman et al., 1983). The fact that these events were initiated from CA1 and occurred simultaneously in multiple hippocampal structures supports the hypothesis that synchronous input from entorhinal cortex was responsible (Yeckel and Berger, 1990). In addition, spontaneous interictal spikes were detected in previously optogenetically kindled animals with nearly identical waveform shapes but without the early ChR2 induced depolarizing potential in CA1. The positive going (presumed inhibitory) phase of the interictal spike was unchanged relative to spontaneous events, as would be predicted by the fact that stimulation was restricted to excitatory neurons. These events (spontaneous or evoked) were followed by activation of contralateral CA1 with a latency of ~12 ms. Conversely, in some spontaneous events, contralateral CA1 preceded the simultaneous interictal spike on the ipsilateral side by about the same amount, suggesting that either hemisphere was capable of generating the spike and propagating it to the contralateral side.

Through the use of a tightly controlled LED light source, we were able to measure population spike thresholds with high resolution. As the light levels increase, the probability of observing a population spike increases. The

relationship between light intensity and spike probability follows a sigmoidal curve, which indicates a clear threshold effect. In contrast, the short latency depolarizing potential in CA1 increased gradually with increasing light intensity as a result of the dose-dependent relationship between intensity and ChR2 currents (Lin, 2010).

Finally, Thy 1 mice express ChR2 at low levels in areas other than the targeted CA1 – thus we cannot completely rule out antidromic responses generating the population spikes; however, this is unlikely since the longer latencies observed are consistent with a feed forward propagation of activity rather than short latencies (~2 ms) observed with antidromic stimulation (Yeckel and Berger, 1990). The fact that activation occurs simultaneously in multiple areas (including CA1) also argues against antidromic activation. In either case, the high degree of similarity between spontaneous and evoked interictal spikes suggests that optogenetic activation serves simply to initiate the event, rather than influence its expression.

Conclusions

We have demonstrated that optogenetic stimulation is sufficient to produce interictal spikes, AD and behavioral seizure. This new model of electrographic and behavioral seizure has several important features; first, it provides some of the first direct evidence for the hypothesized link between the population discharges underlying interictal spikes and ictal activity underlying behavioral seizure; second, it produces robust high amplitude, high frequency population bursts associated with the transition from interictal to ictal activity. In addition, it represents a first step

towards more detailed optogenetic investigation of seizure mechanisms using the full array of optogenetic tools.

Brief Experimental Procedures (See Detailed Methods in Supplement)

Subjects

Male Thy1-ChR2-YFP (founder line 18) transgenic mice (Arenkiel et al., 2007; Wang et al., 2007) (Stock # 007612, The Jackson Laboratory) were used for chronic optogenetic stimulation and recording (n = 27). All animal experiments were approved by the Institutional Animal Care and Use Committee (IACUC) of Wake Forest University and in agreement with National Institutes of Health and United States Department of Agriculture guidelines, including practices to eliminate suffering and reduce animal numbers to the extent possible.

Chronic Implant

Details of the implantation surgery and chronic recording array are described in a previous publication (Klorig and Godwin, 2014b). Briefly, custom arrays were built using 35 µm tungsten microwires and a custom low-noise interface. A total of 8 micro-wires were implanted in a satellite array in cortical, subcortical, and hippocampal locations: prefrontal cortex, anterior medial thalamic nucleus, entorhinal cortex, dentate gyrus, subiculum, hippocampus, and left CA1 (Fig. 1A). A magnetic rotary fiber connector with an attached microwire (optrode) was placed in CA1. The optotrode was configured to minimize the photovoltaic effect (<0.02% LFP amplitude) by cutting the electrode at an angle so that the exposed metal surface was not directly illuminated by the implanted fiber (Cardin et al., 2010). This design allowed for high quality recordings, free of movement artifacts, even

during stage 6 seizure.

Light stimulation and recordings

Wideband (0.3-20kHz, sampled at 40kHz) depth recordings were made using the SciWorks recording system (DataWave Technologies), AM-3600 extracellular amplifiers (A-M Systems), and T8G100 headstage amplifiers (TBSI). Photo stimulation was performed with a custom fiber-coupled LED (Philips Lumileds). LED intensity was controlled using a LED driver with analog modulation (Mightex Systems or ThorLabs). Two estimates of light intensity are provided, the radiant flux (mW) at the tip of the source fiber, as well as the light power density at the recording site (mW/mm^2) estimated using the empirically derived model as described (Aravanis et al., 2007; Yizhar et al., 2011). In addition, a linearized stimulation intensity curve was generated (see Fig. 5D).

Data Analysis

Data analysis was performed using SciWorks, NeuroExplorer (Nex Technologies), and custom software written in MATLAB (MathWorks).

References

Adrian, E.D., and Matthews, B.H. (1934). The interpretation of potential waves in the cortex. J. Physiol. *81*, 440–471.

Aravanis, A.M., Wang, L.P., Zhang, F., Meltzer, L.A., Mogri, M.Z., Schneider, M.B., and Deisseroth, K. (2007). An optical neural interface: in vivo control of rodent motor cortex with integrated fiberoptic and optogenetic technology. J Neural Eng *4*, S143–S156.

Arenkiel, B.R., Peca, J., Davison, I.G., Feliciano, C., Deisseroth, K., Augustine, G.J., Ehlers, M.D., and Feng, G. (2007). In vivo light-induced activation of neural circuitry in transgenic mice expressing channelrhodopsin-2. Neuron *54*, 205–218.

Avoli, M., D'Antuono, M., Louvel, J., Köhling, R., Biagini, G., Pumain, R., D'Arcangelo, G., and Tancredi, V. (2002). Network and pharmacological mechanisms leading to epileptiform synchronization in the limbic system in vitro. Prog. Neurobiol. *68*, 167–207.

Barbarosie, M., and Avoli, M. (1997). CA3-driven hippocampal-entorhinal loop controls rather than sustains in vitro limbic seizures. J. Neurosci. Off. J. Soc. Neurosci. *17*, 9308–9314.

Barbarosie, M., Louvel, J., Kurcewicz, I., and Avoli, M. (2000). CA3-released entorhinal seizures disclose dentate gyrus epileptogenicity and unmask a temporoammonic pathway. J. Neurophysiol. *83*, 1115–1124.

Buzsaki, G. (2006). Rhythms of the Brain (Oxford University Press, USA).

Buzsáki, G., Hsu, M., Slamka, C., Gage, F.H., and Horváth, Z. (1991). Emergence and propagation of interictal spikes in the subcortically denervated hippocampus. Hippocampus *1*, 163–180.

Cardin, J.A., Carlén, M., Meletis, K., Knoblich, U., Zhang, F., Deisseroth, K., Tsai, L.-H., and Moore, C.I. (2010). Targeted optogenetic stimulation and recording of neurons in vivo using cell-type-specific expression of Channelrhodopsin-2. Nat. Protoc. *5*, 247–254.

Cenquizca, L.A., and Swanson, L.W. (2006). Analysis of direct hippocampal cortical field CA1 axonal projections to diencephalon in the rat. J. Comp. Neurol. *497*, 101–114.

Cenquizca, L.A., and Swanson, L.W. (2007). Spatial organization of direct hippocampal field CA1 axonal projections to the rest of the cerebral cortex. Brain Res. Rev. *56*, 1–26.

Chatrian, G.E., Bergamini, L., Dondey, M., Klass, D.W., Petersén, I., and Lennox-Buchthal, M. (1974). A glossary of terms most commonly used by clinical electroencephalographers. Electroencephalogr. Clin. Neurophysiol. *37*, 538–548.

Connors, B.W. (1984). Initiation of synchronized neuronal bursting in neocortex. Nature *310*, 685–687.

de Curtis, M., and Avanzini, G. (2001). Interictal spikes in focal epileptogenesis. Prog. Neurobiol. *63*, 541–567.

Gotman, J. (1980). Quantitative measurements of epileptic spike morphology in the human EEG. Electroencephalogr. Clin. Neurophysiol. *48*, 551–557.

Johnston, D., and Brown, T.H. (1981). Giant synaptic potential hypothesis for epileptiform activity. Science *211*, 294–297.
Johnston, D., and Brown, T.H. (1984). The synaptic nature of the paroxysmal depolarizing shift in hippocampal neurons. Ann. Neurol. *16 Suppl*, S65-71.
Khoshkhoo, S., Vogt, D., and Sohal, V.S. (2017). Dynamic, Cell-Type-Specific Roles for GABAergic Interneurons in a Mouse Model of Optogenetically Inducible Seizures. Neuron *93*, 291–298.
Klorig, D., and Godwin, D.W. (2014a). Optogenetic light-ramp induction of fast-gamma and sharp-wave ripples in vivo. In preparation.
Klorig, D.C., and Godwin, D.W. (2014b). A magnetic rotary optical fiber connector for optogenetic experiments in freely moving animals. J. Neurosci. Methods *227C*, 132–139.
Lin, J.Y. (2010). A User's Guide to Channelrhodopsin Variants: Features, Limitations and Future Developments. Exp. Physiol.
Miles, R., Wong, R.K.S., and Traub, R.D. (1984). Synchronized afterdischarges in the hippocampus: Contribution of local synaptic interactions. Neuroscience *12*, 1179–1189.
Osawa, S., Iwasaki, M., Hosaka, R., Matsuzaka, Y., Tomita, H., Ishizuka, T., Sugano, E., Okumura, E., Yawo, H., Nakasato, N., et al. (2013). Optogenetically Induced Seizure and the Longitudinal Hippocampal Network Dynamics. PLoS ONE *8*, e60928.
Wadman, W.J., Da Silva, F.H., and Leung, L.W. (1983). Two types of interictal transients of reversed polarity in rat hippocampus during kindling. Electroencephalogr. Clin. Neurophysiol. *55*, 314–319.
Wang, H., Peca, J., Matsuzaki, M., Matsuzaki, K., Noguchi, J., Qiu, L., Wang, D., Zhang, F., Boyden, E., Deisseroth, K., et al. (2007). High-speed mapping of synaptic connectivity using photostimulation in Channelrhodopsin-2 transgenic mice. ProcNatl AcadSciUSA *104*, 8143–8148.
Yeckel, M.F., and Berger, T.W. (1990). Feedforward excitation of the hippocampus by afferents from the entorhinal cortex: redefinition of the role of the trisynaptic pathway. Proc. Natl. Acad. Sci. U. S. A. *87*, 5832–5836.
Yizhar, O., Fenno, L.E., Davidson, T.J., Mogri, M., and Deisseroth, K. (2011). Optogenetics in neural systems. Neuron *71*, 9–34.

CHAPTER 3

A NOVEL OPTICALLY-INDUCED POPULATION DISCHARGE THRESHOLD AS A SENSITIVE MEASURE OF CNS HYPEREXCITABILITY DURING ALCOHOL WITHDRAWAL

G. E. Alberto; D.C. Klorig; D. W. Godwin

Abstract

Alcohol abuse is a large scale societal problem. Cessation of chronic alcohol use may produce alcohol withdrawal syndrome (AWS), which is accompanied by significant public health burdens. The mechanisms by which chronic alcohol use leads to hyperexcitability in the central nervous system (CNS) have been well characterized. AWS requires immediate and aggressive treatment in order to prevent seizure and ensure favorable outcomes. Current first line treatment relies almost exclusively on the benzodiazepine (BZD) class of drugs. While BZDs are effective at preventing seizure there are risks inherent to their use and more favorable options are needed. However, development of targeted pharmacotherapies for AWS has been slow, due in part to the lack of availability of animal models that capture the key features of human AWS, and allow high precision *in vivo* monitoring of the electrophysiological correlates of hyperexcitability with the concurrent benefit of pharmacological intervention. Here we have applied a newly developed model for the detailed assessment of CNS excitability, termed the optically-induced Population Discharge Threshold (oPDT), to the well-characterized chronic intermittent exposure model of alcohol withdrawal. We demonstrate that oPDT is sensitive to the effects alcohol withdrawal, allows detailed assessment of compensatory changes to the balance of excitation and inhibition during chronic alcohol exposure, as well as how these changes contribute to rebound hyperexcitability and behavioral seizure when alcohol is removed from the system. oPDT promises to enable greater precision in the preclinical development of next generation pharmacotherapies for AWS.

Introduction

Alcohol is the most commonly consumed drug of abuse in the country. According to the National Institute on Alcohol Abuse and Alcoholism (NIAAA), 86.4% of adults report having consumed alcohol at some point in their lifetime, with more than 15 million of those individuals qualifying as having an Alcohol Use Disorder (AUD) (NSDUH, 2016). AUD is primarily diagnosed through identification of a suite of psychosocial features of a patient's history, including compulsive drinking and excessive alcohol intake (*Diagnostic and Statistical Manual of Mental Disorders* 2013). The patterns of drinking associated with AUD predispose individuals to be at risk for alcohol withdrawal syndrome (AWS) on cessation of alcohol consumption. AWS is characterized by a number of psychological and physiological symptoms related to central nervous system (CNS) hyperexcitability (Jesse et al. 2017). The syndrome is associated with high morbidity and mortality and requires rapid and intense treatment.

The Benzodiazepine (BZD) class of drugs is the most commonly prescribed treatment (Jesse et al. 2017; Ait-Daoud, Malcolm, and Johnson 2006) because they are effective at reducing the most severe symptoms of AWS, notably seizure, which will occur in up to 15% of patients with AUD (Mennecier et al. 2008; Chan et al. 2009; Jesse et al. 2017). When observed in AWS, seizures tend to occur within 24-48 hours of cessation of alcohol intake but in severe cases the risk of seizure remains for up to 1 week (Victor and Brausch 1967;

Bråthen et al. 1999), and is associated with high mortality related to cardiac arrhythmias (Kattimani and Bharadwaj 2013; Mainerova et al. 2015).

BZDs bind gamma-aminobutryic acid type A receptors ($GABA_AR$) to increase the flux of Cl^- ions across the membrane thereby increasing inhibitory tone. BZD action mimics the acute effects of ethanol, which elicit a profound shift in the excitability state of neurons to increase inhibitory tone and reduce excitatory drive (Davies and Alkana 2001; Davies 2003; Morisot and Ron 2017; Valenzuela et al. 1998; Cardoso et al. 1999). Under chronic exposure to ethanol, this shift toward inhibition creates a strong homeostatic pressure to amplify the native excitatory drive. This amplification happens predominately through reduction and alterations of $GABA_ARs$ (Cagetti et al. 2003) and increases in N-methyl-D-aspartate Receptor (NMDAR) expression (Kalluri et al. 1998); however mounting evidence indicates that the effects are much wider, reaching and include changes to a wide variety of intrinsic modulators of excitability (Kourrich et al. 2015) that affect the neurocircuitry of the brain. In sum, AWS results in part from compensatory changes to the CNS that render the brain hyperexcitable when alcohol is not present (Becker 2008).

Several pre-clinical models exist for assessment of AWS, based on behavioral and electrographic observations often coupled with pharmacologic intervention (reviewed in Becker 2000). However, there is no model by which the CNS can be precisely monitored and probed in order to test for the emergence and maintenance of hyperexcitability in neuronal circuits. Here we report a newly developed paradigm, termed optically-induced Population Discharge Threshold

(oPDT) testing (Chapter 2), in the context of chronic alcohol exposure and withdrawal using the chronic intermittent ethanol (CIE) exposure paradigm (Becker and Hale 1993). We demonstrate that oPDT testing permits assessment of the mechanisms of AWS along several dimensions, including increases in spontaneous spiking activity (Veatch and Gonzalez 1996), increases in seizure severity (Becker and Hale 1993), and reduction in seizure threshold to a given stimulus (Kokka et al. 1993). We suggest that oPDT testing comports with conventional measures of withdrawal, but further provides the unique ability to observe changes in the excitability state of an intact system, and to probe the extent of those changes with targeted, cell population specific optical stimulation making it well suited for preclinical discovery of novel pharmacotherapeutics for the treatment of AWS.

Materials and Methods

Animals

Male Thy1-ChR2-YFP (founder line 18) transgenic mice (Arenkiel et al. 2007; Wang et al. 2007) (Stock # 007612, The Jackson Laboratory) were used for chronic optogenetic stimulation and recording (n = 8). The Thy1 transgenic animal expresses the light sensitive cation channel ChR2 consistently in the excitatory neurons of hippocampus. Power calculations on the highly stereotyped response to optical stimulation indicate that significant differences in oPDT are detectable in cohorts of 4 animals. All animal experiments were approved by the Institutional Animal Care and Use Committee (IACUC) of Wake Forest University

and in agreement with National Institutes of Health and United States Department of Agriculture guidelines, including practices to reduce suffering and animal numbers to the extent possible.

Chronic Implant

Custom built satellite microelectrode recording arrays were constructed from eight 35µm tungsten micro-wires for chronic implantation in each animal (Klorig and Godwin 2014). Stereotactic coordinates were calculated for 8 areas to include cortical, subcortical, and hippocampal locations: prefrontal cortex, (PFC, AP: 4.54, L: 0.23, DV: -1.18, in mm, from the interaural plane), anterior medial thalamic nucleus (AM, AP: 2.98, L: 0.58, DV: -3.24), entorhinal cortex (Ent, AP: 0.88, L: 3.86, DV: -3.03), dentate gyrus (DG, AP: 2.10, L: 0.78, DV: -1.72), subiculum (sub, AP: 0.88, L: 1.09, DV: -1.45), hippocampus (CA3, AP: 2.10, L: 1.85, DV: -1.61), and left CA1(AP: 0.88, L: 0.-2.36, DV: -1.34). A custom built optical fiber with magnetic rotary connection was attached to the final micro-wire to serve as the stimulating/recording optrode in CA1 (AP: 0.88, L: 2.36, DV: -1.34). The design of the implant allows for high quality, low artifact, field potential recordings while the animal is freely moving in a recording cage.

Surgery

Thy1 mice (age 8-12 weeks) were anesthetized with isoflurane and placed in a stereotaxic device that allowed continuous administration of isoflurane. An incision was made to expose the cranium in which two silver screws were placed posteriorly over the cerebellum. 8 small craniotomies were then drilled above

each target location and the micro-wires were advanced slowly into each. The optrode was the final implant placed into CA1. A silver ground wire was wrapped tightly around the ground screws and bonded with silver-epoxy. The entire incision was then sealed with dental acrylic and rubberized cyanoacrylic. Surgical procedures were performed under red light to avoid activation of ChR2. The mice were then allowed to recover for at least 1 week before exposure to ethanol vapor or recording.

Chronic Intermittent Ethanol (CIE)

After recovery, implanted mice were exposed to a chronic intermittent ethanol inhalation paradigm as described by Becker and Hale and used previously in the Godwin lab (Becker and Hale 1993; Graef et al. 2011; Riegle et al. 2014). Custom vapor chambers were constructed from Plexiglas and kept in the animal housing room. The animals' home cages were placed inside the chamber giving the animals free access to food and water during exposure. The room was on a 12-12 light-dark cycle, with lights off from 6:00 PM to 6:00 AM. 95% ethanol was volatilized in a glass beaker and pumped into the sealed chamber by an air pump. Animals were kept in the vapor chamber for 16h (5:00 PM to 9:00 AM). Prior to placement in the chamber the alcohol dehydrogenase inhibitor, pyrazole (PYR), was administered to each animal subcutaneously to maintain blood ethanol concentration (BEC; 100mg/kg PYR, Sigma Aldrich; St. Louis, MO). After removal from the vapor chamber an immediate 5µL tail blood sample was collected and stored in trichloroacetic acid (6.25%) for BEC measurement with NAD-ADH enzyme assay (mean BEC=101.3±17.1; Carolina Biological;

Burlington, NC). Animals were then allowed to remain in their home cages for the next 8 hrs constituting the withdrawal period. This process was repeated four times to complete a single cycle of CIE (H. C. Becker and Hale 1993).

Stimulation and Recording

Wideband (0.3-20kHz, sampled at 40kHz) depth recordings were made using the SciWorks recording system (DataWave Technologies), AM-3600 extracellular amplifiers (A-M Systems), and T8G100 headstage amplifiers (TBSI). Photo stimulation was performed with a custom fiber-coupled LED (Philips Lumileds). LED intensity was controlled using a LED driver with analog modulation (Mightex Systems). Analog output pulses were generated within SciWorks and used to control the LED driver.

Optically-Induced Population Discharge Threshold (oPDT) Testing

Kindling-naïve, implanted animals (n=4) were subjected to oPDT testing before and during CIE. The use of optogenetics allows control of neural responses through control of the intensity of light stimulation. Square pulses (10 ms) of light were delivered to CA1 of hippocampus at a range of intensities (10 levels, 0.43 - 1.8 mW at fiber tip, 0.13 – 0.53 mW/mm^2 at the recording site). Sixty repetitions of each intensity were presented in randomly ordered blocks with a 3s interval between pulses. A synchronous timing pulse was used to precisely align responses to the onset of the LED. oPDT testing was not performed in kindled animals. oPDT testing occurred prior to ethanol exposure and between 4-8 hours of removal from the ethanol vapor chamber. Population discharges were defined

by amplitude and waveform shape determined by the second derivative taken on the local field potential (LFP) recording between ~0.005-0.03s. A threshold amplitude of the second derivative was determined uniquely for each animal, due to minor variations in electrode placement that can affect waveshape and amplitude. If a population discharge was detected it was then verified visually (Figure 2.1A). The ratio of population discharges to total stimulations at each optical intensity was used to calculate a population spike (PS) ratio. The ratio at each level was then plotted and fit with a Boltzmann Curve (Figure 2.1B; Chapter 2). This was then used to calculate the intensity at which the ratio of PS to presentations was 0.5, termed I_{50}. The intensity levels were then normalized to the I_{50} in order to align each animal's unique curve. The I_{50} was used to determine significant shifts in the PS curve.

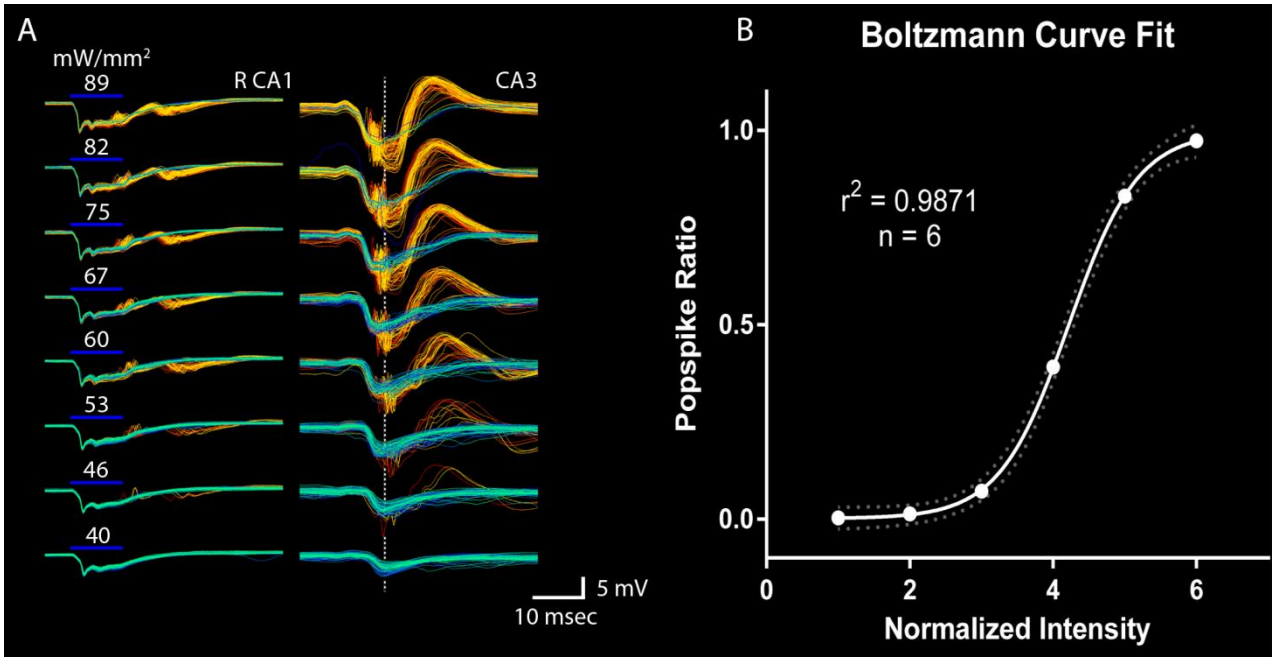

Figure 2.1. Representative PS thresholding procedure and Boltzmann curve used for oPDT testing. A. Representative LFP traces segregated by meeting threshold (yellow) or not (blue) at the middle 8 levels used for oPDT testing. It is clear what constitutes a PS and what does not. The ratio of blue to yellow traces is considered the PS ratio for a given level. **B.** The average normalized PS curve of 6 implanted animals shows the goodness of fit to the Boltzmann curve and the high degree of reproducibility as indicated by 95% confidence intervals (dotted lines).

Kindling and Seizure Threshold Testing

A cohort of animals (n=4) went through an optically based modified kindling procedure such that they experienced overt behavioral seizure in response to stereotyped optical stimulation prior to CIE. Optical kindling was conducted through repeated 6.67Hz train stimulation (10s train, 4ms pulse) at increasing light intensities every 2min until an after discharge (AD) was evoked. This optical intensity represented the AD threshold. AD was observed in real time and defined by high amplitude, rhythmic activity which continued for >5s after optical stimulation had ended. When an AD was observed, the experimenter interrupted

the protocol to stop any further stimulation. The procedure was repeated daily for fifteen days; during this time all of the animals convert from electrographic AD to behavioral seizure. At 15 days the threshold for seizure is stable and does not change (Chapter 2). Only one AD was evoked per 24 hour period. The kindling procedure is similar to electrically based kindling methods and provides the same utility in determining seizure threshold (Pinel et al. 1976; Bragin et al. 2002).

Behavioral Scoring and Spontaneous Spiking

Electrophysiology recording sessions were video recorded. An infrared LED was timelocked to the onset of the recording and stimulus onset allowing for temporal alignment between video and electrophysiological recordings. Video was used to score the severity of evoked seizure using a modified Racine scale (Figure 2.2; Racine 1972).

Spontaneous spikes were counted by hand from the raw electrophysiological recordings in four animals during each WD period of two independent cycles of CIE. CIE cycles were repeated only after spontaneous spike frequency had returned to baseline. Spikes were determined to be high amplitude, fast events that matched the time course and waveform of optically induced spikes, and those observed by Veatch and Gonzalez (Veatch and Gonzalez 1996). Video recordings were used to ensure that the presumed spike was not associated with abnormal behavior or some other environmental effect influencing the recording. Spikes were counted during 10 min, no-stimulation baseline periods performed

each day. Total spikes counted were then divided by total time observed to estimate a frequency of spontaneous spikes in spikes/min.

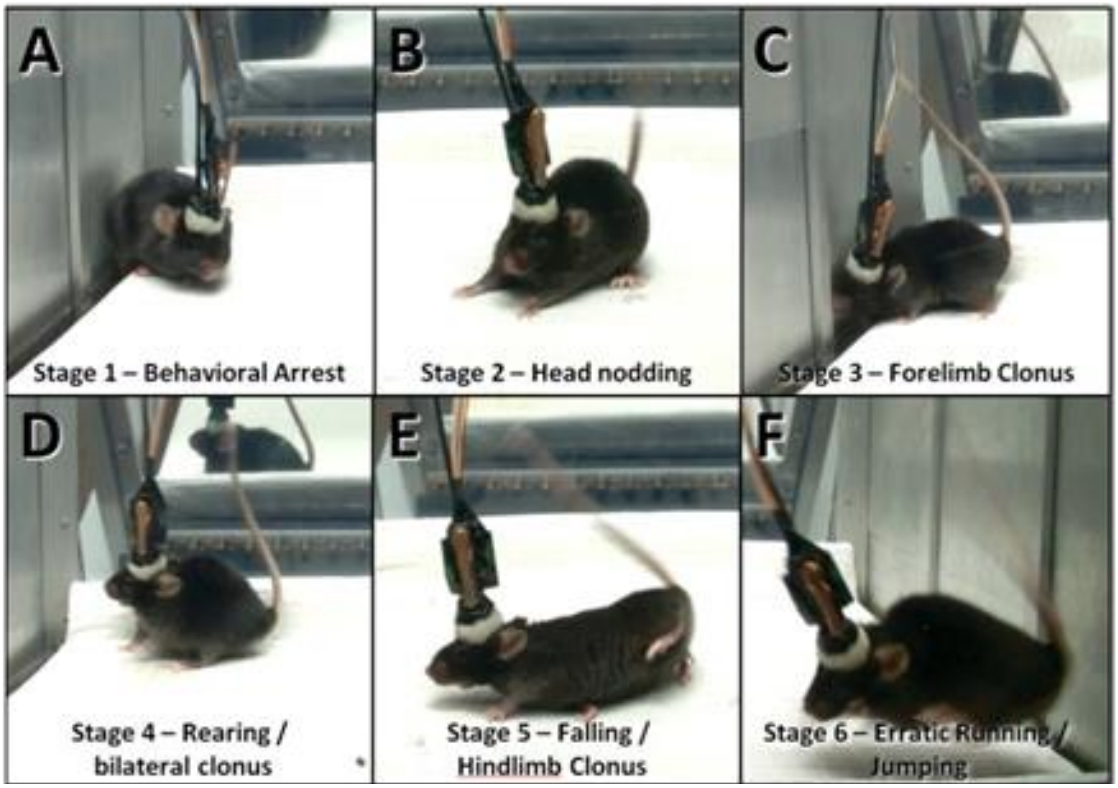

Figure 2.2 The modified Racine Scale used to score seizure severity with corresponding examples of each behavior. Still frames were pulled from the video to show the stereotypic behaviors used to score seizure with stage 6 being the most severe and stage 1 being the mildest.

Data Analysis and Statistics

Data analysis was performed using SciWorks, NeuroExplorer (Nex Technologies), and custom scripts developed in MatLab (MathWorks). Electrophysiological data used for oPDT testing were high pass filtered below 200Hz using an 8^{th} order Butterworth filter. Statistical testing was performed using Prism (GraphPad). A K^2 omnibus test was used to determine normality (D'Agostino and Belanger 1990). Comparisons of seizure parameters before and

after CIE were performed using paired t-tests. Measures of spontaneous spiking during each WD compared to baseline were conducted using two-way analysis of variance (ANOVA) with Dunnett's multiple comparisons test comparing the mean of each baseline period for each animal to the mean of each WD period. I_{50} significance was determined using a paired t-test to compare I_{50} at baseline to I_{50} during the final WD episode. Correlation coefficients were calculated using Pearson's method.

Results

Spontaneous Population Spikes

A group of alcohol naïve and unkindled animals (n=4) were recorded without stimulation for ten minutes, and the number of spontaneously occurring PS were counted. Spontaneous PS were similar to evoked PS as well as those observed in multiple CNS areas by Veatch and Gonzalez on EEG (Veatch and Gonzalez 1996). Animals were then exposed to 1 cycle of CIE. During each WD period as well as at 72 hours after final exposure the animals were recorded for ten minutes without stimulation. Total number of PS was counted for each recording period to generate a PS frequency. Spontaneous PS occurred significantly more frequently during than 3rd WD period (p=0.001) as well as during the 4th WD period (p=0.0001; Figure 2.3). After the final WD period the frequency of spontaneous spiking had returned to a level that was no longer different from baseline when measured at 72 hours (Figure 2.3).

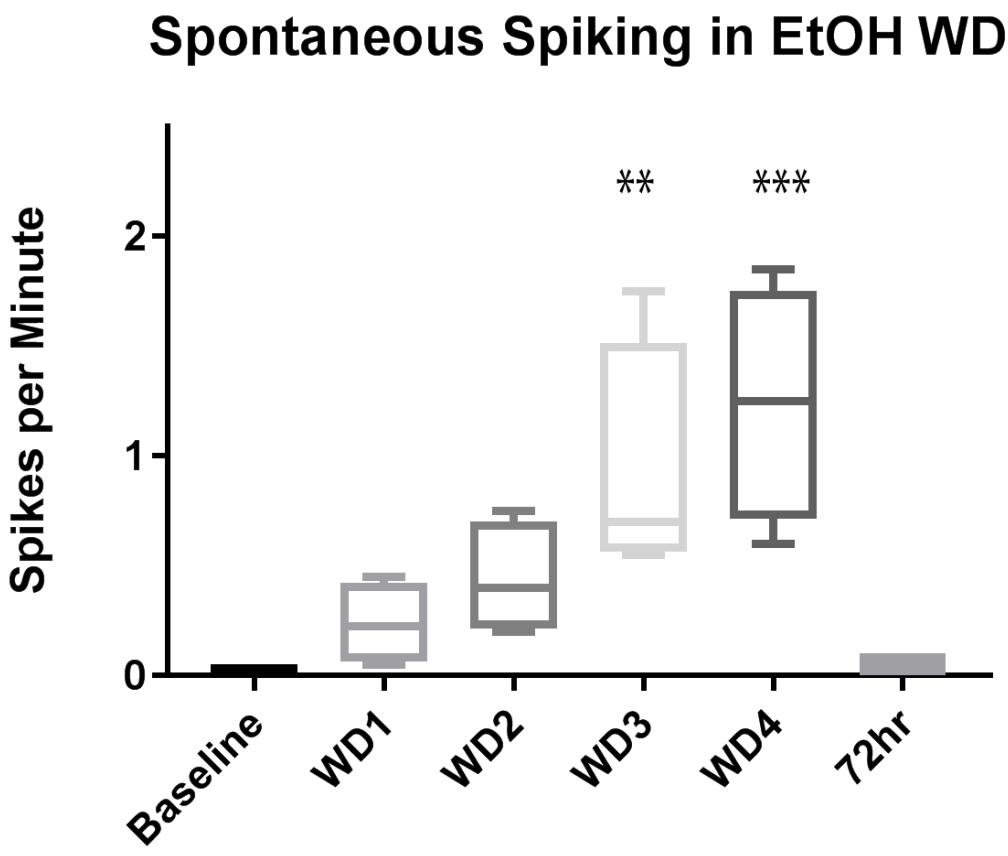

Figure 2.3. Spontaneous Spiking increases during alcohol WD in CIE exposure paradigm. Exposure to CIE ethanol vapor increased the frequency of spontaneous PS during each WD. This increase was significant compared to ethanol naïve animals during the third and fourth WD periods, and was no longer signifcantly different at 72 hours after the final WD period. ** p=0.001; ***p=0.0001. Two-way ANOVA with Dunnett's multiple comparison test.

Seizure Severity and Duration increase while Seizure Threshold decreases during WD

A separate cohort (n=4) underwent a modified kindling protocol for fifteen days. During this time AD threshold was stable with no differences in the slope between animals (Figure 2.4a). Additionally, behavioral seizure manifested with stage 1 early in the kindling process and continued to increase until every animal

had at least a stage 5 seizure (Figure 2.4b; Racine 1972). Seizure severity through the course of the kindling process was not different between animals.

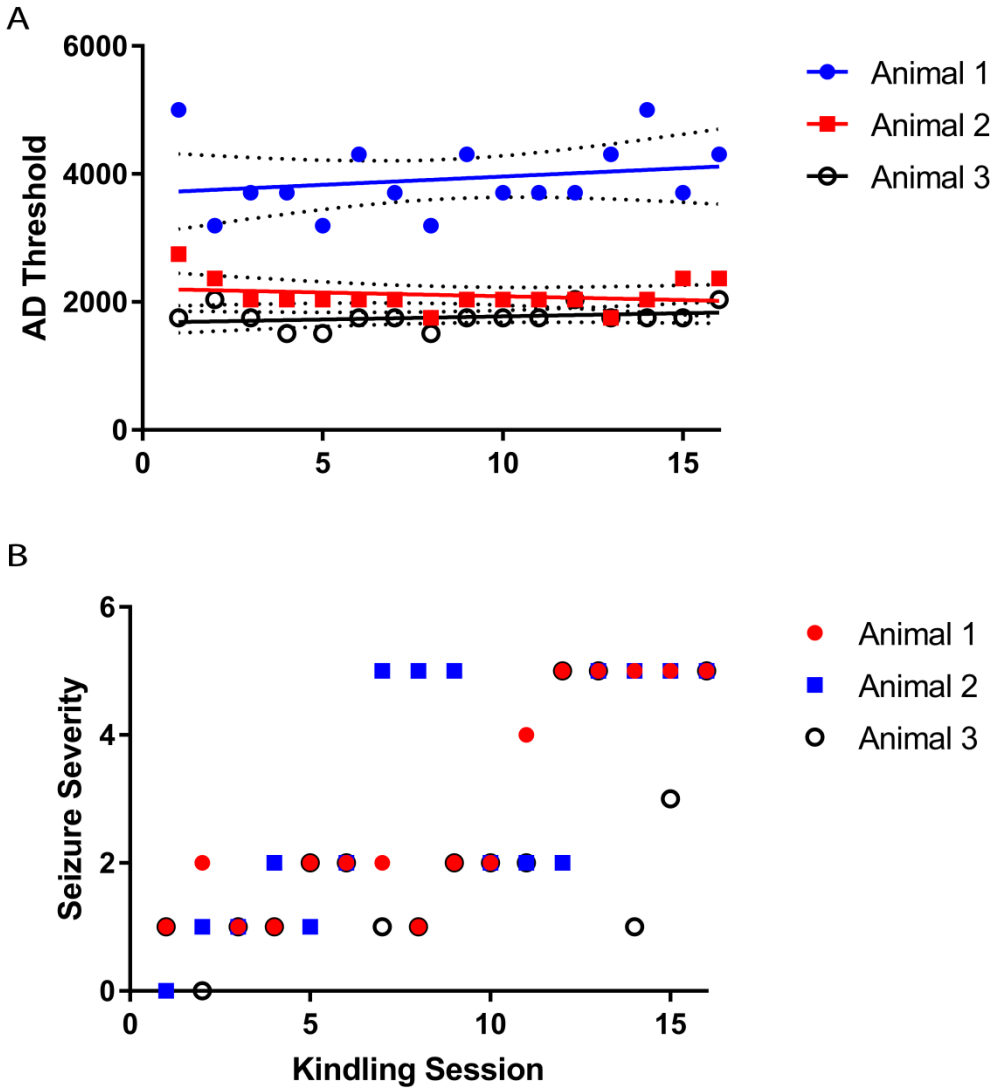

Figure 2.4 Kindling with a modified optical kindling protocol over 15 days elicits stable AD thresholds and increasing but stable seizure severity. A. Three kindled animals had no change in the threshold for AD over the course of kindling. Changes in AD threshold can be interpreted as being related to any subsequent intervention. **B.** The severity of behavioral seizure increases from at or near zero to a consistent stage 5 seizure by the end of kindling. No animal experienced a stage 6 seizure.

After kindling, animals were exposed to CIE exposure for one cycle. During the 4th WD animals were tested again with AD threshold testing. One animal did not

survive the 4th WD and was excluded from analysis. The threshold for seizure was significantly reduced following CIE exposure ($p<0.02$; Figure 2.5a). Additionally, seizure durations and severity were significantly increased ($p<0.05$; Figure 2.5b and Figure 2.5c).

Figure 2.5 Optical seizure threshold is reduced in WD while severity and duration is increased. A. The threshold for generating an AD and behavioral seizure in previously kindled animals was significantly reduced following WD from CIE exposure $p<0.02$. The seizure threshold had previously been stable with no significant differences in threshold from one kindling session to the next. **B.** The severity of seizure was significantly increased with each animal experiencing the most severe seizure score, stage 6; $p<0.05$. Only after CIE exposure did any animal have a stage 6 seizure. **C.** The duration of behavioral seizure also increased significantly; $p<0.041$. Prior to CIE exposure animals had behavioral seizure lasting on average 23.67 ± 1.86s after CIE exposure average seizure increased significantly to 81 ± 19.31s; $p=0.041$.

oPDT testing is a sensitive measure of CNS hyperexcitability during ethanol WD

A group of ethanol naïve animals (n=4) were tested using the oPDT protocol to determine the PS threshold of each. These animals then underwent CIE. During each WD period the oPDT protocol was repeated to test for changes in the PS threshold. The Boltzmann Curve was generated to fit the distribution of PS ratios at each stimulation intensity (Figure 2.6a; Chapter 2). An intensity at which the ratio of PS to presentations was 0.5 was determined, I_{50} (Figure 2.6b). The change in I_{50} was significant during the 3rd and 4th WD periods (Figure 2.6c).

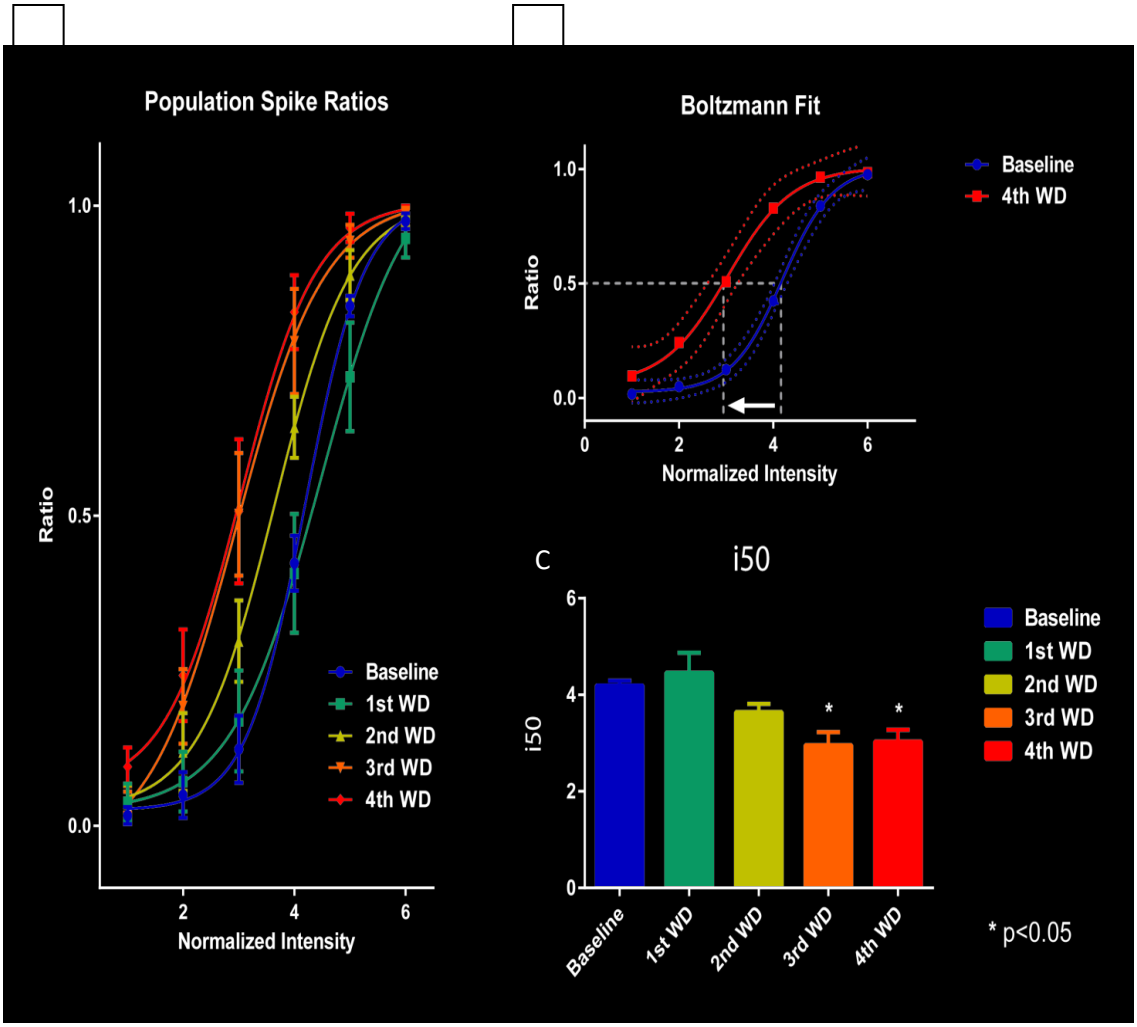

Figure 2.6 oPDT testing is a sensitive measure of CNS hyperexcitability during CIE exposure related WD. A. The average PS curve for each animal at baseline and during each subsequent WD reveals that upon each subsequent exposure to and removal from the ethanol vapor chamber animals become more sensitive to oPDT testing. The curves shift toward the left indicating that they are having a higher ratio of PS to presentations at every level. **B.** A representative comparison of the I_{50} at baseline to the I_{50} during the 4^{th} WD. This measure demonstrates that at the 50% level has shifted lower. This same comparison was conducted for each WD period compared to baseline. **C.** The I_{50} during the 3^{rd} and 4^{th} WD were significantly different from baseline. $p<0.05$ in both conditions; Wilcoxon matched-pairs ranked test.

Discussion

Commonly used methods for understanding alcohol withdrawal-related CNS hyperexcitability rely on indirect surrogates of excitability, including responsiveness to chemoconvulsants (Squires et al. 1984; Kokka et al. 1993; Szabó et al. 1984; Grant et al. 1990; Riegle et al. 2015); quantification of passively observed EEG phenomenon (Veatch and Becker 2002; Veatch and Gonzalez 1996; Wiggins et al. 2013; Riegle et al. 2014); as well as behavioral indicators of CNS hyperexcitability (Maxson and Sze 1976; Kosobud and Crabbe 1990; Becker and Hale 1993). These methods have all been well characterized, and the metrics are consistent with molecular changes to the CNS following alcohol WD. Additionally, the utility of these methods in aiding our understanding of CNS hyperexcitability have been demonstrated through the application of known modulators of alcohol withdrawal symptoms (Becker 2000; Jesse et al. 2017).

However, these methods all fall short of allowing for directly probing the excitability state of affected populations of neurons, and many methods cannot assess levels of excitability until overt electrographic or behavioral seizures are observed. Here we demonstrate the effectiveness of utilizing optogenetic methods to probe the balance of excitation and inhibition of a discrete neural circuit following ethanol WD. By modulating the membrane potentials of local populations of neurons through carefully controlled activation of light sensitive cation channels, ChR2, we demonstrate the susceptibility to population

discharges is decreased and that optically-induced Population Discharge Threshold is a sensitive measure of CNS hyperexcitability during alcohol WD.

The kinetics of ChR2 have been characterized as has the relationship between stimulation intensity (total number of photons) and the number of open channels (Boyden et al. 2005; Klorig and Godwin 2014). In oPDT testing we use this relationship between light intensity and cation channel opening to probe the shift in population excitability during alcohol WD. Modern optics allow for a high degree of control over the intensity of light being introduced into neural tissue (Klorig and Godwin 2014). oPDT capitalizes on this precision to identify changes in excitation that are not limited to single neurons, but manifest as a result as the complex interactions of populations of neurons. The balance of excitation and inhibition is tightly controlled not simply at the individual neuron level, but also by reciprocal and feedforward relationships through groups of neurons (Lovett-Barron et al. 2012; Ben-Yishai et al. 1995; Larkum 2013; Vaidya and Johnston 2013). These population-based interactions add a layer of complexity beyond any single ion channel or modulator of excitability. Through the use of widespread circuit observation with the multi-site satellite array we are able to observe the effects of alcohol WD on population interactions**.**

The results of this study indicate that shifts in the oPDT curve are consistent with previously described measures of CNS hyperexcitability, including seizure. Importantly, work conducted on the model indicates that the I_{50} comports closely with seizure threshold suggesting that it can function as a surrogate marker (Chapter 2).

Employing targeted pharmacology may allow for dissecting the relevant molecular and functional influence on circuit level hyperexcitability. Pairing pharmacology with oPDT testing presents a novel opportunity to not only look at efficacy of treatment strategies for alcohol WD, but also to understand the mechanistic relevance of those strategies. Furthermore, the strategy may allow for differentiating major causes of circuit hyperexcitability from more tangential, or secondary, causes. For example, pharmacology with high specificity for a receptor or intrinsic modulator of excitability that is able to affect the curve can be seen as more efficacious than a drug that has a target with known changes resulting from alcohol exposure fails to affect the curve. This result would suggest that while the molecular target is affected by alcohol exposure those changes are not as influential in circuit wide modulation of excitation and inhibition.

However, it should be noted that there are many phenotypes of alcohol WD seizure and CNS excitability, some of which rely on the seizure susceptibility of selected strains of animals (Kokka et al. 1993; H C Becker 2000), which may not fully capture the complex circuit changes produced in AWS. oPDT testing more closely resembles the phenotype of temporal-lobe and cortically involved tonic-clonic seizures (Becker 2000; Veatch and Gonzalez 1996; Hughes 2009). It may be the case that other phenotypes of CNS hyperexcitability (e.g. BSE, sleep-disturbance, or anxiety (Mu et al. 2003; Wiggins et al. 2013; Riegle et al. 2014; Becker and Hale 1993)) may be differentially modulated and so results of oPDT testing should not be overextended beyond the specific relationship to temporal-

lobe, tonic-clonic seizure. Here oPDT testing has been shown to effectively demonstrate circuit-specific hyperexcitability following CIE exposure. The relationship between oPDT and seizure has also been described. We feel that this method can be applied broadly to investigations of CNS excitability as it relates to mesial temporal and neocortical seizure types

Acknowledgments

This work was supported by NIH grants F30 AA023708, T32AA07565, R01AA016852, P01AA021099, and the Tab Williams Family Fund. The authors declare no competing financial or other conflicts of interest.

References

Ait-Daoud, Nassima, Robert J. Malcolm, and Bankole A. Johnson. 2006. “An Overview of Medications for the Treatment of Alcohol Withdrawal and Alcohol Dependence with an Emphasis on the Use of Older and Newer Anticonvulsants.” *Addictive Behaviors* 31 (9): 1628–49. doi:10.1016/j.addbeh.2005.12.029.

Arenkiel, Benjamin R, Joao Peca, Ian G Davison, Catia Feliciano, Karl Deisseroth, George J Augustine, Michael D Ehlers, and Guoping Feng. 2007. “In Vivo Light-Induced Activation of Neural Circuitry in Transgenic Mice Expressing Channelrhodopsin-2.” *Neuron* 54 (2): 205–18. doi:10.1016/j.neuron.2007.03.005.

Becker, H C. 2000. “Animal Models of Alcohol Withdrawal.” *Alcohol Research & Health: The Journal of the National Institute on Alcohol Abuse and Alcoholism* 24 (2): 105–13.

Becker, H. C., and R. L. Hale. 1993. “Repeated Episodes of Ethanol Withdrawal Potentiate the Severity of Subsequent Withdrawal Seizures: An Animal Model of Alcohol Withdrawal ‘Kindling.’” *Alcoholism, Clinical and Experimental Research* 17 (1): 94–98.

Becker, Howard C. 2008. “Alcohol Dependence, Withdrawal, and Relapse.” *Alcohol Research & Health* 31 (4): 348–61.

Ben-Yishai, R., R. L. Bar-Or, and H. Sompolinsky. 1995. “Theory of Orientation Tuning in Visual Cortex.” *Proceedings of the National Academy of Sciences of the United States of America* 92 (9): 3844–48.

Boyden, E.S., F. Zhang, E. Bamberg, G. Nagel, and K. Deisseroth. 2005. “Millisecond-Timescale, Genetically Targeted Optical Control of Neural Activity.” *Nat Neurosci.* 8 (9): 1263–68.

Bragin, Anatol, Charles L. Wilson, and Jerome Engel. 2002. “Increased Afterdischarge Threshold during Kindling in Epileptic Rats.” *Experimental Brain Research* 144 (1): 30–37. doi:10.1007/s00221-002-1023-y.

Bråthen, G., E. Brodtkorb, G. Helde, T. Sand, and G. Bovim. 1999. “The Diversity of Seizures Related to Alcohol Use. A Study of Consecutive Patients.” *European Journal of Neurology* 6 (6): 697–703.

Cagetti, Elisabetta, Jing Liang, Igor Spigelman, and Richard W. Olsen. 2003. “Withdrawal from Chronic Intermittent Ethanol Treatment Changes Subunit Composition, Reduces Synaptic Function, and Decreases Behavioral Responses to Positive Allosteric Modulators of $GABA_A$ Receptors.” *Molecular Pharmacology* 63 (1): 53–64. doi:10.1124/mol.63.1.53.

Cardoso, R. A., S. J. Brozowski, L. E. Chavez-Noriega, M. Harpold, C. F. Valenzuela, and R. A. Harris. 1999. “Effects of Ethanol on Recombinant Human Neuronal Nicotinic Acetylcholine Receptors Expressed in Xenopus Oocytes.” *The Journal of Pharmacology and Experimental Therapeutics* 289 (2): 774–80.

Chan, Gar Ming, Robert S. Hoffman, Jeffrey A. Gold, Paula J. Whiteman, Lewis R. Goldfrank, and Lewis S. Nelson. 2009. “Racial Variations in the Incidence of Severe Alcohol Withdrawal.” *Journal of Medical Toxicology: Official Journal of the American College of Medical Toxicology* 5 (1): 8–14.

D’Agostino, Ralph B., and Albert Belanger. 1990. “A Suggestion for Using Powerful and Informative Tests of Normality.” *The American Statistician* 44 (4): 316–21. doi:10.2307/2684359.

Davies, D. L., and R. L. Alkana. 2001. “Ethanol Enhances GABAA Receptor Function in Short Sleep and Long Sleep Mouse Brain Membranes.” *Alcoholism, Clinical and Experimental Research* 25 (3): 478–83.

Davies, Martin. 2003. “The Role of GABAA Receptors in Mediating the Effects of Alcohol in the Central Nervous System.” *Journal of Psychiatry and Neuroscience* 28 (4): 263.

Diagnostic and Statistical Manual of Mental Disorders. 2013. 5th ed. American Psychiatric Association.

Graef, J. D., T. W. Huitt, B. K. Nordskog, J. H. Hammarback, and D. W. Godwin. 2011. “Disrupted Thalamic T-Type Ca2+ Channel Expression and Function During Ethanol Exposure and Withdrawal.” *Journal of Neurophysiology* 105 (2): 528–40. doi:10.1152/jn.00424.2010.

Grant, K. A., P. Valverius, M. Hudspith, and B. Tabakoff. 1990. “Ethanol Withdrawal Seizures and the NMDA Receptor Complex.” *European Journal of Pharmacology* 176 (3): 289–96.

Hughes, John R. 2009. “Alcohol Withdrawal Seizures.” *Epilepsy & Behavior* 15 (2): 92–97. doi:10.1016/j.yebeh.2009.02.037.

Jesse, S., G. Bråthen, M. Ferrara, M. Keindl, E. Ben-Menachem, R. Tanasescu, E. Brodtkorb, M. Hillbom, M.a. Leone, and A.c. Ludolph. 2017. “Alcohol Withdrawal Syndrome: Mechanisms, Manifestations, and Management.” *Acta Neurologica Scandinavica* 135 (1): 4–16. doi:10.1111/ane.12671.

Kalluri, Haviryaji S. G, Ashok K Mehta, and Maharaj K Ticku. 1998. “Up-Regulation of NMDA Receptor Subunits in Rat Brain Following Chronic Ethanol Treatment.” *Molecular Brain Research* 58 (1–2): 221–24. doi:10.1016/S0169-328X(98)00112-0.

Kattimani, Shivanand, and Balaji Bharadwaj. 2013. “Clinical Management of Alcohol Withdrawal: A Systematic Review.” *Industrial Psychiatry Journal* 22 (2): 100–108. doi:10.4103/0972-6748.132914.

Klorig, David C., and Dwayne W. Godwin. 2014. “A Magnetic Rotary Optical Fiber Connector for Optogenetic Experiments in Freely Moving Animals.” *Journal of Neuroscience Methods* 227 (April): 132–39. doi:10.1016/j.jneumeth.2014.02.013.

Kokka, N., D. W. Sapp, A. M. Taylor, and R. W. Olsen. 1993. “The Kindling Model of Alcohol Dependence: Similar Persistent Reduction in Seizure Threshold to Pentylenetetrazol in Animals Receiving Chronic Ethanol or Chronic Pentylenetetrazol.” *Alcoholism, Clinical and Experimental Research* 17 (3): 525–31.

Kosobud, A. E., and J. C. Crabbe. 1990. “Genetic Correlations among Inbred Strain Sensitivities to Convulsions Induced by 9 Convulsant Drugs.” *Brain Research* 526 (1): 8–16.

Kourrich, Saïd, Donna J. Calu, and Antonello Bonci. 2015. “Intrinsic Plasticity: An Emerging Player in Addiction.” *Nature Reviews. Neuroscience* 16 (3): 173–84. doi:10.1038/nrn3877.

Larkum, Matthew. 2013. “A Cellular Mechanism for Cortical Associations: An Organizing Principle for the Cerebral Cortex.” *Trends in Neurosciences* 36 (3): 141–51. doi:10.1016/j.tins.2012.11.006.

Lovett-Barron, Matthew, Gergely F. Turi, Patrick Kaifosh, Peter H. Lee, Frédéric Bolze, Xiao-Hua Sun, Jean-François Nicoud, Boris V. Zemelman, Scott M. Sternson, and Attila Losonczy. 2012. “Regulation of Neuronal Input Transformations by Tunable Dendritic Inhibition.” *Nature Neuroscience* 15 (3): 423–30. doi:10.1038/nn.3024.

Mainerova, Barbora, Jan Prasko, Klara Latalova, Karel Axmann, Monika Cerna, Rostislav Horacek, and Romana Bradacova. 2015. “Alcohol Withdrawal Delirium - Diagnosis, Course and Treatment.” *Biomedical Papers of the Medical Faculty of the University Palacky, Olomouc, Czechoslovakia* 159 (1): 44–52. doi:10.5507/bp.2013.089.

Maxson, S. C., and P. Y. Sze. 1976. “Electroencephalographic Correlates of Audiogenic Seizures during Ethanol Withdrawal in Mice.” *Psychopharmacology* 47 (1): 17–20.

Mennecier, D., M. Thomas, P. Arvers, D. Corberand, L. Sinayoko, S. Bonnefoy, F. Harnois, and C. Thiolet. 2008. “Factors Predictive of Complicated or Severe Alcohol Withdrawal in Alcohol Dependent Inpatients.” *Gastroenterologie Clinique Et Biologique* 32 (8–9): 792–97. doi:10.1016/j.gcb.2008.06.004.

Morisot, N., and D. Ron. 2017. “Alcohol-Dependent Molecular Adaptations of the NMDA Receptor System.” *Genes, Brain and Behavior* 16 (1): 139–48. doi:10.1111/gbb.12363.

Mu, Jian, W. Breckinridge Carden, Nuwan C. Kurukulasuriya, Georgia M. Alexander, and Dwayne W. Godwin. 2003. “Ethanol Influences on Native T-Type Calcium Current in Thalamic Sleep Circuitry.” *The Journal of Pharmacology and Experimental Therapeutics* 307 (1): 197–204. doi:10.1124/jpet.103.053272.

Pinel, J. P., R. Skelton, and R. F. Mucha. 1976. “Kindling-Related Changes in Afterdischarge ‘Thresholds.’” *Epilepsia* 17 (2): 197–206.

Racine, R. J. 1972. “Modification of Seizure Activity by Electrical Stimulation. II. Motor Seizure.” *Electroencephalography and Clinical Neurophysiology* 32 (3): 281–94.

Riegle, Melissa A., Melissa L. Masicampo, Erin H. Caulder, and Dwayne W. Godwin. 2014. “Ethosuximide Reduces Electrographical and Behavioral Correlates of Alcohol Withdrawal Seizure in DBA/2J Mice.” *Alcohol (Fayetteville, N.Y.)* 48 (5): 445–53. doi:10.1016/j.alcohol.2014.01.010.

Riegle, Melissa A., Melissa L. Masicampo, Hong Qu Shan, Victoria Xu, and Dwayne W. Godwin. 2015. “Ethosuximide Reduces Mortality and Seizure Severity in Response to Pentylenetetrazole Treatment During Ethanol Withdrawal.” *Alcohol and Alcoholism (Oxford, Oxfordshire)* 50 (5): 501–8. doi:10.1093/alcalc/agv033.

Squires, R. F., E. Saederup, J. N. Crawley, P. Skolnick, and S. M. Paul. 1984. “Convulsant Potencies of Tetrazoles Are Highly Correlated with Actions on GABA/Benzodiazepine/Picrotoxin Receptor Complexes in Brain.” *Life Sciences* 35 (14): 1439–44.

Szabó, G., G. L. Kovács, and G. Telegdy. 1984. “Increased Sensitivity to Picrotoxin as an Index of Physical Dependence on Alcohol in the Mouse.” *Drug and Alcohol Dependence* 14 (2): 187–95.

Vaidya, Sachin P., and Daniel Johnston. 2013. “Temporal Synchrony and Gamma-to-Theta Power Conversion in the Dendrites of CA1 Pyramidal Neurons.” *Nature Neuroscience* 16 (12): 1812–20. doi:10.1038/nn.3562.

Valenzuela, C. F., R. A. Cardoso, M. J. Wick, J. L. Weiner, T. V. Dunwiddie, and R. A. Harris. 1998. “Effects of Ethanol on Recombinant Glycine Receptors Expressed in Mammalian Cell Lines.” *Alcoholism, Clinical and Experimental Research* 22 (5): 1132–36.

Veatch, L. M., and L. P. Gonzalez. 1996. “Repeated Ethanol Withdrawal Produces Site-Dependent Increases in EEG Spiking.” *Alcoholism, Clinical and Experimental Research* 20 (2): 262–67.

Veatch, Lynn M., and Howard C. Becker. 2002. “Electrographic and Behavioral Indices of Ethanol Withdrawal Sensitization.” *Brain Research* 946 (2): 272–82. doi:10.1016/S0006-8993(02)02895-0.

Victor, M., and C. Brausch. 1967. “The Role of Abstinence in the Genesis of Alcoholic Epilepsy.” *Epilepsia* 8 (1): 1–20.

Wang, H., J. Peca, M. Matsuzaki, K. Matsuzaki, J. Noguchi, L. Qiu, D. Wang, et al. 2007. “High-Speed Mapping of Synaptic Connectivity Using Photostimulation in Channelrhodopsin-2 Transgenic Mice.” *Proc.Natl Acad.Sci.U.S.A.* 104 (19): 8143–48.

Wiggins, Walter F., John D. Graef, Tiffany W. Huitt, and Dwayne W. Godwin. 2013. “Ethosuximide Reduces Ethanol Withdrawal-Mediated Disruptions in Sleep-Related EEG Patterns.” *Alcoholism, Clinical and Experimental Research* 37 (3): 372–82. doi:10.1111/j.1530-0277.2012.01938.x.

CHAPTER 4

LEVETIRACETAM BUT NOT ETHOSUXIMIDE IS EFFECTIVE IN REDUCING OPTICALLY-INDUCED POPULATION DISCHARGE THRESHOLD (oPDT) IN MODELS OF CNS HYPEREXCITABILITY

G.E. Alberto; D.C. Klorig; D.W. Godwin

Abstract

Alcohol withdrawal (WD) produces a pathological state of central nervous system (CNS) hyperexcitability. Individuals who suffer from alcohol use disorder (AUD) are susceptible to experiencing WD upon cessation of alcohol consumption. During WD there is an increased risk of seizure and death requiring aggressive pharmacologic intervention to reduce CNS hyperexcitability and the risk of seizure. Behavioral and electrophysiological investigations of WD have documented a number of molecular changes contributing to CNS hyperexcitability that occur in response to chronic ethanol exposure. These molecular changes represent potential targets for novel pharmacotherapies for treatment of WD seizure. One such change is the upregulation of T-type Ca^{2+} channels, which contribute to neuronal burst firing. Treatment with a T-type Ca^{2+} channel blocker, ethosuximide (ETX), has been shown to be effective at reducing some measures of CNS hyperexcitability in WD. We employ a novel method for probing the excitability state of a hippocampal circuit, which we term optically-induced Population Discharge Threshold (oPDT) testing, in order to test whether ETX can be effective in offsetting CNS hyperexcitability during WD as measured with oPDT. Additionally, we utilize the drug pentylenetetrazole (PTZ) to mimic CNS hyperexcitability in order to test a drug with a much broader influence on circuit excitability, Levetiracetam (LEV). We show that while ETX is effective in reducing oPDT in alcohol naïve animals it is unable to counteract the hyperexcitability associated with WD as measured by oPDT, nor is it effective in reducing the number of spontaneously occurring population spikes (PS). We go

on to show that LEV is effective at reducing oPDT in the hyperexcitable brain. We suggest that circuit level excitation such as that associated with PS is a complex circuit phenomenon, which can be insensitive to the effects of modulating a single ion channel

.

Introduction

Alcohol withdrawal syndrome (AWS) represents a dangerous pathological condition that manifests upon cessation of alcohol consumption following long-term chronic alcohol abuse (Jesse et al. 2017). Enhanced central nervous system (CNS) inhibitory drive in the presence of acute alcohol intoxication promotes molecular and functional changes in the CNS to upregulate the excitatory processes (Becker 1998, 2000, 2008). When alcohol is removed from the system, the excess excitatory drive is unmasked resulting in a hyperexcitable CNS (Gonzalez et al. 2001). It is this CNS hyperexcitability that is responsible for many of the symptoms of AWS, including seizure (Jesse et al. 2017). Clinically, seizure represents the most concerning symptom of AWS as it is associated with high mortality (Kattimani and Bharadwaj 2013; Mainerova et al. 2015). Seizure will occur in up to 15% of patients within 24-48 hours of alcohol cessation (Mennecier et al. 2008; Chan et al. 2009; Victor and Brausch 1967; Bråthen et al. 1999), and currently requires aggressive treatment with benzodiazepines (BZDs) (Jesse et al. 2017; Ait-Daoud et al. 2006).

BZDs selectively bind and potentiate gamma-aminobutryic acid type A receptors ($GABA_AR$) leading to increased influx of Cl^- ions. This amplification of inhibitory tone by BZDs mirrors the effects of alcohol to aid in the prevention of WD seizure (Davies and Alkana 2001; Davies 2003; Amato et al. 2010). The effects of chronic alcohol use on excitability are broad, modulating not only $GABA_ARs$ (Cagetti et al. 2003) but also N-methyl-D-aspartate receptors (NMDAR) (Kalluri et

al. 1998) and other modulators of intrinsic excitability (Kourrich et al. 2015). Dysregulation at any molecular subsystem of the CNS represents a potential therapeutic target for the treatment of aspects of AWS and associated seizure.

One such target of interest is the T-type Ca^{2+} channel. Our lab has demonstrated in an animal model of chronic ethanol exposure that T-type Ca^{2+} channels are inhibited during acute ethanol exposure and upregulated during WD in C57 Bl/6 mice (Graef et al. 2011; Shan et al. 2013), and that treatment with the T-type Ca^{2+} channel blocker ethosuximide (ETX) improves WD symptoms (Wiggins et al. 2013; Riegle et al. 2014, 2015) in DBA/2J mice, including improved survival.

T-type Ca^{2+} channels are expressed throughout the brain, particularly in the thalamus and hippocampus (Cain and Snutch 2013). These channels are responsible for pacing specific thalamocortical oscillations associated with sleep and pathological dysrhythmias associated with a specific seizure type, absence seizure (Kandel and Buzsáki 1997; Lee et al. 2004; Astori et al. 2011). Importantly, in animal models of WD a thalamocortical rhythm, brief spindle episode (BSE), associated with the T-type Ca^{2+} channel has been used as a metric of CNS hyperexcitability (Veatch and Becker 2002; Riegle et al. 2014). BSEs occur in all rodents typically during sleep, however the DBA/2J mouse experiences BSEs during active wakefulness making it an attractive model for BSE based studies of WD hyperexcitability (Ryan 1984; Riegle et al. 2014). Dysfunction of T-type Ca^{2+} reduces thalamocortical rhythms in animal models (Lee et al. 2004; Astori et al. 2011), and T-type Ca^{2+} channel blockade with ETX during WD reduces the frequency of BSEs (Riegle et al. 2014).

In this study we set out to determine if Ca^{2+} channel blockade alone using ETX would be sufficient to reduce a phenotype of WD associated with temporal-lobe seizure using a newly developed method called optically-induced Population Discharge Threshold (oPDT) (Chapter 1, Chapter 2). We test whether ETX can reduce the frequency of spontaneous population spikes (PS) and if it can increase the oPDT during WD. We then compare that to the anti-epileptic drug (AED) levetiracetam (LEV) which has broad circuit level mechanisms for reducing pentylenetetrazol (PTZ) induced hyperexcitability (Lee et al. 2009; Fukuyama et al. 2012; Wakita et al. 2014; Nagarkatti et al. 2008; Yan et al. 2013). We find that while in alcohol naïve animals Ca^{2+} alone is sufficient for increasing oPDT it does not do so during WD hyperexcitability nor does it reduce the frequency of spontaneous PS. Conversely, the wide range effects of LEV are able to increase oPDT in a hyperexcitable state. This result suggests that circuit hyperexcitability measureable with oPDT testing is profoundly complex such that blockade of a single ion channel is not sufficient to ameliorate it. Furthermore, these results indicate differentiable phenotypes associated with hyperexcitability: those that are a consequence of complex reciprocal circuitry and those that are associated with single molecule changes.

Materials and Methods

For a detailed discussion of the methods refer to Chapters 1 and 2.

Animals

Male Thy1-ChR2-YFP (founder line 18) transgenic mice (Arenkiel et al. 2007; Wang et al. 2007) (Stock # 007612, The Jackson Laboratory) were used for chronic optogenetic stimulation and recording (n = 8). All animal experiments were approved by the Institutional Animal Care and Use Committee (IACUC) of Wake Forest University and in agreement with National Institutes of Health and United States Department of Agriculture guidelines, including practices to reduce suffering and animal numbers to the extent possible.

Chronic Implant and surgery

The same implant preparation was used as in Chapter 2 (detailed in Klorig and Godwin 2014). Eight 35µm tungsten micro-wires were implanted in a satellite array throughout hippocampal and perihippocampal structures. These include: prefrontal cortex (PFC), anterior medial thalamic nucleus (AM), entorhinal cortex (Ent), dentate gyrus (DG), subiculum (Sub), CA1 of hippocampus contralateral to the site of stimulation (rCA1), CA3 of hippocampus (CA3), and CA1 of the stimulated hippocampus (CA1). The site of stimulation, CA1, was implanted with a custom optrode constructed from a length of fiber optic and a tungsten micro-wire. A ground was placed over the cerebellum aiding in high quality, low artifact, field potential recordings. The design of the implant allows for the animals to move freely in the recording cage. Surgery was conducted under isoflurane, and animals were allowed to recover for at least 1 week prior to testing.

Chronic Intermittent Ethanol (CIE)

After recovery implanted mice (n=6) were exposed to a chronic intermittent ethanol inhalation paradigm as described by Becker and Hale and used previously in the Godwin lab (Becker and Hale 1993; Graef et al. 2011; Riegle et al. 2014). The protocol used for CIE was identical to Chapter 3, there were four 16h periods of ethanol vapor exposure followed by four 8h periods of WD.

Stimulation and Recording

Recording and stimulation protocols were identical to Chapter 3. Wideband (0.3-20kHz) depth recordings were conducted at 40kHz sampling rate using SciWorks recording system (DataWave Technologies). LED stimulation was controlled using an LED driver with analog modulation (Mightex Systems).

Pharmacology testing and oPDT

The oPDT test was conducted as detailed in Chapter 2 and Chapter 3. Ten levels of optical intensity were each pulsed for 10ms in random order to test oPDT. oPDT was conducted prior to CIE and during each withdrawal period in a cohort of animals (n=6). In the final WD period animals were subjected to oPDT testing then immediately injected with 250 mg/kg ETX. After 20 min, animals were retested with oPDT. Additionally, spontaneous PS were counted during 10 min no stimulation baseline periods or oPDT testing during each WD.

In a second cohort of animals (n=4) baseline oPDT was determined. PTZ was then used to induce CNS hyperexcitability (Squires et al. 1984; Psarropoulou et

al. 1994) and oPDT was retested. Finally, LEV was administered (40 mg/kg) while the animal was still in a hyperexcitable state and oPDT was retested. Power analysis reveals that a cohort of 4 animals is sufficient to detect significant shifts in oPDT I_{50} as low as 0.4 of normalized intensity.

Data Analysis and Statistics

Data were analyzed in the same fashion as Chapter 3 using Sciworks, NeuroExplorer (Nex Tehcnologies), and custom scripts in MatLab (Mathworks). Data were filtered and spikes were thresholded to sort PS; suspected PS were then visually inspected. Statistical testing was performed using Prism (GraphPad). Measures of spontaneous spiking during each WD compared to baseline were conducted using one-way analysis of variance (ANOVA) or Kruskal-Wallis Test with Tukey's or Dunn's multiple comparisons test where appropriate comparing the mean of each WD period for each animal to the mean of every other condition. I_{50} significance was determined using one-way ANOVA or Kruskal-Wallis Test with Tukey's or Dunn's multiple comparisons test to compare the means of each condition where appropriate. Correlation coefficients were calculated using Pearson's method.

Results

CIE led to a significant increase in spontaneous PS frequency during the 4^{th} WD period compared to baseline ($p<0.013$). Treatment with 250 mg/kg ETX did not significantly reduce spontaneous PS frequency compared to the 4^{th} WD ($p>0.999$), and the treatment condition remained significantly different from

baseline (p<0.035; Figure 3.1).

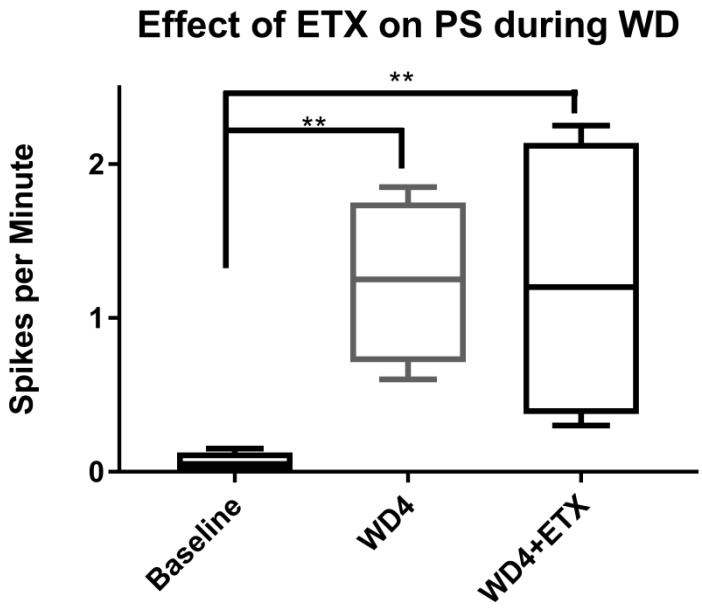

Figure 3.1 ETX does not significantly reduce the frequency of spontaneous PS during EtOH WD. The frequency of spontaneously occurring PS increases significantly by the 4th WD from CIE exposure indicating CNS hyperexcitability (p=0.013, Kruskal-Wallis test with Dunn's multiple comparisons test). Treatment with the Ca^{2+} blocker ETX does not significantly reduce PS frequency compared to the untreated condition and the treatment condition remained significantly increased from baseline (p>0.9999 and p<0.035; Kruskal-Wallis test with Dunn's multiple compariscont).

oPDT was measured during each WD period of CIE. Consistent with results from Chapter 3 oPDT was sensitive to CNS hyperexcitability during WD. The entire Boltzmann curve shifts left during the 4th WD, indicating a reduction in PS threshold (Figure 3.2a). Significance testing was again conducted using the I_{50} and was significant during the 4th WD (Figure 3.2b). ETX was applied after the initial test and oPDT was conducted again. Upon retesting, the optical threshold for induced PS continued to shift left (Figure 3.2a), and the I_{50} was significantly

reduced compared to both baseline and the untreated 4th WD condition (Figure 3.2b).

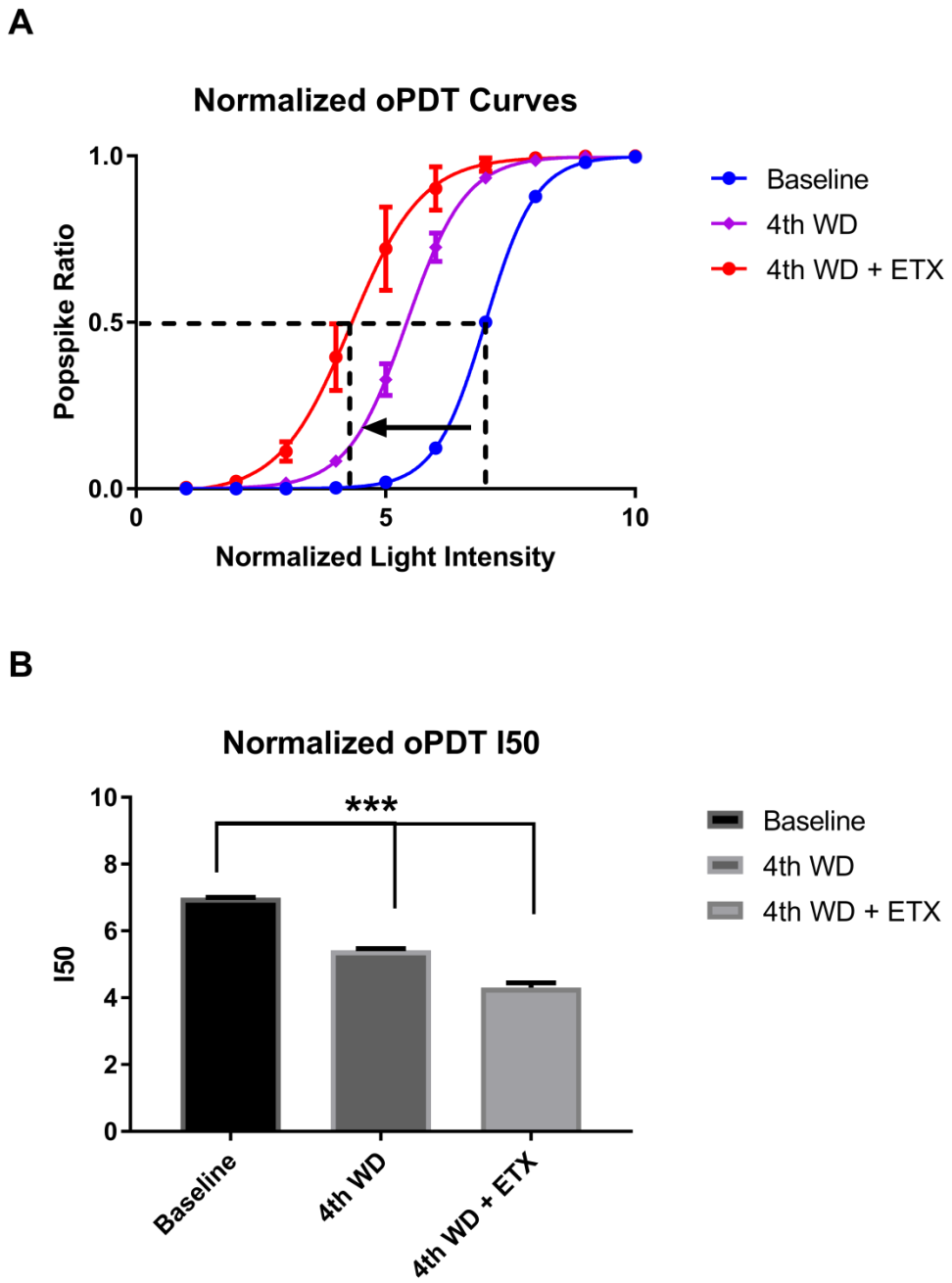

Figure 3.2 Ethosuximide does not raise oPDT during WD. A. oPDT was tested during each WD period of CIE exposure. A PS curve was generated and fit with a Boltzmann Curve in order to estimate the I_{50}. There is a leftward shift in threshold during WD and ETX does not reconcile that shift. **B.** Quantification of I_{50} indicates a significant reduction in the PS threshold during WD. I_{50} during WD remained significantly reduced from baseline upon treatment with ETX (***p<0.0001; F(3.15)=5.796; DF=5, one way ANOVA with Tukey's multiple comparisons test)

PTZ was used to induce hyperexcitability in the CNS (Squires et al. 1984; Psarropoulou et al. 1994). Treatment with a subconvulstant dose of PTZ, 20 mg/kg, significantly reduced oPDT (Figure 3.3). Treatment with the AED LEV, 40 mg/kg, reversed this reduction in oPDT returning it to a level that was no longer significantly different to baseline (Figure 3.3).

A

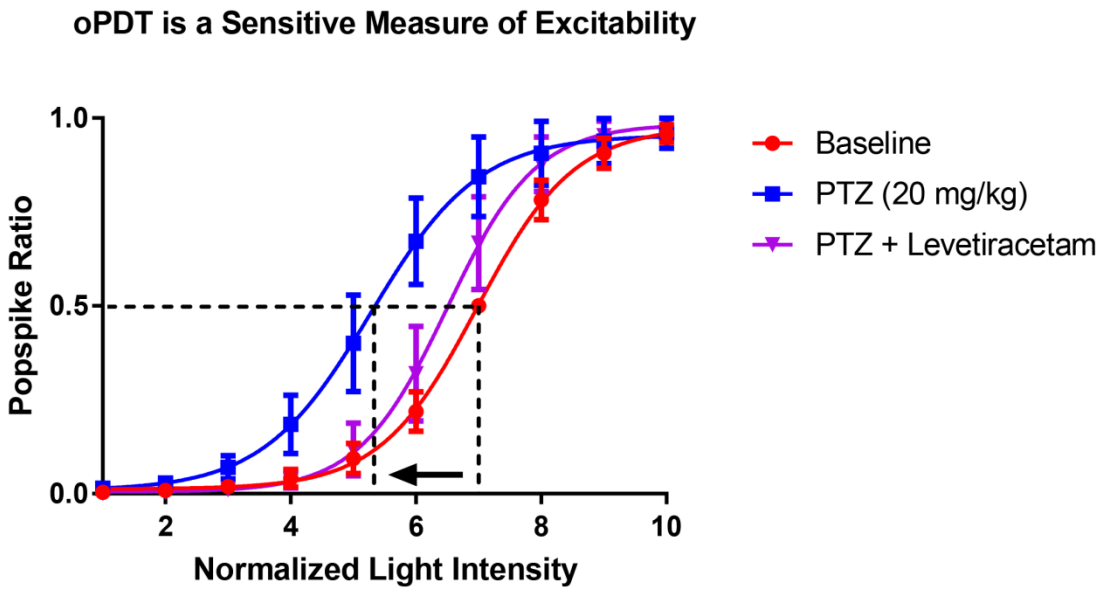

B

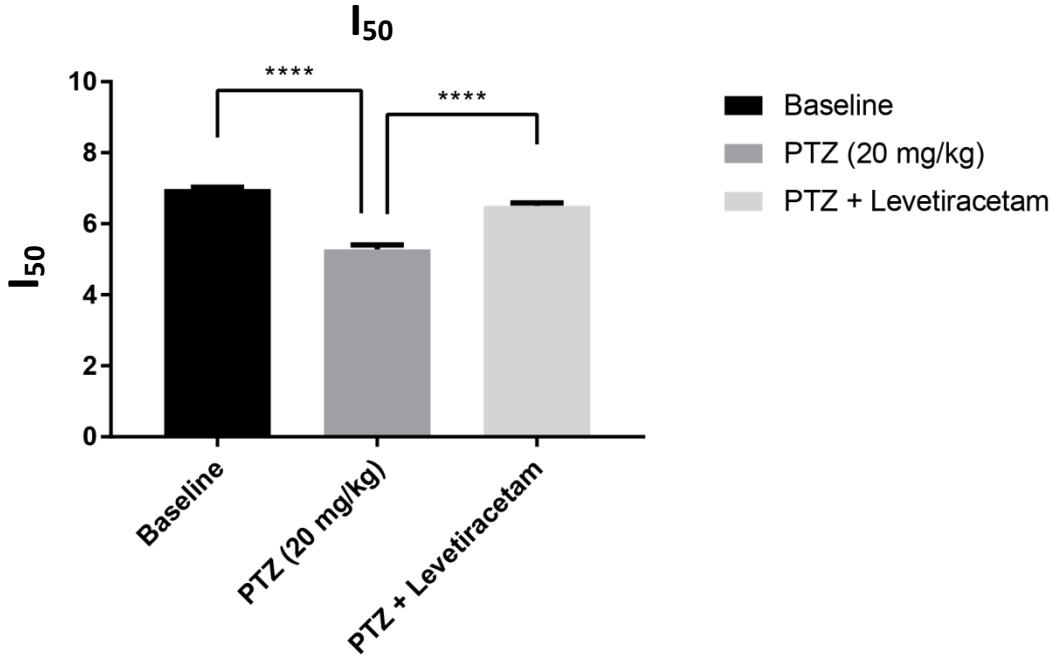

Figure 3.3 Levetiracetam returns oPDT to baseline level in PTZ induced hyperexcitability. A. PS curve shows a shift to the left following treatment with PTZ indicating hyperexcitability. This shift is reversed to baseline upon treatment with LEV. **B.** Quantification of I_{50} demonstrates that PTZ significantly reduces PS threshold, and that LEV significantly raises the threshold (***p<0.0001; ANOVA with Tukey's multiple comparisons test.

Discussion

The T-type Ca^{2+} channel blocking anti-epileptic drug ethosuximide was tested after a single cycle of CIE exposure. During WD the frequency of spontaneous PS was increased, consistent with previous findings (Veatch and Gonzalez 1996). ETX had no significant effect on the frequency of spiking in the hippocampal circuit. Similarly, oPDT was reduced during WD indicating hyperexcitability in the observed neural circuit (Chapter 2, Chapter 3). After treatment with ETX oPDT did not return to baseline. Alternatively, treatment with LEV during PTZ induced hyperexcitability was effective at returning oPDT to baseline levels.

The drug PTZ was used to induce hyperexcitability because it mimics the functional and molecular effects of WD from alcohol and allows for rapid screening without the need for CIE. PTZ inhibits the $GABA_AR$ complex and reduces the total density of $GABA_AR$ in hippocampus and cortex (Squires et al. 1984; Psarropoulou et al. 1994). Additionally, PTZ treatment in kindling upregulates NMDA receptor expression (Zhu et al. 2015) and blocking NMDAR reduces PTZ related seizure (Zaitsev et al. 2015) suggesting a role for NMDA excitability in PTZ seizure similar to that which is seen in alcohol WD seizure. At higher doses (>50mg/kg) PTZ induces seizure when administered systemically. However, in this study a sub-convulsant dose (20 mg/kg) was administered to induce a mild CNS hyperexcitability similar to that seen in WD. Hyperexcitability was detectable with oPDT providing additional support that PTZ treatment produced a WD-like hyperexcitable state. In both WD and PTZ treatment oPDT is

reduced by about 23-30%. Of course, PTZ treatment is not identical to ethanol WD, and further testing of LEV in a WD condition will be required to fully elucidate the efficacy of circuit level excitability reductions attributable to LEV specifically during WD. It is clear from these results however, that LEV functions in such a way as to reduce circuit excitability which affects the optically-induced PS more effectively than ETX when in a hyperexcitable state.

ETX acts to reduce low-threshold T-type Ca^{2+} channel currents by binding to and blocking the channel (Gören and Onat 2007). The T-type Ca^{2+} channel is expressed throughout the brain but the densest expression is in thalamic structures where it participates in pacing of thalamocortical oscillations related to sleep (Cain and Snutch 2013; Kandel and Buzsáki 1997). An important pathology related to the T-type Ca^{2+} channel is the absence seizure. This seizure type produces a thalamocortical rhythm similar to the sleep rhythm (Kandel and Buzsáki 1997; Pinault et al. 2001; Seidenbecher and Pape 2001). This seizure type appears to rely specifically on the presence of functional T-type Ca^{2+} channels, and when they are dysfunctional or absent characteristic spike-and-wake discharges are significantly reduced or absent (Becker et al. 2008; Lee 2004; Astori et al. 2011). Similarly, blockade of T-type Ca^{2+} channels with ETX is effective at reducing spike-and-wave discharges clinically and in genetic models of absence epilepsy (Gilbert et al. 2002; Ishige et al. 2001; Gören and Onat 2007). Importantly, ETX does not appear to be effective in reducing afterdischarges or behavioral seizure in kindling models (Albright and Burnham

1980; Gilbert et al. 2002; Gilbert and Teskey 2007), and is not used in myoclonic seizure disorders other than as adjunctive therapy (Gören and Onat 2007).

Studies of alcohol WD which show efficacy with ETX have utilized the DBA/2J mouse which experiences a thalamocortical rhythm called the brief spindle episode (BSE) (Ryan 1984). Increases in the occurrence of BSE have been used as a measure of CNS hyperexcitability during EtOH WD (Veatch and Becker 2002; Riegle et al. 2014). ETX was shown to be effective at reducing tonic-clonic seizure and improving survival induced by PTZ administration during WD in DBA/2J mice (Riegle et al. 2015). The context of these studies, though, may be limited to thalamocortical rhythms and their increased occurrence during WD.

On the other hand, LEV has a wide range of molecular interactions that affect the excitability state of a neuronal population. The functional effects of LEV include reductions in vesicular release (Lee et al. 2009; Fukuyama et al. 2012), increased presynaptic $GABA_AR$ activity (Wakita et al. 2014), decreased intracellular Ca^{2+} release (Nagarkatti et al. 2008), and decreased extracellular Ca^{2+} entry (Yan et al. 2013). In the context of population based activity, as indicated by oPDT, it appears that broad modulation of excitation is required. Additionally, potent amplification of the overall inhibitory tone by modulation of $GABA_AR$ whereby the activity of the entire CNS diminishes is effective (Davies 2003; Davies and Alkana 2001; Wakita et al. 2014). This suggests a role for population based modulation of the excitability state in the manifestation of particular pathological phenotypes associated with alcohol WD, specifically tonic-clonic seizure as indicated by the PS.

Based on the findings presented here the population dynamics governing tonic-clonic generalized seizure, and correlates thereof (e.g. oPDT), appear to be insensitive to modulation of single ion channels, which are highly effective in mice that possess a baseline seizure phenotype. This result then differentiates pathological thalamocortical rhythms (e.g. BSE), which are governed by the functioning of a single molecule from population hyperexcitability, which plays a role in PS and tonic-clonic seizure. We propose that a distinction exists amongst the multiple observable electrographic and behavioral phenotypes associated with WD hyperexcitability. It is clear that many effector molecules and circuits behave inappropriately as a result of WD hyperexcitability, but the context of the population, or circuit, in which those maladaptive changes occur, and the complexity therein, determines the efficacy of pharmacologic intervention and likely the appropriateness of treatment choices. It will be paramount in the discovery of novel pharmacotherapies for AWS and WD seizure to identify compounds which effectively modulate the circuits related to the specific symptom of interest as opposed to compounds which address hyperexcitability as a simple catchall.

Acknowledgments

This work was supported by NIH grants F30 AA023708, T32AA07565, R01AA016852, P01AA021099, and the Tab Williams Family Fund. The authors declare no competing financial or other conflicts of interest.

References

Ait-Daoud, Nassima, Robert J. Malcolm, and Bankole A. Johnson. 2006. “An Overview of Medications for the Treatment of Alcohol Withdrawal and Alcohol Dependence with an Emphasis on the Use of Older and Newer Anticonvulsants.” *Addictive Behaviors* 31 (9): 1628–49. doi:10.1016/j.addbeh.2005.12.029.

Albright, P. S., and W. M. Burnham. 1980. “Development of a New Pharmacological Seizure Model: Effects of Anticonvulsants on Cortical- and Amygdala-Kindled Seizures in the Rat.” *Epilepsia* 21 (6): 681–89.

Amato, Laura, Silvia Minozzi, Simona Vecchi, and Marina Davoli. 2010. “Benzodiazepines for Alcohol Withdrawal.” *The Cochrane Database of Systematic Reviews*, no. 3 (March): CD005063. doi:10.1002/14651858.CD005063.pub3.

Arenkiel, Benjamin R, Joao Peca, Ian G Davison, Catia Feliciano, Karl Deisseroth, George J Augustine, Michael D Ehlers, and Guoping Feng. 2007. “In Vivo Light-Induced Activation of Neural Circuitry in Transgenic Mice Expressing Channelrhodopsin-2.” *Neuron* 54 (2): 205–18. doi:10.1016/j.neuron.2007.03.005.

Astori, Simone, Ralf D. Wimmer, Haydn M. Prosser, Corrado Corti, Mauro Corsi, Nicolas Liaudet, Andrea Volterra, Paul Franken, John P. Adelman, and Anita Lüthi. 2011. “The Ca(V)3.3 Calcium Channel Is the Major Sleep Spindle Pacemaker in Thalamus.” *Proceedings of the National Academy of Sciences of the United States of America* 108 (33): 13823–28. doi:10.1073/pnas.1105115108.

Becker, Albert J, Julika Pitsch, Dmitry Sochivko, Thoralf Opitz, Matthäus Staniek, Chien-Chang Chen, Kevin P Campbell, Susanne Schoch, Yoel Yaari, and Heinz Beck. 2008. “Transcriptional Upregulation of Cav3.2 Mediates Epileptogenesis in the Pilocarpine Model of Epilepsy.” *The Journal of Neuroscience: The Official Journal of the Society for Neuroscience* 28 (49): 13341–53. doi:10.1523/JNEUROSCI.1421-08.2008.

Becker, H C. 1998. “Kindling in Alcohol Withdrawal.” *Alcohol Health and Research World* 22 (1): 25–33.

Becker, H. C., and R. L. Hale. 1993. “Repeated Episodes of Ethanol Withdrawal Potentiate the Severity of Subsequent Withdrawal Seizures: An Animal Model of Alcohol Withdrawal ‘Kindling.’” *Alcoholism, Clinical and Experimental Research* 17 (1): 94–98.

Becker, Howard C. 2000. “Animal Models of Alcohol Withdrawal.” *Alcohol Research and Health; Washington* 24 (2): 105–13.

———. 2008. “Alcohol Dependence, Withdrawal, and Relapse.” *Alcohol Research & Health* 31 (4): 348–61.

Bråthen, G., E. Brodtkorb, G. Helde, T. Sand, and G. Bovim. 1999. “The Diversity of Seizures Related to Alcohol Use. A Study of Consecutive Patients.” *European Journal of Neurology* 6 (6): 697–703.

Cagetti, Elisabetta, Jing Liang, Igor Spigelman, and Richard W. Olsen. 2003. “Withdrawal from Chronic Intermittent Ethanol Treatment Changes

Subunit Composition, Reduces Synaptic Function, and Decreases Behavioral Responses to Positive Allosteric Modulators of $GABA_A$ Receptors." *Molecular Pharmacology* 63 (1): 53–64. doi:10.1124/mol.63.1.53.

Cain, Stuart M., and Terrance P. Snutch. 2013. "T-Type Calcium Channels in Burst-Firing, Network Synchrony, and Epilepsy." *Biochimica et Biophysica Acta (BBA) - Biomembranes*, Calcium Channels, 1828 (7): 1572–78. doi:10.1016/j.bbamem.2012.07.028.

Chan, Gar Ming, Robert S. Hoffman, Jeffrey A. Gold, Paula J. Whiteman, Lewis R. Goldfrank, and Lewis S. Nelson. 2009. "Racial Variations in the Incidence of Severe Alcohol Withdrawal." *Journal of Medical Toxicology: Official Journal of the American College of Medical Toxicology* 5 (1): 8–14.

Davies, D. L., and R. L. Alkana. 2001. "Direct Evidence for a Cause-Effect Link between Ethanol Potentiation of GABA(A) Receptor Function and Intoxication from Hyperbaric Studies in C57, LS, and SS Mice." *Alcoholism, Clinical and Experimental Research* 25 (8): 1098–1106.

Davies, Martin. 2003. "The Role of GABAA Receptors in Mediating the Effects of Alcohol in the Central Nervous System." *Journal of Psychiatry and Neuroscience* 28 (4): 263.

Fukuyama, Kouji, Shunsuke Tanahashi, Masanori Nakagawa, Satoshi Yamamura, Eishi Motomura, Takashi Shiroyama, Hisashi Tanii, and Motohiro Okada. 2012. "Levetiracetam Inhibits Neurotransmitter Release Associated with CICR." *Neuroscience Letters* 518 (2): 69–74. doi:10.1016/j.neulet.2012.03.056.

Gilbert, Trevor H., Shannon M. Corley, and G. Campbell Teskey. 2002. "Conventional Anticonvulsant Drugs in the Guinea Pig Kindling Model of Partial Seizures: Effects of Acute Phenobarbital, Valproate, and Ethosuximide." *Experimental Brain Research* 146 (3): 336–44. doi:10.1007/s00221-002-1183-9.

Gilbert, Trevor H., and G. Campbell Teskey. 2007. "Conventional Anticonvulsant Drugs in the Guinea-Pig Kindling Model of Partial Seizures: Effects of Repeated Administration." *Experimental Brain Research* 178 (1): 115–25. doi:10.1007/s00221-006-0716-z.

Gonzalez, Larry P., Lynn M. Veatch, Maharaj K. Ticku, and Howard C. Becker. 2001. "Alcohol Withdrawal Kindling: Mechanisms and Implications for Treatment." *Alcoholism: Clinical and Experimental Research* 25 (May): 197S–201S. doi:10.1111/j.1530-0277.2001.tb02396.x.

Gören, M. Zafer, and Filiz Onat. 2007. "Ethosuximide: From Bench to Bedside." *CNS Drug Reviews* 13 (2): 224–39. doi:10.1111/j.1527-3458.2007.00009.x.

Graef, J. D., T. W. Huitt, B. K. Nordskog, J. H. Hammarback, and D. W. Godwin. 2011. "Disrupted Thalamic T-Type Ca2+ Channel Expression and Function During Ethanol Exposure and Withdrawal." *Journal of Neurophysiology* 105 (2): 528–40. doi:10.1152/jn.00424.2010.

Ishige, K., H. Endo, H. Saito, and Y. Ito. 2001. "Repeated Administration of CGP 46381, a Gamma-Aminobutyric AcidB Antagonist, and Ethosuximide

Suppresses Seizure-Associated Cyclic Adenosine 3’5’ Monophosphate Response Element- and Activator Protein-1 DNA-Binding Activities in Lethargic (Lh/Lh) Mice.” *Neuroscience Letters* 297 (3): 207–10.
Jesse, S., G. Bråthen, M. Ferrara, M. Keindl, E. Ben-Menachem, R. Tanasescu, E. Brodtkorb, M. Hillbom, M.a. Leone, and A.c. Ludolph. 2017. “Alcohol Withdrawal Syndrome: Mechanisms, Manifestations, and Management.” *Acta Neurologica Scandinavica* 135 (1): 4–16. doi:10.1111/ane.12671.
Kalluri, Haviryaji S. G, Ashok K Mehta, and Maharaj K Ticku. 1998. “Up-Regulation of NMDA Receptor Subunits in Rat Brain Following Chronic Ethanol Treatment.” *Molecular Brain Research* 58 (1–2): 221–24. doi:10.1016/S0169-328X(98)00112-0.
Kandel, Adam, and György Buzsáki. 1997. “Cellular–Synaptic Generation of Sleep Spindles, Spike-and-Wave Discharges, and Evoked Thalamocortical Responses in the Neocortex of the Rat.” *The Journal of Neuroscience* 17 (17): 6783–97.
Kattimani, Shivanand, and Balaji Bharadwaj. 2013. “Clinical Management of Alcohol Withdrawal: A Systematic Review.” *Industrial Psychiatry Journal* 22 (2): 100–108. doi:10.4103/0972-6748.132914.
Klorig, David C., and Dwayne W. Godwin. 2014. “A Magnetic Rotary Optical Fiber Connector for Optogenetic Experiments in Freely Moving Animals.” *Journal of Neuroscience Methods* 227 (April): 132–39. doi:10.1016/j.jneumeth.2014.02.013.
Kourrich, Saïd, Donna J. Calu, and Antonello Bonci. 2015. “Intrinsic Plasticity: An Emerging Player in Addiction.” *Nature Reviews. Neuroscience* 16 (3): 173–84. doi:10.1038/nrn3877.
Lee, Chun-Yao, Chih-Chuan Chen, and Horng-Huei Liou. 2009. “Levetiracetam Inhibits Glutamate Transmission through Presynaptic P/Q-Type Calcium Channels on the Granule Cells of the Dentate Gyrus.” *British Journal of Pharmacology* 158 (7): 1753–62. doi:10.1111/j.1476-5381.2009.00463.x.
Lee, Jungryun, Daesoo Kim, and Hee-Sup Shin. 2004. “Lack of Delta Waves and Sleep Disturbances during Non-Rapid Eye Movement Sleep in Mice Lacking Alpha1G-Subunit of T-Type Calcium Channels.” *Proceedings of the National Academy of Sciences of the United States of America* 101 (52): 18195–99. doi:10.1073/pnas.0408089101.
Mainerova, Barbora, Jan Prasko, Klara Latalova, Karel Axmann, Monika Cerna, Rostislav Horacek, and Romana Bradacova. 2015. “Alcohol Withdrawal Delirium - Diagnosis, Course and Treatment.” *Biomedical Papers of the Medical Faculty of the University Palacky, Olomouc, Czechoslovakia* 159 (1): 44–52. doi:10.5507/bp.2013.089.
Mennecier, D., M. Thomas, P. Arvers, D. Corberand, L. Sinayoko, S. Bonnefoy, F. Harnois, and C. Thiolet. 2008. “Factors Predictive of Complicated or Severe Alcohol Withdrawal in Alcohol Dependent Inpatients.” *Gastroenterologie Clinique Et Biologique* 32 (8–9): 792–97. doi:10.1016/j.gcb.2008.06.004.
Nagarkatti, Nisha, Laxmikant S. Deshpande, and Robert J. DeLorenzo. 2008. “Levetiracetam Inhibits Both Ryanodine and IP3 Receptor Activated

Calcium Induced Calcium Release in Hippocampal Neurons in Culture." *Neuroscience Letters* 436 (3): 289–93. doi:10.1016/j.neulet.2008.02.076.
Pinault, D, M Vergnes, and C Marescaux. 2001. "Medium-Voltage 5–9-Hz Oscillations Give Rise to Spike-and-Wave Discharges in a Genetic Model of Absence Epilepsy: In Vivo Dual Extracellular Recording of Thalamic Relay and Reticular Neurons." *Neuroscience* 105 (1): 181–201. doi:10.1016/S0306-4522(01)00182-8.
Psarropoulou, C., N. Matsokis, F. Angelatou, and G. Kostopoulos. 1994. "Pentylenetetrazol-Induced Seizures Decrease Gamma-Aminobutyric Acid-Mediated Recurrent Inhibition and Enhance Adenosine-Mediated Depression." *Epilepsia* 35 (1): 12–19.
Riegle, Melissa A., Melissa L. Masicampo, Erin H. Caulder, and Dwayne W. Godwin. 2014. "Ethosuximide Reduces Electrographical and Behavioral Correlates of Alcohol Withdrawal Seizure in DBA/2J Mice." *Alcohol (Fayetteville, N.Y.)* 48 (5): 445–53. doi:10.1016/j.alcohol.2014.01.010.
Riegle, Melissa A., Melissa L. Masicampo, Hong Qu Shan, Victoria Xu, and Dwayne W. Godwin. 2015. "Ethosuximide Reduces Mortality and Seizure Severity in Response to Pentylenetetrazole Treatment During Ethanol Withdrawal." *Alcohol and Alcoholism (Oxford, Oxfordshire)* 50 (5): 501–8. doi:10.1093/alcalc/agv033.
Ryan, Lawrence J. 1984. "Characterization of Cortical Spindles in DBA/2 and C57BL/6 Inbred Mice." *Brain Research Bulletin* 13 (4): 549–58. doi:10.1016/0361-9230(84)90037-6.
Seidenbecher, Thomas, and Hans-Christian Pape. 2001. "Contribution of Intralaminar Thalamic Nuclei to Spike-and-Wave-Discharges during Spontaneous Seizures in a Genetic Rat Model of Absence Epilepsy." *European Journal of Neuroscience* 13 (8): 1537–1546. doi:10.1046/j.0953-816x.2001.01537.x.
Shan, Hong Qu, James A. Hammarback, and Dwayne W. Godwin. 2013. "Ethanol Inhibition of a T-Type Ca^{2}+ Channel through Activity of Protein Kinase C." *Alcoholism, Clinical and Experimental Research* 37 (8): 1333–42. doi:10.1111/acer.12098.
Squires, R. F., E. Saederup, J. N. Crawley, P. Skolnick, and S. M. Paul. 1984. "Convulsant Potencies of Tetrazoles Are Highly Correlated with Actions on GABA/Benzodiazepine/Picrotoxin Receptor Complexes in Brain." *Life Sciences* 35 (14): 1439–44.
Veatch, L. M., and L. P. Gonzalez. 1996. "Repeated Ethanol Withdrawal Produces Site-Dependent Increases in EEG Spiking." *Alcoholism, Clinical and Experimental Research* 20 (2): 262–67.
Veatch, Lynn M., and Howard C. Becker. 2002. "Electrographic and Behavioral Indices of Ethanol Withdrawal Sensitization." *Brain Research* 946 (2): 272–82. doi:10.1016/S0006-8993(02)02895-0.
Victor, M., and C. Brausch. 1967. "The Role of Abstinence in the Genesis of Alcoholic Epilepsy." *Epilepsia* 8 (1): 1–20.
Wakita, Masahito, Naoki Kotani, Kyuya Kogure, and Norio Akaike. 2014. "Inhibition of Excitatory Synaptic Transmission in Hippocampal Neurons

by Levetiracetam Involves Zn^{2+}-Dependent GABA Type A Receptor-Mediated Presynaptic Modulation." *The Journal of Pharmacology and Experimental Therapeutics* 348 (2): 246–59. doi:10.1124/jpet.113.208751.

Wang, H., J. Peca, M. Matsuzaki, K. Matsuzaki, J. Noguchi, L. Qiu, D. Wang, et al. 2007. "High-Speed Mapping of Synaptic Connectivity Using Photostimulation in Channelrhodopsin-2 Transgenic Mice." *Proc.Natl Acad.Sci.U.S.A.* 104 (19): 8143–48.

Wiggins, Walter F., John D. Graef, Tiffany W. Huitt, and Dwayne W. Godwin. 2013. "Ethosuximide Reduces Ethanol Withdrawal-Mediated Disruptions in Sleep-Related EEG Patterns." *Alcoholism, Clinical and Experimental Research* 37 (3): 372–82. doi:10.1111/j.1530-0277.2012.01938.x.

Yan, Hai-Dun, Kumatoshi Ishihara, Takahiro Seki, Ryosuke Hanaya, Kaoru Kurisu, Kazunori Arita, Tadao Serikawa, and Masashi Sasa. 2013. "Inhibitory Effects of Levetiracetam on the High-Voltage-Activated L-Type Ca^{2+} Channels in Hippocampal CA3 Neurons of Spontaneously Epileptic Rat (SER)." *Brain Research Bulletin* 90 (January): 142–48. doi:10.1016/j.brainresbull.2012.10.006.

Zaitsev, Aleksey V., Kira Kh Kim, Dmitry S. Vasilev, Nera Ya Lukomskaya, Valeria V. Lavrentyeva, Natalia L. Tumanova, Igor A. Zhuravin, and Lev G. Magazanik. 2015. "N-Methyl-D-Aspartate Receptor Channel Blockers Prevent Pentylenetetrazole-Induced Convulsions and Morphological Changes in Rat Brain Neurons." *Journal of Neuroscience Research* 93 (3): 454–65. doi:10.1002/jnr.23500.

Zhu, Xinjian, Jingde Dong, Kai Shen, Ying Bai, Yuan Zhang, Xuan Lv, Jie Chao, and Honghong Yao. 2015. "NMDA Receptor NR2B Subunits Contribute to PTZ-Kindling-Induced Hippocampal Astrocytosis and Oxidative Stress." *Brain Research Bulletin* 114 (May): 70–78. doi:10.1016/j.brainresbull.2015.04.002.

CHAPTER 5

Discussion and Future Directions

G. E. Alberto

Summary of Results

Ingestion of alcohol has profound neurobiological affects both acutely and when administered chronically. Acutely, alcohol increases the overall inhibitory tone of the CNS (Becker 2008). When the CNS is chronically exposed to the amplified inhibition of alcohol intoxication, homeostatic pressure to increase excitatory drive leads to complex and diverse molecular changes. The cycle of intoxication followed by withdrawal from alcohol accelerates this homeostatic drive, leading to CNS hyperexcitability when alcohol is not present in the system (Ballenger and Post 1978; Becker 1998). Clinically, this type of CNS hyperexcitability presents as Alcohol Withdrawal Syndrome (AWS) and represents a very dangerous pathological state that requires immediate and aggressive pharmacologic intervention, most often with the benzodiazepine (BZD) class of drugs (Holbrook et al. 1999; Amato et al. 2010; Jesse et al. 2017). While BZDs are effective in many cases of AWS, there are associated risks with BZD use, including respiratory depression and abuse potential, and they sometimes fail or only provide partial protection from seizures, which are the most severe and dangerous symptom of AWS (Ait-Daoud et al. 2006; Amato et al. 2010; Jesse et al. 2017).

In order to develop and test novel pharmacotherapies, as well as to simply gain a more detailed understanding of the etiology and pathophysiology of AWS, it is critical to have high quality pre-clinical models. There are a large number of animal models that faithfully reproduce the features of alcohol use disorder (AUD) (Becker 2013) and AWS (Becker 2000), which have been instrumental in

advancing the understanding of this disease process. Here, we have combined a well-established model of AUD, chronic intermittent ethanol (CIE) vapor exposure (Becker and Hale 1993), with a newly developed method for investigating CNS excitability, in order to probe CNS hyperexcitability during alcohol WD. We are able to demonstrate that optically-induced Population Discharge Threshold (oPDT) testing is a sensitive measure of alcohol WD hyperexcitability. We then used the metric to test efficacy of the drug ethosuximide (ETX) in affecting the oPDT curve during WD.

Using an 8-channel satellite recording array we were able to detect significant increases in the frequency of spontaneous population spikes (PS) during WD, specifically the 3rd and 4th WD periods of CIE. The occurrence of spontaneous PS during WD on EEG is a known indicator of CNS hyperexcitability during WD (Veatch and Gonzalez 1996). In optically kindled animals the threshold for optically induced seizure was lowered during WD. Seizure threshold measured by susceptibility to chemoconvulsant-induced seizure as well as electrical stimulation is another known indicator of CNS hyperexcitability during WD (Velísek et al. 1989; Grant et al. 1990; Kokka et al. 1993; Riegle et al. 2015). The reduction of seizure threshold was accompanied by increased seizure severity and duration following CIE exposure. Again, these results are consistent with observed indications of CNS hyperexcitability using other models (Becker and Hale 1993; Becker 1994). After demonstrating that the transgenic animals used for oPDT testing experienced the same electrographic and behavioral indications

of CNS hyperexcitability during WD, we aimed to determine whether oPDT testing was sensitive to WD-related CNS hyperexcitability.

Single 10ms pulses of optical stimulation at 10 different intensity levels were repeatedly presented to the light sensitive excitatory neurons of CA1 of hippocampus of the transgenic mouse. At maximum stimulation intensity a PS is evoked on nearly every presentation, below maximum stimulation the likelihood of a PS occurring is probabilistic. The distribution of PS to total presentations at each level is fit by a Boltzmann curve, representing each animal's unique sensitivity to the optical probe, termed the PS curve. The intensity at which the ratio of PS to presentations is 0.5 was termed the I_{50}, analogous to the V_{50} in ion channel studies (Chapter 2). The I_{50} was used to test for significant differences in the PS curve between conditions. A reduction in I_{50} indicates that stimulation evoked a PS at lower stimulation intensity, and therefore an increase in circuit excitability compared to baseline. We show that the I_{50} is significantly reduced during the 3rd and 4th WD periods of CIE when compared to a baseline period prior to EtOH exposure. These results indicate that oPDT testing to generate an I_{50} is a sensitive measure for probing the excitability state of a population of neurons. It is an interesting observation that spontaneous PS frequency was significantly increased at the same point in CIE that I_{50} was significantly decreased, during the 3rd and 4th WD periods.

In a second series of experiments the oPDT preparation was used to investigate efficacy of a Ca^{2+} channel blocker during EtOH WD. The drug ETX was chosen because the lab's previous investigations have demonstrated efficacy in reducing

measures of WD related hyperexcitability (Wiggins et al. 2013; Riegle et al. 2014, 2015) and we saw an increase in oPDT threshold during ETX treatment in alcohol naïve animals. Pentylenetetrazol (PTZ) was used to induce CNS hyperexcitability and the efficacy of the anti-epileptic drug (AED) levetiracetam (LEV) in reducing oPDT was tested. Interestingly, ETX reduced neither spontaneous PS rates, nor did it cause a significant shift in the I_{50} of the oPDT PS curve during WD despite having an effect on the alcohol naïve oPDT. On the other hand, LEV did significantly increase the I_{50} when compared to the PTZ only condition, returning the I_{50} to a level that was no different than the pre-PTZ level. We suggest that the mechanism of generating spontaneous PS and optically-induced population discharges is contingent on vesicular release and circuit interaction. This result disentangles certain WD phenotypes (e.g. brief spindle episodes, sleep dysrhythmia, and anxiety) from the hippocampal and cortical spikes associated with tonic-clonic WD seizure. During global hyperexcitability from WD or PTZ we demonstrate that oPDT is sensitive to specific actions of targeted pharmacology and is useful in distinguishing features of hyperexcitability. We recognize, of course, that while treatment with PTZ recapitulates many of the molecular and functional features of WD hyperexcitability, it is likely not identical to WD hyperexcitability. It would be worthwhile to replicate this result during WD.

Furthermore, there are additional potential pitfalls in this experimental model. First, the transgenic animal is expressing high levels of protein in the neurons which may cause damage and influence function. It will be possible using

alternative transgenes to reduce this effect. For example, the cell-filling variant of ChR2 expression has less membrane disturbance from the eYFP than does classical optogenes. Additionally, there has been some concern that electrographic artifact is associated with optical stimulation. We were able to avoid this problem with careful construction of the optrode (Klorig and Godwin 2014). Another concern to develop this model was whether repeated stimulation would cause spurious shifts in the PS curve. This was addressed with carefully controlled repetitions of stimulation (Chapter 2). Finally, early in our implementation of oPDT testing there were issues with variability in the PS curve. However with careful histology we were able to identify this was a consequence of imprecise stereotactic surgery (Chapter 2). We are confident that the highly stereotyped response is a feature of high quality stereotactic surgery.

The role of population and circuit level excitation in hyperexcitability

The balance of excitation and inhibition is the essential governing feature of observed neural electrophysiology (Lovett-Barron et al. 2012; Beltramo et al. 2013; Wakita et al. 2014; Hass and Glickfeld 2016). When using the term population, or population-based, we are referring to locally recurrent groups of neurons observable with local field potentials (LFPs) (Kajikawa and Schroeder 2011). The LFP is a record of aggregate neuronal activity representing the sum total of local ion flow across neuron membranes. It is analogous to an EEG recording, but specific to the local surrounding tissue. The cellelluar composition of the region, the molecular profiles of those cells, and their local connectivity dictate the observed LFP response to some upstream input or perturbation

(Kajikawa and Schroeder 2011). Changing any one aspect of these local population dynamics affects how the population as a whole behaves. However, changing any one cell will likely not have an effect on the recorded LFP. This is important because it provides the experimenter with the opportunity to observe how activity is meaningfully coordinated across a functional group.

The term circuit, on the other hand, refers to how discrete local populations interact with distant or nearby populations to reciprocally affect the activity in either or both locations (Douglas and Martin 2007; Arenkiel et al. 2007; Beltramo et al. 2013). Because population dynamics are governed by the makeup of local neurons, distinct populations can respond differently to the same treatment (i.e. one population may be sensitized while another may be depressed). This means that circuit level dynamics are dependent on–but not identical to—population dynamics. Just as the population is dependent on the neurons that make it up, its activity profile is not identical to any single neuron. The circuit dynamics are dependent on the local population activity but are not identical to or dictated entirely by any one population. Circuits tend to be highly convergent such that any one population in a circuit receives multiple inputs from unique, distant populations (Douglas and Martin 2007). This convergence further increases the difficulty in deciphering what the primary effector of changes to observed activity may be. In fact, it may be fair to suspect the search for a primary effector is misguided, and we may be better served by searching for key interactions. However, the role of circuit interactions is not more important than population activity which is likely no more important than single cell dynamics; each simply

reflects different levels in the functional organization of neuronal activity. oPDT testing provides a framework in which we can appreciate population activity through the LFP in context of the broader circuit framework observed in the satellite array.

An example of the interplay of populations and circuits can be found in the results from ETX testing in WD compared to LEV testing. In both WD and PTZ treatment the system is hyperexcitable as measured by oPDT. Furthermore, there are known changes to the molecular profiles of neurons that undergo chronic exposure to ethanol, specifically in Ca^{2+} channel expression levels (Graef et al. 2011) and certain symptoms of alcohol WD are ameliorated by treatment with ETX (Wiggins et al. 2013; Riegle et al. 2014, 2015). LEV on the other hand has a poorly understood specific mechanism of action in treating seizure (Deshpande and Delorenzo 2014). It also has little efficacy in treating some types of WD related seizure and some apparent efficacy in others, though identifying which WD seizures will respond to LEV is as yet impossible (Krebs et al. 2006; Richter et al. 2010; Youland et al. 2014). LEV has multiple effects including vesicular release (Lee et al. 2009; Fukuyama et al. 2012), presynaptic $GABA_AR$ activity (Wakita et al. 2014), intracellular Ca^{2+} release (Nagarkatti et al. 2008), and extracellular Ca^{2+} entry (Yan et al. 2013). Nonetheless, targeted pharmacotherapy with ETX was not sufficient to reduce WD hyperexcitability of the circuit measured by oPDT. This indicates that there are likely other aspects of the local population and overall circuit which are more influential in the occurrence of PS than simply upregulation of Ca^{2+} channels. Meanwhile, LEV

has broad effects on the tone of excitability and response to depolarization in the circuit and did lead to an increase in spike threshold when compared to a similar excitable state. BZDs, which are known to be efficacious in WD hyperexcitability, do have a much more specific mechanism of action than LEV, but similarly have a ubiquitous effect on overall tone of excitability through their interaction with a major contributor to hyperpolarization, the $GABA_AR$. From this example we see that oPDT provides insight into population dynamics in a way that is able to differentiate effects of complex circuit interactions from more direct relationships.

Interestingly, the effectiveness of ETX in reducing electrographic correlates of CNS hyperexcitability is predominately associated with BSEs (Ryan 1984; Veatch and Becker 2002; Riegle et al. 2014). The BSE is very similar in waveform and origin to the normally observed sleep spindle (Ryan 1984; Sitnikova 2010; Bonjean et al. 2011). The BSE therefore appears to be an aberrant thalamocortical rhythm that is directly reliant on the pacemaking influence of appropriately functioning Ca^{2+} channels in thalamus (Sitnikova 2010; Cain and Snutch 2013). In this case, using the BSE as a metric for WD hyperexcitability, while entirely appropriate, is limited to a simple feedforward oscillation originating in a single location that is causally dependent on the functioning of a specific channel (Ryan 1984; Kandel and Buzsáki 1997; Lee et al. 2004; Astori et al. 2011; Halassa et al. 2011; Cain and Snutch 2013).

These observations further differentiate the unique symptoms of WD hyperexcitability, and suggest that the catchall term of WD hyperexcitability may be too simplistic. It is clear that hyperexcitability of neurons is a ubiquitous

feature of WD that may involve both isolated and convergent networks, and that reducing excitability with potent BZDs (which may reduce seizure through actions at many, or all, of the populations and circuits of AWS) is effective in addressing WD symptoms. However, the observations made here coupled with existing literature suggest that there are in fact many consequences of hyperexcitability, and what is effective at reducing one consequence of excitability in one system (e.g. ETX for BSEs) may not be effective in another (e.g. ETX in PS). The implication of this is that the context of hyperexcitability is the relevant determinant of what will and will not be effective in treatment. In the case of hyperexcitability in BSEs the context is a simple thalamocortical rhythm driven predominantly by the pacing of a single ion channel (Astori et al. 2011). This is distinct from the context of the hyperexcitability in the PS and generalized tonic-clonic seizure that is complex circuits of populations of distinct populations of neurons. The need for targeted pharmacotherapy necessitates that we consider the specific influence of hyperexcitability in the context of the populations and circuits relevant to a specific symptom of interest rather than as an inclusive pathophysiologic mechanism for all WD symptoms.

Utility of oPDT in studying WD hyperexcitability

In the preceding chapters the newly developed oPDT testing protocol was tested in CIE-induced alcohol WD. It is clear from the results that oPDT testing is sensitive to the excitability state of the circuit being monitored and probed. We suggest that this model has high utility in studying WD hyperexcitability from a neuron population perspective, as it respects the intrinsic population circuit

dynamics that govern neural activity. Population circuit dynamics are related to the excitability of the individual neurons that make up the populations in the circuit, but circuits, or interacting populations, are reliant on complex, multifactorial modulations that cannot necessarily be uniquely attributed to a single molecule or cell type (Douglas and Martin 2007; Lee and Reid 2011; Cutsuridis and Taxidis 2013). Because oPDT is a measure of population circuit level excitability, it provides a unique platform for testing pharmacotherapies that may be effective in modulating WD hyperexcitability as it relates to disturbances in population dynamics.

Importantly, there are a number of clinical seizure phenotypes related to alcohol withdrawal (Bråthen et al. 1999; Hughes 2009; Rathlev et al. 2006). In fact, the vast majority of patients who present to the hospital do not have characteristic EEG findings similar to those found in patients with seizure disorder (Deisenhammer et al. 1984; Krauss and Niedermeyer 1991; Sand et al. 2002; Rathlev et al. 2006). However, in cases in which abnormal spiking activity was detected with EEG, the tendency was for those patients to have generalized tonic-clonic seizure (Krauss and Niedermeyer 1991), and amongst patients with prior seizure disorder, abnormal EEG findings are worsened during WD and outcomes are worse (Sand et al. 2002). These clinical observations, coupled with results from our studies which differentiate pharmacologic efficacy in hyperexcitability, suggest that alcohol WD hyperexcitability has multiple manifestations dependent on patient genetics, history, and related

symptomology. We propose that oPDT testing has utility in studying WD hyperexcitability related to seizure of the generalized tonic-clonic type.

oPDT testing provides a model for a specific pathology that allows for precise investigations related to temporal lobe excitability. By differentiating unique phenotypes within the general term WD hyperexcitability we can develop targeted pharmacotherapies that address individual features of hyperexcitability. For example, while ETX has been shown to be effective at reducing anxiety-like behavior, sleep disturbances, brief spindle episodes (BSEs), and improving survival (Riegle et al. 2014; Wiggins et al. 2013; Riegle et al. 2015) it did not raise the threshold of optically-induced PS nor reduce the frequency of spontaneously occurring PS during WD. This indicates that there is differentiable control over these WD related phenotypes, and that appropriate targeted therapy may be discernable based on a clinical presentation. However, in the pre-WD condition, ETX did raise oPDT suggesting that Ca^{2+} flux does participate in evoked PS which is to be expected as the target molecule T-type Ca^{2+} channel opens in response to depolarization, but that it is not the major driver during WD. Using oPDT in conjunction with other studies of WD (e.g. behavioral testing) it may be possible to identify which aspects of WD hyperexcitability are responsive to specific interventions. In the future, these types of targeted studies may allow for the development of a look-up table whereby rather than simply giving BZD to everyone with AWS the specific symptoms and signs are identified and targeted therapy is provided.

Future Directions

We have demonstrated the efficacy of using oPDT testing to probe circuit excitability as it relates to generalized tonic-clonic seizure. We will continue to utilize this methodology to develop a deeper mechanistic understanding of how circuit level excitability influences disease processes as well as normal functioning.

Specifically related to alcohol WD, there are important questions regarding the time course of seizure that we can investigate using this method. For example, we show that spontaneous spike frequency returns to baseline 72h after the last exposure to ethanol which is consistent with clinical observations (Hughes 2009). However, subsequent relapses are known to further potentiate AWS (Becker and Hale 1993; Becker 1998). Using oPDT testing we may be able to track the baseline changes to excitability that are present following WD, but remain subclinical. We have thus far only subjected animals to single, isolated cycles of CIE, and have yet to use oPDT to track excitability beyond 24h past alcohol cessation. The subclinical changes that are present in the complex circuits of hippocampus may be revealed with the sensitivity of oPDT. In these investigations we can utilize pharmacologic intervention during the abstinent period to potentially reverse or prevent the kindling-like effect of repeated WD.

Furthermore, the utility of optogenetics is not limited to investigations of hippocampal circuitry (Cardin et al. 2010). It would be possible to use different promoter systems to target, specific regions in thalamus to directly probe

thalamic hyperexcitablility in order to further distinguish thalamocortical disturbances from those of hippocampal and cortical origin. Specifically, inducible expression systems like the Cre/lox system allow targeted expression in any cell type of interest (Sauer 1998; Lo and Anderson 2011). It would be possible to target, for example, cells expressing T-type Ca^{2+} channels with a viral transfection in thalamus and stimulate the neurons with a modified oPDT protocol. We predict that ETX would be effective in raising threshold specifically in those neurons. Furthermore, using a c-fos-promoter-driven system to express GFP and ChR2 in active neurons during oPDT testing and kindling it would be possible to identify the specific downstream neurons which participate in the PS (Liu et al. 2012). Investigations into the identity of the neurons involved in PS and seizure could provide the basis for outlining a genetic, morphological, or functional profile of neurons susceptible to hyperactivity.

It will also be important to further characterize which symptoms of AWS are responsive to specific treatments. Using oPDT we have already shown that the efficacy of ETX relates more to thalamocortical interactions than to the generalized tonic-clonic seizures associated with hippocampus and cortex. A full suite of available and experimental compounds could be applied to this model to generate a library of effective interventions for alleviating tonic-clonic seizure related signs and symptoms. This pre-clinical work will be essential in developing novel compounds and treatment paradigms based on the specific features of a patient's AWS.

Additionally, a non-human primate self-administration model of alcohol use disorder has been employed for use in magnetoencephalography (MEG) (Appendix B; (Rowland et al. 2017)). MEG functions similarly to EEG, however it has the potential to generate virtual LFP-like timeseries from anywhere in the brain (Hillebrand and Barnes 2005). We have begun to develop a modified oPDT paradigm for use in non-human primates (Appendix C). Combining oPDT with MEG recordings in a volitional model of AUD in non-human primates will provide an unprecedented opportunity for investigation. The oPDT testing would not be limited to the number of available implanted micro-electrodes, and the animals would determine their own drinking patterns in a way that recapitulates more faithfully human drinking behaviors.

Finally, oPDT testing does not need to be limited to investigations of alcohol WD hyperexcitability. For example, recent studies regarding the neuronal underpinnings of depression have begun to suggest a role of excitation (Zheng and Zhang 2015). It may be possible to utilize oPDT in animal models of depression to study novel pharmaceutical approaches to treatment. The NMDAR system has been a subject of interest as there is increasing evidence that potent NMDAR antagonists can act as rapid antidepressants (Caddy et al. 2015; Newport et al. 2015). A proposed mechanism for their efficacy relies on a rebound of the excitability of neural circuits following high dose exposure to the antagonist. This increase in excitability should be detectable using oPDT.

Conclusion

oPDT testing is an effective measure of circuit level excitability. It is possible using this technique to detect alcohol WD hyperexcitability in the circuit as it relates to WD seizure. Furthermore, oPDT provides a platform for pharmacologic discovery and pre-clinical testing in a highly controlled model. We suggest that its applicability is not limited to WD hyperexcitability, but instead that it has utility in investigating many questions related to circuit excitability. Moving forward it will become more and more important to appreciate the role of complex circuits in governing the normal and pathological activity observed in the brain. We suggest that the oPDT preparation is well suited for the type of study required to appreciate the complexity of interacting populations of neurons, and that it provides an excellent platform for discovery.

Using oPDT we differentiate the functional consequences of hyperexcitability. We demonstrate that the system wide changes during AWS are differentiable based on the circuit of interest. Previous work in our lab has demonstrated the efficacy of T-type Ca^{2+} channel blockers at reducing thalamic dysfunction, BSEs during WD. In this study, we show that blocking of T-type Ca^{2+} channels alone does not reduce pathologic activity, spontaneous PS, or measures of excitability, oPDT, in hippocampal circuits. Despite ubiquitous upregulation of T-type Ca^{2+} channel expression the hippocampal seizure circuit remains resistant to modulation with targeted Ca^{2+} channel blockade. We interpret this result to suggest that the context and circuitry involved in a WD phenotype is as important as changes in molecular expression associated with WD hyperexcitability. We have

demonstrated differentiation of pathologies associated with WD indicating that the circuit in which alterations occur dictates the manifestation of symptoms. Symptom specific therapy may be possible as a result of nuanced investigations into the relevant circuit for the symptom.

References

Ait-Daoud, Nassima, Robert J. Malcolm, and Bankole A. Johnson. 2006. “An Overview of Medications for the Treatment of Alcohol Withdrawal and Alcohol Dependence with an Emphasis on the Use of Older and Newer Anticonvulsants.” *Addictive Behaviors* 31 (9): 1628–49. doi:10.1016/j.addbeh.2005.12.029.

Amato, Laura, Silvia Minozzi, Simona Vecchi, and Marina Davoli. 2010. “Benzodiazepines for Alcohol Withdrawal.” *The Cochrane Database of Systematic Reviews*, no. 3 (March): CD005063. doi:10.1002/14651858.CD005063.pub3.

Arenkiel, Benjamin R, Joao Peca, Ian G Davison, Catia Feliciano, Karl Deisseroth, George J Augustine, Michael D Ehlers, and Guoping Feng. 2007. “In Vivo Light-Induced Activation of Neural Circuitry in Transgenic Mice Expressing Channelrhodopsin-2.” *Neuron* 54 (2): 205–18. doi:10.1016/j.neuron.2007.03.005.

Astori, Simone, Ralf D. Wimmer, Haydn M. Prosser, Corrado Corti, Mauro Corsi, Nicolas Liaudet, Andrea Volterra, Paul Franken, John P. Adelman, and Anita Lüthi. 2011. “The Ca(V)3.3 Calcium Channel Is the Major Sleep Spindle Pacemaker in Thalamus.” *Proceedings of the National Academy of Sciences of the United States of America* 108 (33): 13823–28. doi:10.1073/pnas.1105115108.

Ballenger, J. C., and R. M. Post. 1978. “Kindling as a Model for Alcohol Withdrawal Syndromes.” *The British Journal of Psychiatry: The Journal of Mental Science* 133 (July): 1–14.

Becker, H C. 1998. “Kindling in Alcohol Withdrawal.” *Alcohol Health and Research World* 22 (1): 25–33.

———. 2000. “Animal Models of Alcohol Withdrawal.” *Alcohol Research & Health: The Journal of the National Institute on Alcohol Abuse and Alcoholism* 24 (2): 105–13.

Becker, H. C., and R. L. Hale. 1993. “Repeated Episodes of Ethanol Withdrawal Potentiate the Severity of Subsequent Withdrawal Seizures: An Animal Model of Alcohol Withdrawal ‘Kindling.’” *Alcoholism, Clinical and Experimental Research* 17 (1): 94–98.

Becker, Howard C. 1994. “Positive Relationship between the Number of Prior Ethanol Withdrawal Episodes and the Severity of Subsequent Withdrawal Seizures.” *Psychopharmacology* 116 (1): 26–32.

———. 2008. “Alcohol Dependence, Withdrawal, and Relapse.” *Alcohol Research & Health* 31 (4): 348–61.

———. 2013. “Animal Models of Excessive Alcohol Consumption in Rodents.” *Current Topics in Behavioral Neurosciences* 13: 355–77. doi:10.1007/7854_2012_203.

Beltramo, Riccardo, Giulia D’Urso, Marco Dal Maschio, Pasqualina Farisello, Serena Bovetti, Yoanne Clovis, Glenda Lassi, Valter Tucci, Davide De Pietri Tonelli, and Tommaso Fellin. 2013. “Layer-Specific Excitatory Circuits Differentially Control Recurrent Network Dynamics in the Neocortex.” *Nature Neuroscience* 16 (2): 227–34. doi:10.1038/nn.3306.

Bonjean, Maxime, Tanya Baker, Maxime Lemieux, Igor Timofeev, Terrence Sejnowski, and Maxim Bazhenov. 2011. “Corticothalamic Feedback Controls Sleep Spindle Duration in Vivo.” *The Journal of Neuroscience: The Official Journal of the Society for Neuroscience* 31 (25): 9124–34. doi:10.1523/JNEUROSCI.0077-11.2011.

Bråthen, G., E. Brodtkorb, G. Helde, T. Sand, and G. Bovim. 1999. “The Diversity of Seizures Related to Alcohol Use. A Study of Consecutive Patients.” *European Journal of Neurology* 6 (6): 697–703.

Caddy, Caroline, Ben H. Amit, Tayla L. McCloud, Jennifer M. Rendell, Toshi A. Furukawa, Rupert McShane, Keith Hawton, and Andrea Cipriani. 2015. “Ketamine and Other Glutamate Receptor Modulators for Depression in Adults.” *The Cochrane Database of Systematic Reviews*, no. 9 (September): CD011612. doi:10.1002/14651858.CD011612.pub2.

Cain, Stuart M., and Terrance P. Snutch. 2013. “T-Type Calcium Channels in Burst-Firing, Network Synchrony, and Epilepsy.” *Biochimica et Biophysica Acta (BBA) - Biomembranes*, Calcium Channels, 1828 (7): 1572–78. doi:10.1016/j.bbamem.2012.07.028.

Cardin, Jessica A, Marie Carlén, Konstantinos Meletis, Ulf Knoblich, Feng Zhang, Karl Deisseroth, Li-Huei Tsai, and Christopher I Moore. 2010. “Targeted Optogenetic Stimulation and Recording of Neurons in Vivo Using Cell-Type-Specific Expression of Channelrhodopsin-2.” *Nature Protocols* 5 (2): 247–54. doi:10.1038/nprot.2009.228.

Cutsuridis, Vassilis, and Jiannis Taxidis. 2013. “Deciphering the Role of CA1 Inhibitory Circuits in Sharp Wave-Ripple Complexes.” *Frontiers in Systems Neuroscience* 7: 13. doi:10.3389/fnsys.2013.00013.

Deisenhammer, E., D. Klingler, and H. Trägner. 1984. “Epileptic Seizures in Alcoholism and Diagnostic Value of EEG after Sleep Deprivation.” *Epilepsia* 25 (4): 526–30.

Deshpande, Laxmikant S., and Robert J. Delorenzo. 2014. “Mechanisms of Levetiracetam in the Control of Status Epilepticus and Epilepsy.” *Frontiers in Neurology* 5: 11. doi:10.3389/fneur.2014.00011.

Douglas, Rodney J, and Kevan A C Martin. 2007. “Recurrent Neuronal Circuits in the Neocortex.” *Current Biology: CB* 17 (13): R496-500. doi:10.1016/j.cub.2007.04.024.

Fukuyama, Kouji, Shunsuke Tanahashi, Masanori Nakagawa, Satoshi Yamamura, Eishi Motomura, Takashi Shiroyama, Hisashi Tanii, and Motohiro Okada. 2012. “Levetiracetam Inhibits Neurotransmitter Release Associated with CICR.” *Neuroscience Letters* 518 (2): 69–74. doi:10.1016/j.neulet.2012.03.056.

Graef, J. D., T. W. Huitt, B. K. Nordskog, J. H. Hammarback, and D. W. Godwin. 2011. “Disrupted Thalamic T-Type Ca2+ Channel Expression and Function During Ethanol Exposure and Withdrawal.” *Journal of Neurophysiology* 105 (2): 528–40. doi:10.1152/jn.00424.2010.

Grant, K. A., P. Valverius, M. Hudspith, and B. Tabakoff. 1990. “Ethanol Withdrawal Seizures and the NMDA Receptor Complex.” *European Journal of Pharmacology* 176 (3): 289–96.

Halassa, Michael M, Joshua H Siegle, Jason T Ritt, Jonathan T Ting, Guoping Feng, and Christopher I Moore. 2011. “Selective Optical Drive of Thalamic Reticular Nucleus Generates Thalamic Bursts and Cortical Spindles.” *Nature Neuroscience* 14 (9): 1118–20. doi:10.1038/nn.2880.

Hass, Charles A., and Lindsey L. Glickfeld. 2016. “High Fidelity Optical Excitation of Cortico-Cortical Projections at Physiological Frequencies.” *Journal of Neurophysiology*, August, jn.00456.2016. doi:10.1152/jn.00456.2016.

Hillebrand, Arjan, and Gareth R. Barnes. 2005. “Beamformer Analysis of MEG Data.” In , edited by BT - International Review of Neurobiology, 68:149–71. Magnetoencephalography. Academic Press. http://www.sciencedirect.com/science/article/pii/S0074774205680063.

Holbrook, A. M., R. Crowther, A. Lotter, C. Cheng, and D. King. 1999. “Diagnosis and Management of Acute Alcohol Withdrawal.” *CMAJ: Canadian Medical Association Journal = Journal de l’Association Medicale Canadienne* 160 (5): 675–80.

Hughes, John R. 2009. “Alcohol Withdrawal Seizures.” *Epilepsy & Behavior* 15 (2): 92–97. doi:10.1016/j.yebeh.2009.02.037.

Jesse, S., G. Bråthen, M. Ferrara, M. Keindl, E. Ben-Menachem, R. Tanasescu, E. Brodtkorb, M. Hillbom, M.a. Leone, and A.c. Ludolph. 2017. “Alcohol Withdrawal Syndrome: Mechanisms, Manifestations, and Management.” *Acta Neurologica Scandinavica* 135 (1): 4–16. doi:10.1111/ane.12671.

Kajikawa, Yoshinao, and Charles E Schroeder. 2011. “How Local Is the Local Field Potential?” *Neuron* 72 (5): 847–58. doi:10.1016/j.neuron.2011.09.029.

Kandel, Adam, and György Buzsáki. 1997. “Cellular–Synaptic Generation of Sleep Spindles, Spike-and-Wave Discharges, and Evoked Thalamocortical Responses in the Neocortex of the Rat.” *The Journal of Neuroscience* 17 (17): 6783–97.

Klorig, David C., and Dwayne W. Godwin. 2014. “A Magnetic Rotary Optical Fiber Connector for Optogenetic Experiments in Freely Moving Animals.” *Journal of Neuroscience Methods* 227 (April): 132–39. doi:10.1016/j.jneumeth.2014.02.013.

Kokka, N., D. W. Sapp, A. M. Taylor, and R. W. Olsen. 1993. “The Kindling Model of Alcohol Dependence: Similar Persistent Reduction in Seizure Threshold to Pentylenetetrazol in Animals Receiving Chronic Ethanol or Chronic Pentylenetetrazol.” *Alcoholism, Clinical and Experimental Research* 17 (3): 525–31.

Krauss, G. L., and E. Niedermeyer. 1991. “Electroencephalogram and Seizures in Chronic Alcoholism.” *Electroencephalography and Clinical Neurophysiology* 78 (2): 97–104.

Krebs, Michael, Karolina Leopold, Christoph Richter, Thorsten Kienast, Axel Hinzpeter, Andreas Heinz, and Martin Schaefer. 2006. “Levetiracetam for the Treatment of Alcohol Withdrawal Syndrome: An Open-Label Pilot Trial.” *Journal of Clinical Psychopharmacology* 26 (3): 347–49. doi:10.1097/01.jcp.0000219926.49799.89.

Lee, Chun-Yao, Chih-Chuan Chen, and Horng-Huei Liou. 2009. “Levetiracetam Inhibits Glutamate Transmission through Presynaptic P/Q-Type Calcium Channels on the Granule Cells of the Dentate Gyrus.” *British Journal of Pharmacology* 158 (7): 1753–62. doi:10.1111/j.1476-5381.2009.00463.x.

Lee, Jungryun, Daesoo Kim, and Hee-Sup Shin. 2004. “Lack of Delta Waves and Sleep Disturbances during Non-Rapid Eye Movement Sleep in Mice Lacking Alpha1G-Subunit of T-Type Calcium Channels.” *Proceedings of the National Academy of Sciences of the United States of America* 101 (52): 18195–99. doi:10.1073/pnas.0408089101.

Lee, Wei-Chung Allen, and R Clay Reid. 2011. “Specificity and Randomness: Structure-Function Relationships in Neural Circuits.” *Current Opinion in Neurobiology* 21 (5): 801–7. doi:10.1016/j.conb.2011.07.004.

Liu, Xu, Steve Ramirez, Petti T. Pang, Corey B. Puryear, Arvind Govindarajan, Karl Deisseroth, and Susumu Tonegawa. 2012. “Optogenetic Stimulation of a Hippocampal Engram Activates Fear Memory Recall.” *Nature* 484 (7394): 381. doi:10.1038/nature11028.

Lo, Liching, and David J. Anderson. 2011. “A Cre-Dependent, Anterograde Transsynaptic Viral Tracer for Mapping Output Pathways of Genetically

Marked Neurons." *Neuron* 72 (6): 938–50. doi:10.1016/j.neuron.2011.12.002.

Lovett-Barron, Matthew, Gergely F. Turi, Patrick Kaifosh, Peter H. Lee, Frédéric Bolze, Xiao-Hua Sun, Jean-François Nicoud, Boris V. Zemelman, Scott M. Sternson, and Attila Losonczy. 2012. "Regulation of Neuronal Input Transformations by Tunable Dendritic Inhibition." *Nature Neuroscience* 15 (3): 423–30. doi:10.1038/nn.3024.

Nagarkatti, Nisha, Laxmikant S. Deshpande, and Robert J. DeLorenzo. 2008. "Levetiracetam Inhibits Both Ryanodine and IP3 Receptor Activated Calcium Induced Calcium Release in Hippocampal Neurons in Culture." *Neuroscience Letters* 436 (3): 289–93. doi:10.1016/j.neulet.2008.02.076.

Newport, D. Jeffrey, Linda L. Carpenter, William M. McDonald, James B. Potash, Mauricio Tohen, Charles B. Nemeroff, and APA Council of Research Task Force on Novel Biomarkers and Treatments. 2015. "Ketamine and Other NMDA Antagonists: Early Clinical Trials and Possible Mechanisms in Depression." *The American Journal of Psychiatry* 172 (10): 950–66. doi:10.1176/appi.ajp.2015.15040465.

Rathlev, Niels K., Andrew S. Ulrich, Norman Delanty, and Gail D'Onofrio. 2006. "Alcohol-Related Seizures." *The Journal of Emergency Medicine* 31 (2): 157–63.

Richter, Christoph, Axel Hinzpeter, Folkhard Schmidt, Thorsten Kienast, Ulrich W. Preuss, Thomas Plenge, Andreas Heinz, and Martin Schaefer. 2010. "Levetiracetam for the Treatment of Alcohol Withdrawal Syndrome: A Multicenter, Prospective, Randomized, Placebo-Controlled Trial." *Journal of Clinical Psychopharmacology* 30 (6): 720–25.

Riegle, Melissa A., Melissa L. Masicampo, Erin H. Caulder, and Dwayne W. Godwin. 2014. "Ethosuximide Reduces Electrographical and Behavioral Correlates of Alcohol Withdrawal Seizure in DBA/2J Mice." *Alcohol (Fayetteville, N.Y.)* 48 (5): 445–53. doi:10.1016/j.alcohol.2014.01.010.

Riegle, Melissa A., Melissa L. Masicampo, Hong Qu Shan, Victoria Xu, and Dwayne W. Godwin. 2015. "Ethosuximide Reduces Mortality and Seizure Severity in Response to Pentylenetetrazole Treatment During Ethanol Withdrawal." *Alcohol and Alcoholism (Oxford, Oxfordshire)* 50 (5): 501–8. doi:10.1093/alcalc/agv033.

Rowland, Jared A., Jennifer R. Stapleton-Kotloski, Greg E. Alberto, April T. Davenport, Robert J. Kotloski, David P. Friedman, Dwayne W. Godwin, and James B. Daunais. 2017. "Changes in Nonhuman Primate Brain Function Following Chronic Alcohol Consumption in Previously Naïve Animals." *Drug and Alcohol Dependence* 177 (May): 244–48. doi:10.1016/j.drugalcdep.2017.03.036.

Ryan, Lawrence J. 1984. “Characterization of Cortical Spindles in DBA/2 and C57BL/6 Inbred Mice.” *Brain Research Bulletin* 13 (4): 549–58. doi:10.1016/0361-9230(84)90037-6.

Sand, T., G. Bråthen, R. Michler, E. Brodtkorb, G. Helde, and G. Bovim. 2002. “Clinical Utility of EEG in Alcohol-Related Seizures.” *Acta Neurologica Scandinavica* 105 (1): 18–24.

Sauer, B. 1998. “Inducible Gene Targeting in Mice Using the Cre/Lox System.” *Methods (San Diego, Calif.)* 14 (4): 381–92. doi:10.1006/meth.1998.0593.

Sitnikova, Evgenia. 2010. “Thalamo-Cortical Mechanisms of Sleep Spindles and Spike-Wave Discharges in Rat Model of Absence Epilepsy (a Review).” *Epilepsy Research* 89 (1): 17–26. doi:10.1016/j.eplepsyres.2009.09.005.

Veatch, L. M., and L. P. Gonzalez. 1996. “Repeated Ethanol Withdrawal Produces Site-Dependent Increases in EEG Spiking.” *Alcoholism, Clinical and Experimental Research* 20 (2): 262–67.

Veatch, Lynn M., and Howard C. Becker. 2002. “Electrographic and Behavioral Indices of Ethanol Withdrawal Sensitization.” *Brain Research* 946 (2): 272–82. doi:10.1016/S0006-8993(02)02895-0.

Velísek, L, I Kulhánková, L Roztocilová, P Mares, J Velísková, and H Mirvaldová. 1989. “Ethosuximide Affects Both Pentylenetetrazole- and Kainate-Induced Clonic Seizures but Differentiates between Tonic-Clonic Seizures.” *Canadian Journal of Physiology and Pharmacology* 67 (10): 1357–61.

Wakita, Masahito, Naoki Kotani, Kyuya Kogure, and Norio Akaike. 2014. “Inhibition of Excitatory Synaptic Transmission in Hippocampal Neurons by Levetiracetam Involves Zn^{2+}-Dependent GABA Type A Receptor-Mediated Presynaptic Modulation.” *The Journal of Pharmacology and Experimental Therapeutics* 348 (2): 246–59. doi:10.1124/jpet.113.208751.

Wiggins, Walter F., John D. Graef, Tiffany W. Huitt, and Dwayne W. Godwin. 2013. “Ethosuximide Reduces Ethanol Withdrawal-Mediated Disruptions in Sleep-Related EEG Patterns.” *Alcoholism, Clinical and Experimental Research* 37 (3): 372–82. doi:10.1111/j.1530-0277.2012.01938.x.

Yan, Hai-Dun, Kumatoshi Ishihara, Takahiro Seki, Ryosuke Hanaya, Kaoru Kurisu, Kazunori Arita, Tadao Serikawa, and Masashi Sasa. 2013. “Inhibitory Effects of Levetiracetam on the High-Voltage-Activated L-Type Ca^{2+} Channels in Hippocampal CA3 Neurons of Spontaneously Epileptic Rat (SER).” *Brain Research Bulletin* 90 (January): 142–48. doi:10.1016/j.brainresbull.2012.10.006.

Youland, Kelly M., Ryan F. Miller, Lisa J. Mahoney, Andrew J. Borgert, and Jacob D. Gundrum. 2014. “Levetiracetam as Adjunctive Therapy for Acute Alcohol Withdrawal Syndrome in Hospitalized Patients.” *Journal of Clinical*

Psychopharmacology 34 (6): 704–8. doi:10.1097/JCP.0000000000000209.

Zheng, C., and T. Zhang. 2015. “Synaptic Plasticity-Related Neural Oscillations on Hippocampus-Prefrontal Cortex Pathway in Depression.” *Neuroscience* 292 (April): 170–80. doi:10.1016/j.neuroscience.2015.01.071.

Appendix A

Changes in nonhuman primate brain function following chronic alcohol consumption in previously naïve animals

Jared A. Rowland[a,b,c,], Jennifer R. Stapleton-Kotloski[d], Greg E. Alberto[b], April T. Davenport[e], Robert J. Kotloski[f,g], David P. Friedman[e], Dwayne W. Godwin[b], James B. Daunais[e]

a *Research and Academic Affairs Service Line, Mid-Atlantic Mental Illness Research Education and Clinical Center, W.G. "Bill" Hefner VA Medical Center, Salisbury, NC, USA*
b *Department of Neurobiology and Anatomy, Wake Forest School of Medicine, Winston-Salem, NC, USA*
c *Department of Psychiatry and Behavioral Medicine, Wake Forest School of Medicine, Winston-Salem, NC, USA*
d *Department of Neurology, Wake Forest School of Medicine, Winston-Salem, NC, USA*
e *Department of Physiology and Pharmacology, Wake Forest School of Medicine, Winston-Salem, NC, USA*
f *Department of Neurology, University of Wisconsin School of Medicine and Public Health, Madison, WI, USA*
g *Department of Neurology, William S. Middleton VA Medical Center, Madison, WI, USA*

A B S T R A C T

Introduction: Chronic alcohol abuse is associated with neurophysiological changes in brain activity; however, these changes are not well localized in humans. Non-human primate models of alcohol abuse enable control over many potential confounding variables associated with human studies. The present study utilized high-resolution magnetoencephalography (MEG) to quantify the effects of chronic EtOH self-administration on resting state (RS) brain function in vervet monkeys.

Methods: Adolescent male vervet monkeys were trained to self-administer ethanol (n = 7) or an isocaloric malto-dextrin solution (n = 3). Following training, animals received 12 months of free access to ethanol. Animals then underwent RS magnetoencephalography (MEG) and subsequent power spectral analysis of brain activity at 32 bilateral regions of interest associated with the chronic effects of alcohol use.

Results: demonstrate localized changes in brain activity in chronic heavy drinkers, including reduced power in the anterior cingulate cortex, hippocampus, and amygdala as well as increased power in the right medial orbital and parietal areas.

Discussion: The current study is the first demonstration of whole-head MEG acquisition in vervet monkeys. Changes in brain activity were consistent with human electroencephalographic studies; however, MEG was able to extend these findings by localizing the observed changes in power to specific brain regions. These regions are consistent with those previously found to exhibit

volume loss following chronic heavy alcohol use. The ability to use MEG to evaluate changes in brain activity following chronic ethanol exposure provides a potentially powerful tool to better understand both the acute and chronic effects of alcohol on brain function.

1. Introduction

Alcohol abuse is associated with widespread cortical atrophy and loss of white matter integrity (Buhler and Mann, 2011; Monnig et al.,2013), particularly in frontal cortical areas (Pfefferbaum et al., 1997). These changes may contribute to the characteristic patterns of brain activity associated with alcohol abuse seen both in the resting state (RS) and during task performance (Rangaswamy and Porjesz, 2008). However, it is not clear when during the disease process these patterns are manifested and which specific neurocircuits are affected. Well-characterized non-human primate (NHP) drinking models are a powerful translational science tool that enable control of many variables, including environmental conditions, nutrition, intake patterns, etc. that are a source of uncontrolled variance in clinical populations. Studies of one such model (Grant et al., 2008; Vivian et al., 2001) have demonstrated functional and genomic consequences throughout the brain following 15 months of chronic daily drinking (Acosta et al., 2010; Ariwodola et al., 2003; Budygin et al., 2003; Carden et al., 2006; Cuzon Carlson et al., 2011; Floyd et al., 2004; Grant et al., 2008; Hemby et al., 2006; Mohr et al., 2013; Welsh et al., 2011). Recently, graph theoretical analyses of fMRI data from this model found that chronic heavy drinking altered RS brain network organization (Telesford et al., 2015). These findings are consistent with those from human studies (Zahr, 2013) and indicate that this NHP model of chronic alcohol consumption is a robust representation of the human condition of alcoholism. Noninvasive electrophysiological measures of brain function, such as electroencephalography (EEG), are sensitive to differences in

brain activity due to chronic alcohol consumption (Kamarajan and Porjesz, 2015; Pandey et al., 2012). EEG studies of humans with alcohol use disorders have most consistently reported increased power in the beta and theta bandwidths (Kamarajan and Porjesz, 2015), while findings in other bandwidths have been mixed. Magnetoencephalography (MEG) is another noninvasive method of directly measuring brain function with high temporal resolution and increased spatial resolution relative to EEG. However, MEG has not been previously used to record RS activity in the vervet brain. The present study was designed to assess the feasibility of measuring RS brain activity in the vervet brain using a MEG instrument designed for humans. We obtained RS MEG from vervet monkeys following 15 months of daily EtOH consumption and control animals.

We hypothesized that power would be increased in the beta and theta bandwidths in EtOH animals, consistent with human EEG findings. We anticipated being able to extend current literature by localizing observed differences to particular brain regions due to the superior spatial resolution provided by MEG.

2. Material and methods

All procedures were approved by the Institutional Animal Care and Use Committee of Wake Forest School of Medicine (WFSM) and conformed to the National Institute of Health Guide for the Care and Use of Laboratory Animals (NIH Publications No. 80-23) in research.

2.1. Animals

Adult male vervet monkeys (Chlorocebus aethiops, n = 10, 7 years old; 28 year human equivalent) were acquired from the Primate Center at Wake Forest School of Medicine and currently participating in a separate EtOH self-administration study. The monkeys were trained to self-administer EtOH (EtOH, n = 7) or an isocaloric maltose-dextrin solution (Control, n = 3) (Grant et al., 2008).

2.2. Preparation for MEG scans

Animals were fasted overnight from EtOH and food prior to scans. Duration between the onset of fasting and beginning of scan was 927.3 min (SD = 134.7) for the EtOH group and 879.7 min (SD = 30.5) for the Control group. Across the ten days prior to imaging, the EtOH group consumed an average of 87.5% (SD = 7.3) of their total daily intake by the fasting time. Only one animal consumed less than 85% by this point, consuming on average 74% (SD = 11.69) by the fasting time. Animals were sedated with ketamine (10 mg/kg, i.m.) for transport. Anesthesia was induced with 3.0–4.0 mg/kg propofol and then maintained by continuous infusion of 200 μg/kg/min via syringe pump (Sage, Orion Research Corporation, Cambridge, Mass). The animals were placed in a supine position and artificially ventilated. Vital signs were monitored throughout the scan and recovery sessions. MEG was acquired under propofol anesthesia due to

concerns regarding head motion artifact during scanning if the animals were conscious.

A known linear relationship exists between resting-state activity and propofol anesthesia (Boveroux et al., 2010). Notably, electrophysiological studies suggest propofol sedation is associated with increased power in the beta frequencies (Mahon et al., 2008). Changes in resting state networks observed with fMRI and associated with EtOH consumption have been previously demonstrated in these same animals using an identical preparation (Telesford et al., 2015).

2.3. MEG acquisition

Data were acquired using a whole head CTF Systems Inc. MEG 2005 neuromagnetometer system equipped with 275 first-order axial gradiometers coils. Data were sampled at 600 Hz over a DC–150 Hz bandwidth for 8 min.

Following data acquisition, fiducial coils were replaced with a lipid marker to facilitate MEG co-registration with T1-weighted MRI scans.

2.4. MEG data processing

Data preprocessing, head model creation, and beamforming were performed using CTF MEG™ Software (MISL, Coquitlam, BC, Canada). MEG data were pre-processed using synthetic 3rd order gradient balancing with whole trial DC offset. Data were band pass filtered from 1 to 80 Hz with a 60 Hz notch filter (4 Hz width). Three spherical shell, multiple local-sphere head models were created using the fiducial information and T1-weighted MRI (Huang et al., 1999).

2.5. ROI identification

Using the animal-specific MRI, 32 non-adjacent regions of interest (ROIs, 2 mm□3; see Table 1) were identified in native brain space for each animal. Figures visually displaying the location of ROIs are available as supplementary materials (S1-S12). ROIs were chosen based on existing literature (Buhler and Mann, 2011) and evidence from our laboratories using an identical drinking model that chronic alcohol use affects these areas (cited above).

2.6. Source series

Synthetic Aperture Magnetometry (SAM; Robinson and Vrba, 1998) as implemented in CTF MEG™ Software was used to return source series for each ROI. Source series represent the unique weighted sum of MEG sensor output for a specific location in the brain, and are strongly correlated with the local field potential at that location. Source series retain the same time-frequency characteristics as the original MEG sensor data; here they were constructed for the full time domain of the original scans. SAM source series have been effective in analyzing both RS and event related brain activity (Beal et al., 2010; Cheyne et al.,2007; Cornwell et al., 2012; Cornwell et al., 2008; Douw et al., 2013; Hillebrand et al., 2012; Hung et al., 2010, 2012; Luo et al., 2007; Moses et al., 2009; Quraan et al., 2011; Riggs et al., 2009; Stapleton-Kotloski et al., 2014).

2.7. Signal power

Signal power for each source series was calculated using multi-taper estimation implemented in Chronux (Mitra and Bokil, 2008; http://chronux.org). The mtspectrogramc function was used with a 1 s window and 500 ms overlap. A modified Welch′s method was implemented by averaging within each 6-s epoch of the resulting spectrum (See Fig. 1A). For comparison, the resulting spectrum from applying an identical analysis to sensor level data from a control animal can be seen in Supplementary materials (S13–S18). Next, the maximum power within each of the classic bandwidths was identified for each source series (delta: 1–4 Hz, theta: 4–8 Hz, alpha: 8–13 Hz, beta: 13–30 Hz,gamma: 30–80 Hz) at each time point, creating a vector of values

Table 1

Percent change in power associated with EtOH group membership relative to the Control group. This was calculated as the parameter estimate for EtOH group membership divided by the intercept. Positive values indicate higher levels of

power in drinkers, negative values indicate lower levels of power in drinkers.

	Delta	Theta	Alpha	Beta	Gamma
Left Anterior Cingulate	−6.6	−22.8	**−36.8***	−25.8	**−31.9***
Right Anterior Cingulate	−12.6	−22.4	**−39.3***	**−30.3***	**−39.9***
Bilateral Anterior Cingulate	−10.2	−23.5	**−39.0***	**−28.8***	**−36.5***
Left Medial Orbital Sulcus	36.5	11.1	2.4	6.7	22.7
Right Medial Orbital Sulcus	**253.1***	**200.2***	**139.2***	**152.4***	**137.0***
Left Lateral Orbital Sulcus	50.8	16.9	−17.5	−18.5	−18.9
Right Lateral Orbital Sulcus	13.9	16.3	−12.0	−2.3	−10.1
Left Principle Sulcus	60.4	22.9	4.8	−0.1	−6.6
Right Principle Sulcus	−16.4	−23.2	**−35.9***	−26.0	−29.5
Left Nucleus Accumbens	35.6	12.9	−14.4	−7.2	−3.4
Right Nucleus Accumbens	42.4	39.3	27.2	37.2	25.1
Left Caudate	12.9	−2.0	−14.8	−9.3	−10.2
Right Caudate	−9.6	−16.5	−8.6	−1.1	−10.6
Left Putamen	10.1	2.8	−11.2	−9.8	−19.6
Right Putamen	0.6	3.9	5.4	−0.5	−14.1
Left Parietal	15.4	8.4	4.1	−0.6	1.5
Right Parietal	**84.8***	**108.0***	**124.2***	**103.0***	**86.6***
Left Precuneus	−1.2	2.8	12.8	−3.9	1.38
Right Precuneus	32.1	38.5	48.0	34.6	**54.9***
Left Amygdala	**35.3***	17.4	0.8	−0.3	−7.6
Right Amygdala	−6.3	−10.4	**−21.4***	**−23.3***	**−25.9***
Left Middle Hippocampus	10.7	2.0	−3.2	−6.9	−13.2
Right Middle Hippocampus	−14.7	−16.6	**−21.8***	**−29.8***	**−31.9***
Left Anterior Hippocampus	32.5	18.6	0.9	−3.2	−12.2
Right Anterior Hippocampus	−3.3	−9.2	**−23.7***	**−29.6***	**−32.9***
Left Posterior Hippocampus	19.1	8.5	6.6	−1.8	−4.6
Right Posterior Hippocampus	−6.2	−6.2	−4.8	−11.4	−10.3
Vermis of Cerebellum	0.5	0.6	−3.5	−7.5	−2.0
Left Anterior Lobe Cerebellum	9.0	8.8	3.0	−3.3	2.2
Right Anterior Lobe Cerebellum	8.9	16.2	27.3	21.3	47.8
Left Posterior Lobe Cerebellum	−25.7	−31.6	−28.8	**−34.0***	−27.5
Right Posterior Lobe Cerebellum	−32.5	−30.1	−25.7	−27.9	−22.5

$n = 10$, EtOH group $n = 7$, Control group $n = 3$.
* $p < 0.05$ corrected.

across time (See Fig. 1B). One subject was scanned for only six minutes; therefore, all subjects' data was truncated to six minutes. Results were replicated calculating signal power using 750 ms and 900 ms overlap.

2.8. Analyses

Analyses were conducted using SPSS version 21. Power in each bandwidth at each ROI was analyzed using the Generalized Linear Models approach. A linear model was selected with power in the appropriate bandwidth as the outcome. Group, Time, and the Group*Time interaction were entered into the model. Parameter estimates were calculated using maximum likelihood estimation. The False Discovery Rate (FDR; Benjamini and Hochberg, 1995) was used to control for Type-I error across analyses (160 comparisons) using α = 0.05 (step up method).

3. Results

3.1. Ethanol self-administration

Average daily ethanol intake ranged from 0.73 to 2.57 g/kg (3–10 drink/day equivalent) across the 12-months of free access prior to the scans. Average daily intake across the last 3 months ranged from 1.06 to 3.11 g/kg (equivalent to 4–12 drinks/day). Lifetime intake ranged from 307.1 to 1109.3 g/kg.

3.2. Signal power

Results of the analysis can be seen in Table 1. Values indicate percent change in power due to EtOH group membership. Positive values indicate higher power and negative values indicate lower power in EtOH animals relative to Control animals. EtOH animals displayed significantly lower levels of power in the alpha, beta, and gamma bandwidths in the anterior cingulate cortices, right hippocampus, and right amygdala. Power was also lower in EtOH animals in the right principle sulcus in the alpha bandwidth and left posterior lobe of the cerebellum in the beta bandwidth. EtOH animals displayed significantly higher

power across all bandwidths in the right medial orbital and parietal areas. Power was also higher in EtOH animals in the right precuneus in the gamma bandwidth and left amygdala in the delta bandwidth. There were no significant effects of time, or time*group interactions, indicating that patterns of brain activity did not meaningfully change over the duration of the scan for either group. Results were essentially identical when signal power was calculated using 750 ms and 900 ms overlaps.

4. Discussion

The current study provides the first demonstration of whole-head MEG acquisition in vervet monkeys. Results revealed differences in RS activity in specific brain regions between chronic EtOH consuming monkeys and age-matched controls after 15 months of daily drinking (See Table 1) that are consistent with previous findings in humans. These findings extend our previous report of altered hub connectivity using fMRI (Telesford et al., 2015) by examining changes in the frequency domain in the same animals using an imaging modality less sensitive to potential EtOH-related disruptions of the microvasculature (Altura and Altura, 1984). The current study supports the feasibility of using a human MEG instrument to record from cortical and subcortical brain regions in vervet monkeys.

Additionally, these findings help clarify previous reports examining changes in power associated with alcohol use disorders (Kamarajan and Porjesz, 2015). The relatively poor spatial resolution of EEG may have been a key factor producing inconsistent findings as recent studies have demonstrated unique spectral profiles across brain regions (Keitel and Gross, 2016). The current findings demonstrate that changes in brain activity due to EtOH exposure are dependent on the brain region being examined. Analyses utilizing sensor level EEG may be examining brain activity combined across regions of both increased and decreased activity. Using MEG to spatially localize brain activity, the current results suggest the right parietal and ventral frontal regions as sources of differences in the theta and beta bandwidths with the anterior cingulate and right

limbic areas (amygdala and hippocampus) as generators underlying differences in the alpha bandwidth. Future studies may be able to utilize this NHP model of alcoholism and MEG during task performance to better understand the changes in brain function associated with chronic alcohol consumption. Several limitations of this study should be considered. Although it was possible to detect and localize significant differences in brain activity resulting from chronic EtOH consumption, it is not possible to determine when during the course of EtOH exposure the changes occur due to the cross-sectional nature of the data. Additionally, data were acquired under propofol anesthesia and a known linear relationship exists between resting-state activity and propofol anesthesia (Boveroux et al., 2010). Previous research suggests that propofol has a greater effect on activity in higher frequency ranges, suggesting changes in brain activity in these ranges may not be solely due to EtOH consumption. The EtOH fast minimally interfered with drinking behaviors for all but one animal, suggesting disruption of drinking cannot fully explain the findings. However, propofol is a GABAA agonist that can be used to treat alcohol withdrawal syndrome (Brotherton et al., 2016), it is possible the two groups responded differently to anesthesia due to differences in EtOH exposure, or propofol could have mitigated potential acute withdrawal symptoms in EtOH animals. Overnight fasting from EtOH suggests that the changes in activity are a result of chronic exposure to EtOH, rather than an interaction between acute EtOH and propofol. The ability to acquire data in awake NHPs, particularly during task performance, will better utilize the translational value of these models. Finally, future studies

should determine the optimal analytic approach for NHP data. It is possible that alternative approaches, particularly for head modeling, may be required for optimal results. The ability to use MEG to evaluate changes in brain activity in the NHP following chronic ethanol exposure provides a potentially powerful tool to better understand both the acute and chronic effects of ethanol on brain function.

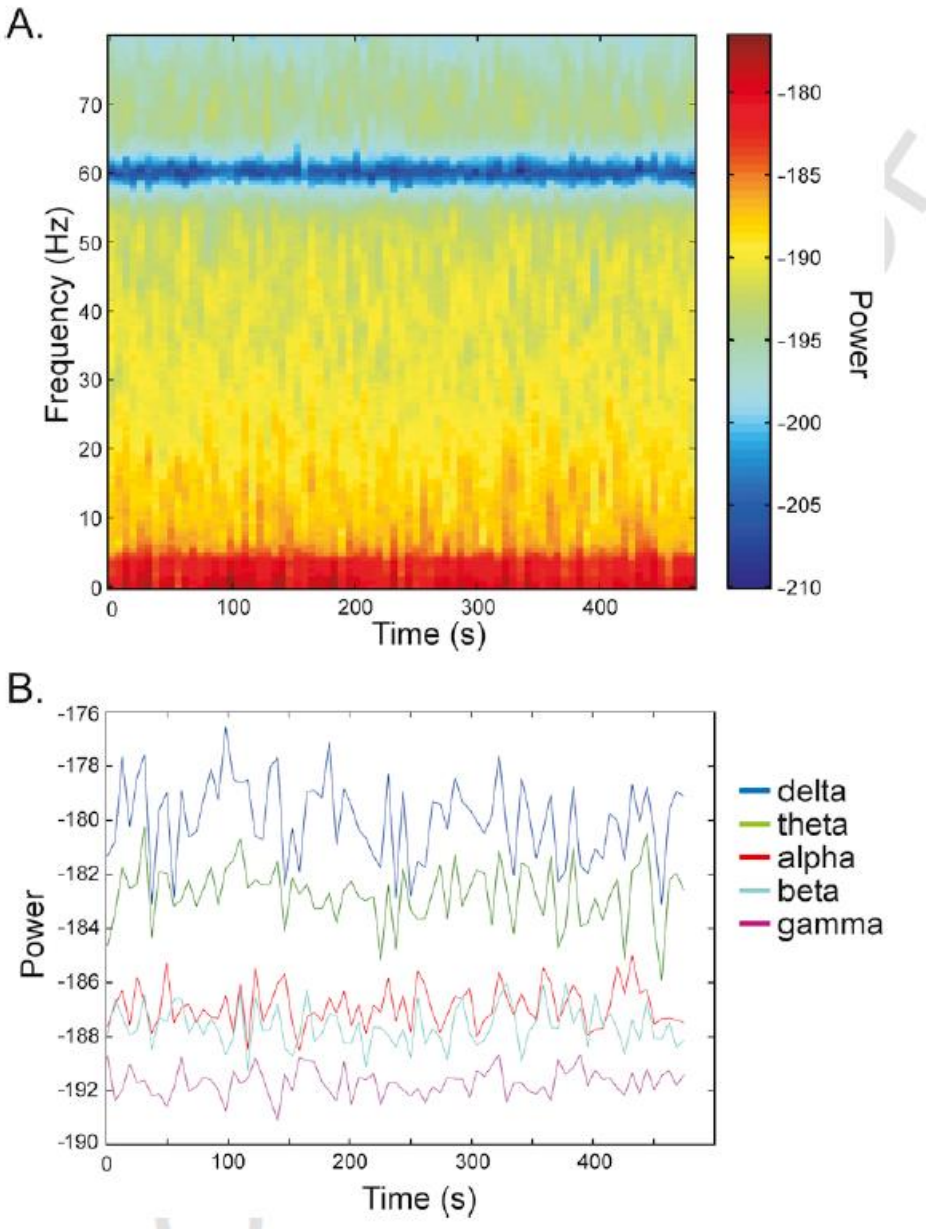

Fig. 1. This figure illustrates the creation of the outcome variables. Data are presented as 10*log10 for ease of viewing. First, the spectrogram is calculated using a 1 s window with 50%overlap. Then every twelve data points are averaged in a modified Welch′s method, as shown in panel A. From the result, the maximum value in each of the delta, theta, alpha, beta, and gamma bandwidths is extracted at each time point, creating a vector of maximum values as shown in panel B. These vectors are extracted from each ROI and used in the analyses.

Role of funding

Source This study was supported by AA019431 and AA016748 (JBD), AA016852 (DWG), AA014106 (DPF), 2T32NS073553-06 and 5F30AA023708-02 (GEA), Ignition Funds from the Wake Forest School of Medicine Translational Sciences Institute (JBD) and a TSI pilot award (DWG). These funding sources had no role in study design, data acquisition, data analysis, or manuscript preparation.

Contributors

JAR, JRSK, GEA, AD, and JBD participated in protocol design and data collection. JAR and JRSK conducted data analyses. All authors participated in hypothesis development, interpretation of results, and manuscript preparation. All authors have approved the final article.

Conflict of interest

No conflict declared.

Acknowledgements

We wish to thank the Department of Neurology for providing scanner time on the MEG and the Center for Biomolecular Imaging for MRI pilot scans. We acknowledge the Wake Forest University Primate Center for providing animals for this study OD010965 (Jay Kaplan), as well as support from the W.G. (Bill) Hefner Veterans Affairs Medical Center and VA Mid-Atlantic Mental Illness, Research, Education, and Clinical Center.

Appendix A. Supplementary data

Supplementary data associated with this article can be found, in the online version, at http://dx.doi.org/10.1016/j.drugalcdep.2017.03.036.

References

Acosta, G., Hasenkamp, W., Daunais, J.B., Friedman, D.P., Grant, K.A., Hemby, S.E., 2010. Ethanol self-administration modulation of NMDA receptor subunit and related synaptic protein mRNA expression in prefrontal cortical fields in cynomolgus monkeys. Brain Res. 1318, 144–154.

Altura, B.M., Altura, B.T., 1984. Alcohol, the cerebral circulation and strokes. Alcohol 1, 325–331.

Ariwodola, O.J., Crowder, T.L., Grant, K.A., Daunais, J.B., Friedman, D.P., Weiner, J.L.,2003. Ethanol modulation of excitatory and inhibitory synaptic transmission in rat and monkey dentate granule neurons. Alcohol. Clin. Exp. Res. 27, 1632–1639.

Beal, D.S., Cheyne, D.O., Gracco, V.L., Quraan, M.A., Taylor, M.J., De Nil, L.F., 2010. Auditory evoked fields to vocalization during passive listening and active generation in adults who stutter. Neuroimage 52, 1645–1653.

Benjamini, Y., Hochberg, Y., 1995. Controlling the false discovery rate: a practical and powerful approach to multiple testing. J. R. Statist. Soc. B 57, 289–300.

Boveroux, P., Vanhaudenhuyse, A., Bruno, M.A., Noirhomme, Q., Lauwick, S., Luxen, A., Degueldre, C., Plenevaux, A., Schnakers, C., Phillips, C., Brichant, J.F., Bonhomme, V.,Maquet, P., Greicius, M.D., Laureys, S., Boly, M., 2010. Breakdown of within- and between-network resting state functional magnetic resonance imaging connectivity during propofol-induced loss of consciousness. Anesthesiology 113, 1038–1053.

Brotherton, A.L., Hamilton, E.P., Kloss, H.G., Hammond, D.A., 2016. Propofol for treatment of refractory alcohol withdrawal syndrome: A review of the literature. Pharmacotherapy 36, 433–442.

Budygin, E.A., John, C.E., Mateo, Y., Daunais, J.B., Friedman, D.P., Grant, K.A., Jones, S.R., 2003. Chronic ethanol exposure alters presynaptic dopamine function in the striatum of monkeys: a preliminary study. Synapse 50, 266–268.

Buhler, M., Mann, K., 2011. Alcohol and the human brain: a systematic review of different neuroimaging methods. Alcohol. Clin. Exp. Res. 35, 1771–1793.

Carden, W.B., Alexander, G.M., Friedman, D.P., Daunais, J.B., Grant, K.A., Mu, J., Godwin, D.W., 2006. Chronic ethanol drinking reduces native T-type calcium current in the thalamus of nonhuman primates. Brain Res. 1089, 92–100.

Cheyne, D., Bostan, A.C., Gaetz, W., Pang, E.W., 2007. Event-related beamforming: a robust method for presurgical functional mapping using MEG. Clin. Neurophysiol. 118, 1691–1704.

Cornwell, B.R., Carver, F.W., Coppola, R., Johnson, L., Alvarez, R., Grillon, C., 2008. Evoked amygdala responses to negative faces revealed by adaptive MEG beamformers. Brain Res. 1244, 103–112.

Cornwell, B.R., Arkin, N., Overstreet, C., Carver, F.W., Grillon, C., 2012. Distinct contributions of human hippocampal theta to spatial cognition and anxiety. Hippocampus 22, 1848–1859.

Cuzon Carlson, V.C., Seabold, G.K., Helms, C.M., Garg, N., Odagiri, M., Rau, A.R., Daunais, J., Alvarez, V.A., Lovinger, D.M., Grant, K.A., 2011. Synaptic and morphological neuroadaptations in the putamen associated with long-term, relapsing alcohol drinking in primates. Neuropsychopharmacology 36, 2513–2528.

Douw, L., de Groot, M., van Dellen, E., Aronica, E., Heimans, J.J., Klein, M., Stam, C.J.,Reijneveld, J.C., Hillebrand, A., 2013. Local MEG networks: the missing link between protein expression and epilepsy in glioma patients?. Neuroimage 75, 195–203.

Floyd, D.W., Friedman, D.P., Daunais, J.B., Pierre, P.J., Grant, K.A., McCool, B.A., 2004.Long-term ethanol self-administration by cynomolgus macaques alters the pharmacology and expression of GABAA receptors in basolateral amygdala. J. Pharmacol. Exp. Ther. 311, 1071–1079.

Grant, K.A., Leng, X., Green, H.L., Szeliga, K.T., Rogers, L.S., Gonzales, S.W., 2008. Drinking typography established by scheduled induction predicts chronic heavy drinking in a monkey model of ethanol self-administration. Alcohol. Clin. Exp. Res. 32, 1824–1838.

Hemby, S.E., O'Connor, J.A., Acosta, G., Floyd, D., Anderson, N., McCool, B.A., Friedman, D., Grant, K.A., 2006. Ethanol-induced regulation of GABA-a subunit mRNAs in prefrontal fields of cynomolgus monkeys. Alcohol. Clin. Exp. Res. 30, 1978–1985.

Hillebrand, A., Barnes, G.R., Bosboom, J.L., Berendse, H.W., Stam, C.J., 2012. Frequency-dependent functional connectivity within resting-state networks: an atlas-based MEG beamformer solution. Neuroimage 590, 3909–3921.

Huang, M.X., Mosher, J.C., Leahy, R.M., 1999. A sensor-weighted overlapping-sphere head model and exhaustive head model comparison for MEG. Phys. Med. Biol. 44, 423–440.

Hung, Y., Smith, M.L., Bayle, D.J., Mills, T., Cheyne, D., Taylor, M.J., 2010. Unattended emotional faces elicit early lateralized amygdala-frontal and fusiform activations. Neuroimage 50, 727–733.

Hung, Y., Smith, M.L., Taylor, M.J., 2012. Development of ACC-amygdala activations in processing unattended fear. Neuroimage 60, 545–552.

Kamarajan, C., Porjesz, B., 2015. Advances in electrophysiological research. Alcohol Res. Curr. Rev. 37, 53–87.

Keitel, A., Gross, J., 2016. Individual human brain areas can be identified from their characteristic spectral activation fingerprints. PLoS Biol. 14, e1002498.

Luo, Q., Holroyd, T., Jones, M., Hendler, T., Blair, J., 2007. Neural dynamics for facial threat processing as revealed by gamma band synchronization using MEG. Neuroimage 34, 839–847.

Mahon, P., Greene, B.R., Greene, C., Boylan, G.B., Shorten, G.G., 2008. Behavior of spectral entropy, spectral edge frequency 90%, and alpha and beta power parameters during low-dose propofol infusion. Br. J. Anaesth. 101, 213–221.

Mitra, P., Bokil, H., 2008. Observed Brain Dynamics. Oxford University Press, New York.
Mohr, C., Kolotushkina, O., Kaplan, J.S., Welsh, J., Daunais, J.B., Grant, K.A., Rossi, D.J., 2013. Primate cerebellar granule cells exhibit a tonic GABAAR conductance that is not affected by alcohol: a possible cellular substrate of the low level of response phenotype. Front. Neural Circ. 7, 189.
Monnig, M.A., Tonigan, J.S., Yeo, R.A., Thoma, R.J., McCrady, B.S., 2013. White matter volume in alcohol use disorders: a meta-analysis. Addict. Biol. 18, 581–592.
Moses, S.N., Ryan, J.D., Bardouille, T., Kovacevic, N., Hanlon, F.M., McIntosh, A.R., 2009. Semantic information alters neural activation during transverse patterning performance. Neuroimage 46, 863–873.
Pandey, A.K., Kamarajan, C., Rangaswamy, M., Porjesz, B., 2012. Event-related oscillations in alcoholism research: a review. J. Addict. Res. Ther. Suppl. 7.
Pfefferbaum, A., Sullivan, E.V., Mathalon, D.H., Lim, K.O., 1997. Frontal lobe volume loss observed with magnetic resonance imaging in older chronic alcoholics. Alcohol. Clin. Exp. Res. 21, 521–529.
Quraan, M.A., Moses, S.N., Hung, Y., Mills, T., Taylor, M.J., 2011. Detection and localization of hippocampal activity using beamformers with MEG: a detailed investigation using simulations and empirical data. Hum. Brain Mapp. 32, 812–827.
Rangaswamy, M., Porjesz, B., 2008. From event-related potential to oscillations: genetic diathesis in brain (dys)function and alcohol dependence. Alcohol Res. Health 31, 238–242.
Riggs, L., Moses, S.N., Bardouille, T., Herdman, A.T., Ross, B., Ryan, J.D., 2009. A complementary analytic approach to examining medial temporal lobe sources using magnetoencephalography. Neuroimage 45, 627–642.
Robinson, S.E., Vrba, J., 1998. Functional neuroimaging by Synthetic Aperture Magnetometry (SAM). In: Biomag98, 11th International Conference on Biomagnetism. Sendai. pp. 1–4.
Stapleton-Kotloski, J.R., Kotloski, R.J., Boggs, J.A., Popli, G., O'Donovan, C.A., Couture, D.E., Cornell, C., Godwin, D.W., 2014. Localization of interictal epileptiform activity using magnetoencephalography with synthetic aperture magnetometry in patients with a vagus nerve stimulator. Front. Neurol. 5, 244.
Telesford, Q.K., Laurienti, P.J., Davenport, A.T., Friedman, D.P., Kraft, R.A., Daunais, J.B., 2015. The effects of chronic alcohol self-administration in nonhuman primate brain networks. Alcohol. Clin. Exp. Res. 39, 659–671.
Vivian, J.A., Green, H.L., Young, J.E., Majerksy, L.S., Thomas, B.W., Shively, C.A., Tobin, J.R., Nader, M.A., Grant, K.A., 2001. Induction and maintenance of ethanol self-administration in cynomolgus monkeys (Macaca fascicularis): long-term characterization of sex and individual differences. Alcohol. Clin. Exp. Res. 25, 1087–1097.

Welsh, J.P., Han, V.Z., Rossi, D.J., Mohr, C., Odagiri, M., Daunais, J.B., Grant, K.A., 2011. Bidirectional plasticity in the primate inferior olive induced by chronic ethanol intoxication and sustained abstinence. Proc. Natl. Acad. Sci. U. S. A. 108, 10314–10319.

Zahr, N.M., 2013. Graphs of brain networks. Alcohol. Clin. Exp. Res. 37, 1813–1815.

Appendix B

Optogenetic activation of brain circuits reveals detection capabilities of MEG source imaging

Alberto, GE[1*]; Klorig, DC[1]; Stapleton-Kotloski[1,2], JR; Constantinidis, C[1]; Daunais, JB[3]; Godwin, DW[1,2,3]

1. Wake Forest School of Medicine Department of Neurobiology and Anatomy
2. Wake Forest School of Medicine Department of Neurology
3. Wake Forest School of Medicine Department of Physiology and Pharmacology

*corresponding author

Abstract

We have developed an experimental platform combining MEG-compatible optogenetic techniques in a non-human primate model. We demonstrate localization of optogenetically-evoked signals to known sources in both the superficial structure of arcuate sulcus of cortex and deep in the hippocampus, at a resolution of 750 μm^3. We also demonstrate detection of a previously described functional network that includes subcortical, including thalamic, structures in response to optical stimulation of a discrete cortical subregion.

Body

A fundamental goal of neuroimaging is to observe and quantify the brain's activity across the spatial and temporal resolutions at which it occurs. Magnetoencephalography (MEG) holds particular promise for improving upon current neuroimaging methods because it has identical temporal resolution to EEG, with the potential for superior spatial resolution[1,2]. Importantly, unlike electric fields, biomagnetic signals are not distorted by the intervening tissues of the head through which they propagate prior to arriving at the sensor, providing magnetic source imaging (MSI) an inherent advantage over source localization with EEG[2].

Despite the exponential drop-off of signal strength with distance from the source, the sensitivity of MEG sensors to magnetic flux provide some MSI analysis techniques, namely synthetic aperture magnetometry (SAM)[3], with a theoretical

spatial resolution in the sub-mm^3 range[4–6]. While SAM has been employed clinically for use in the pre-surgical evaluation of epilepsy[7–9] and in studies of deep structures such as hippocampus[10] and amygdala[11], a detailed investigation of the resolution capabilities of MEG has not been conducted; thus the degree to which the theoretical capabilities of MSI are reflected in the underlying practical abilities remains uncertain.

We have developed a MEG-compatible optogenetic preparation in vervet monkeys that allows simultaneous optical activation of discrete brain areas with MEG recording. Using this combination of approaches, we elicited and measured neuronal activity in the arcuate sulcus of the cerebral cortex and within the CA3 region of the hippocampus in vervet monkeys. We demonstrate the ability of SAM to accurately localize discrete optogenetically-elicited sources of activity throughout the volume of the brain. We further demonstrate the utility of combining optogenetics and MEG/MSI in experimenter-controlled functional brain mapping across a wide range of spatiotemporal scales.

Three vervet monkeys were first injected with the viral vector, AAV10-CaMKIIa-ChR2-eYFP, then in the same surgery implanted with an optical fiber. Two weeks after surgery we determined whether there was a detectable signal during the early expression period. At this time-point a small LFP response was detected that would continue to increase until week seven (Fig 1C-E; one-way ANOVA, cortical: [$F(2, 47) = 21.32$, $p<0.0001$, hippocampal: $F(2, 57) = 82.67$, $p < 0.0001$)]. When two week post-surgical MEG data were analyzed using SAM, consistent with the electrophysiological recordings obtained in the same week,

there was no localization to the site of stimulation, and the activity maps were qualitatively similar to the pre-surgical control scans. This contrasts with visual stimulation experiments conducted at that time that demonstrated peak voxels active in the occipital lobe consistent with the early cortical component of visual evoked potentials[12](Fig. S1). We conclude that expression of ChR2 at two weeks post-injection was insufficient to generate an optically-evoked response that could be identified using SAM.

After eight weeks post-injection, once the neural response to optical stimulation had reached a plateau, broadband (DC-450 Hz) whole-head dual-state SAM analysis of 1 s of data surrounding one hundred pulses (10 ms each) to arcuate sulcus of cortex revealed a tight cluster of peaks in the SPM at the target site of transfection and stimulation (Fig. 2A). Similarly, whole-head SAM analysis of 100 pulses of optical stimulation data identified peak signal generators at the site of stimulation in hippocampus (Fig. 2B). For this analysis, beamforming parameters were confined to unique features of the signal; based on the LFP, 50 ms of data were analyzed at 100-200 Hz.

Additional investigations of SAM based SPMs revealed peak generators in a pattern that conformed to a known motor-associative network, the cortico-striatal-pallido-thalamo-cortical (CSPTC) motor network[13,14]. Wide band (DC-450 Hz) analysis of 1 s of data after 100 stimulations of ChR2-transfected arcuate sulcus indicated peaks of activity in the ipsilateral caudate nucleus of striatum, globus pallidus, ipsilateral and contralateral midline thalamus, and ipsilateral primary

motor cortex (Fig. 3A-D). This result indicates the utility of combining optogenetic techniques with MEG for functional brain mapping, even under anesthesia.

Post-mortem confocal microscopy demonstrated labeled neurons in the posterior wall of arcuate cortex corresponding to area 8a of the NHP cortex[27,28](Fig. 1Ai). Hippocampal imaging revealed GFP labeled neurons in anterior dorsal hippocampus corresponding to area CA3[28] (Fig. 1Bi). Terminal MRI confirmed placement of the optrode in both the posterior wall of arcuate sulcus and in anterior dorsal hippocampus[29] (Fig. 1Aii-iii and Fig. 1Bii-iii).

This study represents the first successful use of optogenetics with magnetic source imaging of MEG signals in non-human primates, and provides additional information on the relationship between MEG signals and the underlying electrical activity in the brain[15]. In this study, we have demonstrated anatomically discrete and temporally precise control over the LFP in a MEG-compatible optogenetic preparation. The LFP is a measure of population-wide changes in the electrical fields in the brain[16]. Control over the LFP via optogenetics provides the unique ability to test certain assumptions regarding the MEG signal and MEG analytics, differentiating it from studies that rely on phantom signals and artificially generated datasets[5,17,18]. This study provides evidence that a signal generated in deep brain structures is detectable with MEG, including hippocampus, caudate nucleus, globus pallidus and thalamus and that the elicited signals are localizable with appropriate use of beamformers.

Studies using NHPs in MEG have previously demonstrated the feasibility of equivalent current dipole[19] and beamformer[20] analyses in monkeys. This study extends these observations to analysis of areas beyond superficial cortex into deep structures, supporting the utility of MSI throughout the volume of the brain. Furthermore, this study uses experimentally controlled, optogenetically generated signals from a known source to demonstrate the *accuracy* of source localization. The reported results suggest that a combination of whole head coverage with axial gradiometers, a low noise floor, low movement, and appropriate use of beamformers allows deep localization of activity that is consistent with theoretical investigations and data from epilepsy patients[2–5,8,9].

The relevance of this finding to the clinical evaluation of epilepsy surgery candidates is significant. Currently, MEG is approved by the United States Food and Drug Administration for pre-surgical evaluation of epilepsy, but use is often limited to dipole analyses only[21–23]. However, dipole analyses break down with low SNR[5], which is often the case with deep signals. The most common epilepsy type requiring surgical resection is mesial temporal lobe epilepsy wherein the seizure generator is deep in the brain[24]; importantly, our results demonstrate that SAM can accurately localize a deep signal to its source.

The results of this study support, through direct measurement, the assumed theoretical ability of MEG/MSI to detect and localize experimentally controlled activity in the brain at very fine temporal and spatial resolutions. We have demonstrated the feasibility of localizing activity in the brains of vervet monkeys

using whole head instrumentation designed for human subjects. By combining optogenetic stimulation in MEG with SAM analyses it is possible to empirically determine the practical abilities and limitations of MEG/MSI. In addition, evaluation of optimal study designs and environment for MEG/MSI will be possible. However, beyond use as a tool for improving MEG/MSI it is clear that this combination of techniques may also permit functional brain mapping in spatial and temporal domains not otherwise possible with current functional imaging techniques.

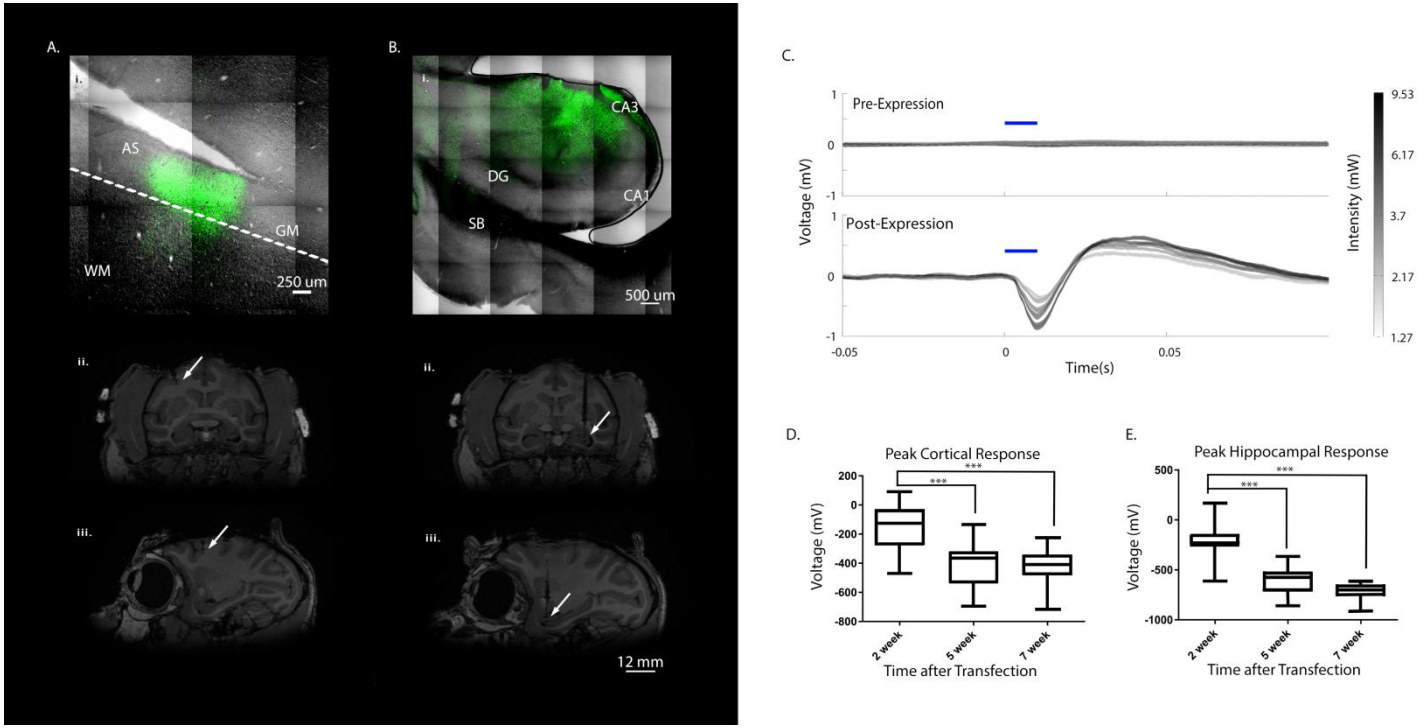

Figure 1. Location of optogenetic proteins and light evoked responses. Ai. GFP labeled neurons confined to gray matter of the posterior wall of arcuate sulcus corresponding to area 8a, white line indicates approximate boundary between gray and white matter. Coronal (Aii) and sagittal (Aiii) MRI demonstrating colocalization of the optrode. Bi. GFP labeled neurons in the anterior dorso-lateral aspect of hippocampus corresponding to area CA3 indicate transgene expression. Coronal (Bii) and sagittal (Biii) MRI demonstrating colocalization of the optrode. C. Example of averaged response to stimulation in hippocampus showing week 2 (upper trace) and week 7 (lower trace). Maximum intensity stimulation of cortex (D) and hippocampus (E) at two weeks post transfection elicited a response as measured by the LFP electrode that was significantly less than at 7 weeks post-transfection. Maximum stimulation intensity elicited a response in both locations that was no different at 5 weeks compared to 7 indicating a sufficient channel expression. Transparent bands indicate 95% confidence intervals when averages were used. Blue bar indicates stimulus onset and duration. *** indicate one-way ANOVA $F(2, 57)=82.67$, $p<0.0001$ hippocampal, and $F(2, 47)=21.32$, $p<0.0001$ cortical. Tukey's correction for multiple comparison hippocampal 2vs5 weeks $q = 13.59$ $p<0.0001$, 2vs7 weeks $q=17.26$ $p<0.0001$, 5vs7 weeks $q=3.672$ $p=0.0316$; cortical 2vs5 weeks $q=6.57$ $p<0.0001$, 2vs7 weeks $q=8.606$ $p<0.001$, 5vs7 weeks $q=0.4566$ $p=0.9442$. AS= arcuate sulcus; GM= gray matter; WM = white matter; DG= dentate gyrus; SB= subiculum

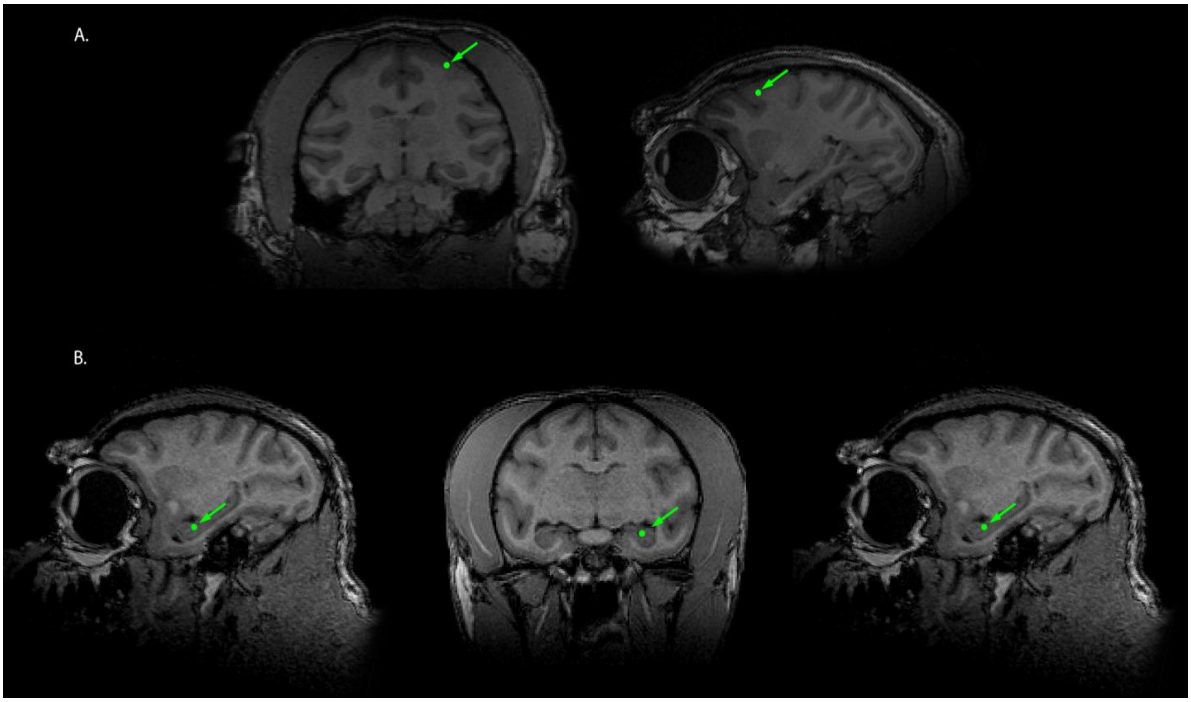

Figure 2. SAM source localization of optogenetically evoked responses. One hundred, 10 ms flashes of light were delivered with a 5 second inter-stimulus interval through an implanted fiber optic to the site of transfection in arcuate sulcus (A) and hippocampus (B) of an anesthetized vervet while the animal was positioned inside the MEG helmet. SAM dual state analysis was employed to calculate pseudo-T scores for each voxel at a resolution of 750 μm^3 for the frequency bin DC-450 Hz over 1 s. (A) and from 100-200Hz over 50ms (B) starting at pulse onset. Green arrows indicate a peak in the statistical parametric map (SPM) generated by SAM analysis. Peak activity reveals a source in the posterior wall of arcuate sulcus (A) and in the antero-medial aspect of hippocampus (B) corresponding to the coordinates of implantation for each respective stimulation.

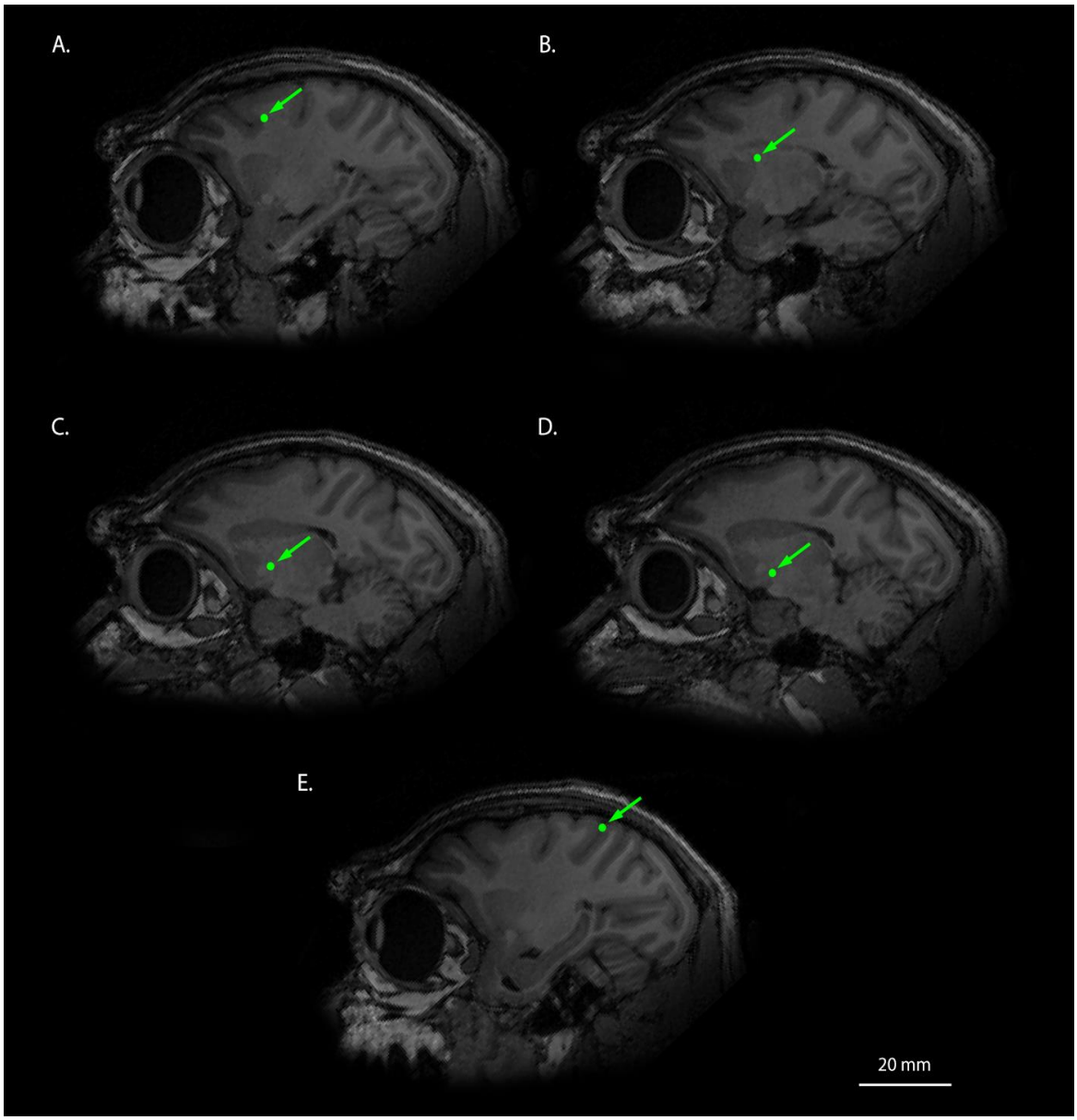

Figure 3. Identification of cortico-striato-pallido-thalamo-cortical (CSPTC) network activity in response to stimulation of arcuate sulcus. SAM analysis of 100 10 ms stimulations to arcuate sulcus reveals a known functional network with peaks in **A.** arcuate sulcus, **B.** caudate nucleus of the striatum, **C.** globus pallidus, **D.** midline thalamus, and **E.** primary motor cortex. Analysis was conducted on trials 1 s of data following stimulation across a broad bandwidth frequency range (DC-450 Hz). Green arrow indicates peak in map at each location. Pseudo-t score = 0.1 in all cases.

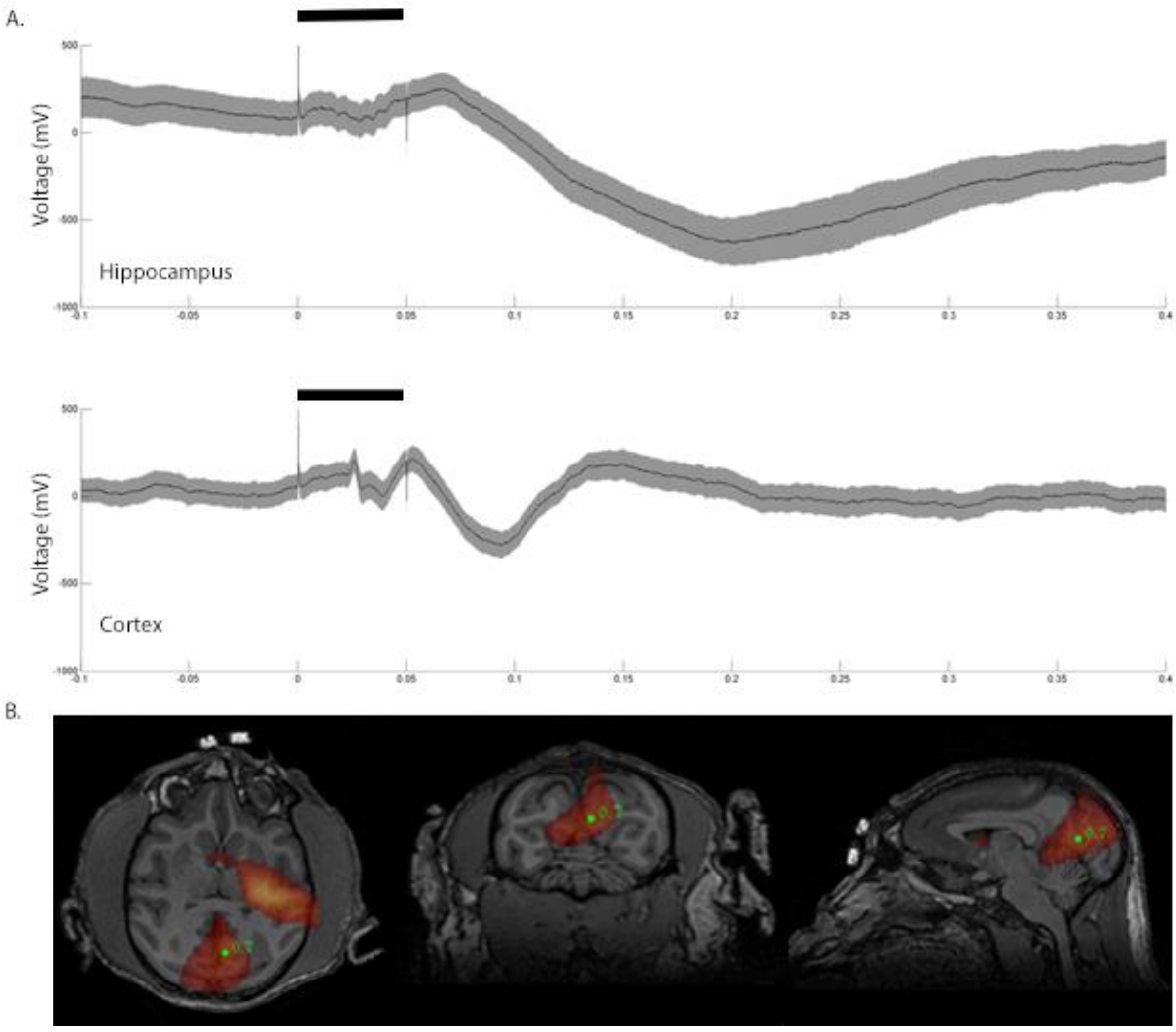

Figure S1. Electrode positive control and Synthetic Aperture Magnetometry (SAM) source localization of visually evoked potential (VEP) at two weeks. A. One hundred twenty, 50 ms flashes of white light were delivered with a 3 second inter-stimulus interval to the left visual field of an anesthetized vervet. The response was measured on the hippocampal (upper trace) and cortical (lower) electrodes. The averaged response is shown and ghosting indicates 95% confidence interval. **B.** The animal was visually stimulated with the same protocol during the MEG scan. SAM dual state analysis was employed to calculate pseudo-t scores for each voxel at a resolution of 750 μm^3 for the frequency bin 20-40 Hz over 50 ms starting at pulse onset, corresponding to latency of the C1 component in VEP studies (Di Russo et al., 2001). Green number indicates peak in the SAM SPM. Field spread is thresholded at the full width half-maximum of the peak. Black bar indicates stimulus onset.

References

1. Nasiotis, K., *et. al*. *NeuroImage* doi:10.1016/j.neuroimage.2016.10.017

2. Vrba, J. & Robinson, S. E. *Methods* **25,** 249–271 (2001).

3. Robinson, S. & Vrba, J. in *11th Int. Conf. on Biomagnetism* (1998).

4. Vrba, J., Robinson, S. E. & McCubbin, J. *Neurol. Clin. Neurophysiol. NCN* **2004,** 99 (2004).

5. Hillebrand, A. & Barnes, G. R. in (ed. Neurobiology, B.-I. R. of) **68,** 149–171 (Academic Press, 2005).

6. Troebinger, L. *et al. NeuroImage* **86,** 583–591 (2014).

7. Stapleton-Kotloski, J. R. *et al. Brain Imaging Methods* **5,** 244 (2014).

8. Robinson, S., *et. al*. *Neurol. Clin. Neurophysiol. NCN* **2004,** 74 (2004).

9. Kirsch, H. E., *et. al. Clin. Neurophysiol.* **117,** 2264–2271 (2006).

10. Cornwell, B. R., *et. al*. *J. Neurosci. Off. J. Soc. Neurosci.* **28,** 5983–5990 (2008).

11. Cornwell, B. R. *et al. Brain Res.* **1244,** 103–112 (2008).

12. Di Russo, F., *et. al*. *Hum. Brain Mapp.* **15,** 95–111 (2002).

13. Worbe, Y., Lehericy, S. & Hartmann, A. *Mov. Disord.* **30,** 1179–1183 (2015).

14. Worbe, Y. *et al. Brain* **138,** 472–482 (2015).

15. Ioannides, A. A. *Neurosci. Rev. J. Bringing Neurobiol. Neurol. Psychiatry* **12,** 524–544 (2006).

16. Buzsáki, G., Anastassiou, C. A. & Koch, C. *Nat. Rev. Neurosci.* **13,** 407–420 (2012).

17. Jonmohamadi, Y. & Jones, R. D. *J. Neural Eng.* **13,** 016005 (2016).

18. Bauer, M., Trahms, L. & Sander, T. *Biomed. Eng. Biomed. Tech.* **60,** 135–145 (2014).

19. Wilson, T. W. *et al. NeuroImage* **46,** 998–1003 (2009).

20. Zumer, J. M. *et al. Brain Res.* **1345,** 110–124 (2010).

21. Kharkar, S. & Knowlton, R. *Epilepsy Behav.* **46,** 19–26 (2015).

22. Kaiboriboon, K., *et. al*. *Clin. Neurophysiol.* **121,** 325–331 (2010).

23. Bagić, A. I. *et. al*. *J. Clin. Neurophysiol.* 1 (2011). doi:10.1097/WNP.0b013e3182272fed

24. Giulioni, M. *et al. J. Neurosurg.* 1–11 (2013).

Materials and Methods

Surgical Targeting.

All studies were approved by the Animal Care and Use Committee of Wake Forest School of Medicine. This study was repeated in three female vervet monkeys, *Chlorocebus aethiops*, aged 15-16 years and weighing between 4.99-6.75 kg, housed in pairs under a 12/12 light/dark cycle. Each animal was mounted in an MRI compatible stereotaxic frame with lipid containing ear bars, and T1-weighted anatomical images were acquired using a 3D-MPRAGE 0.5 mm isotropic sequence in a Siemens 3 T Skyra system with a custom built 8-channel flexible head coil (Dr. Cecil Hayes, Univ. Washington). The animals were removed from the stereotaxic frame and an additional MRI scan was acquired in which the animals were fitted with three lipid biomarkers fixed in the location of the MEG fiducials (placed in the conventional three-point fiducial locations) for co-registration with MEG data. The locations of the MEG fiducials were tattooed on the animals prior to the start of the study to ensure precise co-registration across multiple sessions. In one animal a post-mortem MRI was conducted after implantation and recording to confirm stereotaxic targeting (Fig. 1Aii-iii and Bii-iii).

Using Medical Image Processing, Analysis, and Visualization (MIPAV) software available from the NIH, stereotaxic coordinates were generated for CA3 of hippocampus and for the posterior wall of the contralateral arcuate sulcus.

Surgery

Animals were securely mounted and centered in a surgical stereotaxic frame. The cranium was exposed and ten ceramic screws (Rogue Research Inc.; Montreal, Canada) were placed around the perimeter of the surgical margin. A craniotomy was then drilled over the coordinates for each targeted brain region. A custom polyether ether ketone (PEEK) cannula with a Teflon stop was advanced through the dura on a stainless steel stylette. The stylette was retracted leaving the cannula in place; injection of the viral vector and placement of optrode was done through the cannula to ensure co-localization. A gas-tight, micro volume Hamilton Syringe was then filled with AAV10-CaMKIIa-ChR2-eYFP (Dr. Caroline Bass, SUNY Buffalo) and 4 µL of virus was injected at each coordinate through a 38 G needle at a rate of 0.5 µL/minute. The syringe was left in place for 5 minutes following the injection and slowly removed. A custom made optrode was implanted to a depth of 0.5 mm above the injection coordinates. The optrode consisted of either a 200 or 400 µm diameter fiber optic cable (ThorLabs, Inc.; Newton, NJ) coupled to a 75 µm Pt/Ir (FHC, Inc.; Bowdoin, ME) or a 35 µm formvar-coated Tungsten electrode (California Fine Wire Co.; Grover Beach, CA), which extended 0.7 mm beyond the tip of the optical fiber. Lastly, a custom polyether ether ketone (PEEK) headwell (Crist Instruments Co., Inc.; Bethesda, MD) was fitted over each craniotomy and cemented in place. The craniotomy was sealed with bone cement securing the optrode in place.

To ensure electrical and magnetic silence, we avoided the photovoltaic effect by designing optrodes with a beveled tip so that the conductive surface was in shadow rather than in the cone of light[1,2].

Electrophysiology Recordings

Recordings were conducted under anesthesia, using either propofol (200-400 µg/kg/min) or ketamine (12-15 mg/kg) and dexmedetomidine (0.0075-0.015 mg/kg). MEG recordings were conducted in a magnetically shielded room (MSR; Vacuumschmelze GmbH & Co.; Hanau, Germany) with a CTF MEG™ whole cortex helmet equipped with 275 first-order axial gradiometer coils, each with a 5 cm baseline and 22.4 mm average inter-sensor spacing and 29 reference sensors (CTF MEG International Services Limited Partnership; Coquitlam, BC, Canada). MEG recordings were sampled at 2400 Hz for a bandwidth of DC-600 Hz. Data were powerline filtered at 60 Hz harmonics with a 4 Hz width, and synthetic third-order gradiometry was applied for viewing, but recorded wideband without filtering. Simultaneous LFP data were amplified using a Nicolet intraoperative monitoring system (Natus Medical; Pleasanton, CA) sampled at 5 kHz with maximum range of +/- 5 mV with a bandpass filter of 0.1 Hz to 3 kHz, and recorded as analog channels in line with MEG data. On separate days without MEG recordings, LFP data were recorded using a SciWorks recording system (DataWave Technologies; Loveland, CO), AM-3600 extracellular amplifiers (A-M Systems; Carlsborg, WA), and a T8G100 headstage amplifier

(Triad Biosystems International; Durham, NC) bandpass filtered at 0.3 Hz to 5 kHz, with a gain of 500 and a 40 kHz sampling rate.

Prior to the optrode implantation, 8-minute resting-state MEG scans were acquired to establish baseline activity. Two weeks after surgery (before high level transgene expression, and after the animal had recovered from surgery) animals were stimulated for the first time at a range of optical intensities (10.3-75.6 mW/mm^2 for 200 µm and 2.6-18.9 mW/mm^2 for 400 µm fiber). These recordings were conducted under anesthesia as described in the MEG MSR as well as in separate sessions in a dedicated electrophysiology suite. Stimulations included single 10 ms pulses of 473 nm light from either a light emitting diode (ThorLabs) or from a laser (Shanghai Dream Laser Technology Co., Ltd; Song Jiang, Shanghai, China). The pulse inter-stimulus interval (ISI) was 3 seconds. Pulse duration of the laser was controlled with a 2 mm Uniblitz laser shutter and a D880C Uni-stable driver (Uniblitz Electronic; Rochester, NY). LED pulse durations were controlled with custom MATLAB scripts and a digital-analog converter (DAC; Data Translation, Inc.; Marlborough, MA). After stable transgene expression was determined, the animals were stimulated again using the same paradigms as above and the resulting activity was recorded. Electrophysiological and MEG recordings after stable expression were again done simultaneously using the Nicolet system for acquiring electrophysiology during MEG and also separately.

The optrodes were tested in saline; *in vitro* two weeks after transfection; as well as post mortem. As a positive control of the electrode and MEG/MSI, analysis of visual stimulation was conducted. One hundred twenty, 50 ms pulses of white light were delivered with a 3 s ISI via LED, in both the electrophysiology suite and the MEG MSR.

Analysis

All analyzed data were derived from recordings in which motion was no greater than 0.2 mm. Head motion was nearly eliminated through the use of anesthesia and a carefully supported head.

Data preprocessing, head model creation, and beamforming were performed using CTF MEG™ Software (CTF MEG International Services Limited Partnership, Coquitlam, BC, Canada). MEG preprocessing included DC-offsetting, application of synthetic third-order gradiometry, and powerline filtering[3]. MEG data were then co-registered with the monkey's anatomical MRI data using the standard three-point fiducials. From this, a head model composed of a three spherical shell, multiple-overlapping-spheres model of the whole brain volume was generated[4]. Dual-state SAM[5,6] was applied to each active time segment and an equal length control segment composed of data preceding the stimulus, to construct 3D images of the entire brain volume. Noise normalized t-deviate statistical parametric maps of source power were derived from the beamformer output at a voxel size ranging from 0.75 - 1.5 mm^3. Results will be

shown for 750 μm^3 analyses due to superior accuracy in source localization. Such small voxel sizes were possible because of extremely low motion associated with this preparation. SAM time-frequency analysis parameters were determined in part by the power spectral densities (PSDs) of the neural response measured on the LFP during simultaneous MEG/LFP recordings in the MSR. The degree of activation in each voxel is indicated by a pseudo t-score. Local maxima and minima of the SAM maps were identified as peak activity voxels.

LFP data were analyzed using SciWorks, Neuroexplorer (Nex Technologies, Madison, Al), and custom scripts in MATLAB. Peak amplitude of the LFP in response to optical stimulation of electrophysiology recordings was tested for significance between two week, five week, and seven week time points using a one-way analysis of variance (ANOVA) with Tukey's multiple comparisons test. One-way ANOVA was chosen because the time points are treated as three independent groups with equal variance. Peak amplitudes were identified as maximum voltage between stimulus onset and 30 ms following stimulation.

Histology

At the completion of the imaging study, one animal was necropsied by first sedating with ketamine followed by an overdose with pentobarbital. A thoracotomy was conducted and the animal was transcardially perfused with ice-cold phosphate buffered saline followed by 4% paraformaldehyde fixative. The brain was extracted and sectioned at 50 µm thickness on a modified Vibratome

1000 (Leica Biosystems Inc.; Buffalo Grove, IL). Sections of tissue were mounted on gelatin coated microscope slides and imaged on a Zeiss LSM 710 confocal microscope with 10X and 20X objectives (Carl Zeiss Microscopy, LLC; Thornwood, NY.).

Data Availability

MEG and electrophysiology data analyzed and used for this report are available upon request from the authors.

Methods References

1. Han, X. in *Progress in Brain Research* **196,** 215–233 (Elsevier, 2012)
2. Klorig, D.C. *et. al. J. Neurosci. Methods* **227,** 132-139 (2014).
3. Stapleton-Kotloski, J.R., *et. al. Brain Imaging Methods* **5,** 244 (2014).
4. Huang, M.X., *et. al. Phys. Med. Biol.* **44,** 423 (1999).
5. Robinson, S. & Vrba, J. in *11th Int. Conf. on Biomagnetism* (1998).
6. Hillebrand, A. & Barnes, G.R. *Int. Rev. Neuro.* **68** (2005).

Greg Alberto

417 Corona St. Winston-Salem, NC 27103; Phone: 317-225-8456; e-mail: galberto@wakehealth.edu

Education

Graduate: Wake Forest School of Medicine combined MD/PhD program (2011-present)

PhD Dissertation: *Optically-induced Population Discharge Threshold Testing: A Novel Investigation of a Murine Model of Alcohol Withdrawal Induced CNS Hyperexcitability.*

Undergraduate: Wake Forest University

Bachelor of Science in Biology (Honors) with a minor in Neuroscience (2011)

Honor's Thesis: *Identification of Hormone Receptors that Mediate Metabolic Homeostasis in Drosophila melanogaster.*

Experience

Wake Forest School of Medicine Graduate School 2012-Present

- Student researcher, 2012-present, Wake Forest School of Medicine, Laboratory of Dwayne Godwin, PhD
- Skills: Neurophysiology, Magnetoencephalography, Neuroimaging, Murine and Nonhuman Primate Models, Addiction

Wake Forest University 2009-2012

- Student researcher Wake Forest University, Laboratory of Erik Johnson, PhD
- Skills: Genetics, Invertebrate physiology and pharmacology

Publications

- Braco JT; Gillespie EL; Alberto GE; Brenman JE; and Johnson EC. "Energy-dependent modulation of glucagon-like signaling in *Drosophila* via the AMP-activated kinase." *GENETICS*. 2012 192: 457-466.
- Rowland JA; Stapleton-Kotloski JR; Alberto GE; Rawley JA, Kotloski RJ, Taber KH; and Godwin DW. "Contrasting effects of posttraumatic stress disorder and mild traumatic brain injury on the whole-brain resting-state network: a magnetoencephalography study." *Brain Connectivity*. 2016

- Rowland JA; Alberto GE; Stapleton-Kotloski JR; Kotloski RJ; Godwin DW; Friedman D; Daunais JB. “Changes in brain function following chronic alcohol consumption in previously naïve individuals.” *Drug and Alcohol Dependence.* 2017.
- Alberto GE; Klorig DC; Stapleton-Kotloski JR; Constantinidis C; Daunais JB; Godwin DW. “Optogenetic activation of brain circuits reveals detection capabilities of MEG source imaging.” *Nature Neuroscience.* Under review.

Presentations

- Alberto, Greg. “Identification of Hormone Receptors that Mediate Metabolic Homeostasis in Drosophila melanogaster.” Granted travel award to present talk at the Symposium for Young Neuroscientists and Professors of the Southeast (SYNaPSe) at Wake Forest University. (2011)
- Alberto, Greg. “Localization of Optogenetically Induced Population Discharges in Vervet Hippocampus using MEG.” Neuroscience Research at Wake Forest School of Medicine Retreat. (2015)
- Alberto G.E, Klorig D.C., Masicampo M., Godwin D.W. “Ethanol withdrawal produces hyperexcitability and lowers seizure threshold in an optogenetic model of seizure.” Selected speaker for NIDA-NIAAA Early Career Investigator Showcase. (2015)
- Alberto, Greg. “optoMEG: Combining optogenetics and MEG for whole brain functional mapping.” Invited speaker at University of Glasgow Institute of Neuroscience and Psychology. (2016)

Abstracts

- Alberto, Greg. “Peptide signaling in maintenance of metabolic homeostasis in the fruitfly *Drosophila melanogaster*.” Poster presented at Wake Forest University, Undergraduate Research Day (2010).
- Alberto, Greg. “A novel method for developing and examining functional brain networks with magnetoencephalography for translational neuroimaging.” Poster presented at Wake Forest School of Medicine, Medical Student Research Day (2012).
- Alberto G., Klorig D., Stapleton-Kotloski J., McGowin I., Constantinidis C., Daunais J., Popli G., Godwin D. “Localization of Optogenetically Induced Population Discharges in Vervet Hippocampus using MEG.” Poster

presented at Wake Forest School of Medicine, Medical Student Research Day (2014).

- Alberto G., Klorig D., Stapleton-Kotloski J., McGowin I., Constantinidis C., Daunais J., Popli G., Godwin D. “Mapping optogenetic activation of the non-human primate brain using MEG.” Poster presented at Society for Neuroscience (2015).
- Alberto G., Klorig D., Stapleton-Kotloski J., McGowin I., Constantinidis C., Daunais J., Popli G., Godwin D. “Mapping optogenetic activation of the non-human primate brain using MEG.” Poster presented at Cell Symposia: Engineering the Brain – Technologies for Neurobiological Applications (2015).
- Klorig D.C., Alberto G.E, Masicampo M., Godwin D.W. “Ethanol withdrawal produces hyperexcitability and lowers seizure threshold in an optogenetic model of seizure.” Poster presented at Society for Neuroscience (2015).
- Alberto G., Klorig D., Stapleton-Kotloski J., McGowin I., Constantinidis C., Daunais J., Popli G., Godwin D. “Toward a combined optogenetic/MEG model of epilepsy in non-human primates.” Poster presented at American Epilepsy Society National Conference (2015).
- Alberto G., Klorig D., Stapleton-Kotloski J., Constantinidis C., Daunais J., Popli G., Godwin D. “Reconstruction of Optogenetic Induced Oscillations using Magnetoencephalography (MEG).” Poster presented at Society for Neuroscience (2016).

Awards and Honors:

- Norman M. Sulkin Scholarship Award in Neuroanatomy, 2017
- Governor’s Institute Scholarship to attend the Addiction Medicine 2017 Conference, 2017
- Poster Award Winner: Wake Forest Neuroscience Research Day, 2016
- Invited speaker to University of Glasgow Institute of Neuroscience and Psychology, 2016
- Invited speaker and travel award recipient for NIDA-NIAA Early Career Investigator Showcase Symposium, 2015
- Poster Award Winner: Wake Forest Neuroscience Research Day Poster 2014
- Invited attendee at “Combining Clinical and Research Careers in Neuroscience”, 2014
- SYNaPSe Travel Award winner, 2011
- Magna cum laude, 2011
- Honors in Biology, 2011
- Carolina Biological Undergraduate Research Student of the Year, 2011
- Florence Robinson Neuroscience Award, 2011

- Undergraduate Dean's List, 2007-2011

Grants and Fellowships:

- NRSA Individual Training Fellowship; NIH F30; 2015-2019
- Multisensory Training Grant; NIH T32, 2014
- Wake Forest Baptist Health Sciences Department of Neurology Sponsored Training Fellow; 2013
- Medical School Research Program; NIH T35 training grant, 2012
- Wake Forest Undergraduate Research Fellowship, 2010
- Robert L. Sullivan Scholarship, 2009